

For Reference

NOT TO BE TAKEN FROM THIS ROOM

For Reference

NOT TO BE TAKEN FROM THIS ROOM

Ex LIBRIS
UNIVERSITATIS
ALBERTAEISIS



UNIVERSITY OF ALBERTA
LIBRARY

Regulations Regarding Theses and Dissertations

Typescript copies of theses and dissertations for Master's and Doctor's degrees deposited in the University of Alberta Library, as the official Copy of the Faculty of Graduate Studies, may be consulted in the Reference Reading Room only.

A second copy is on deposit in the Department under whose supervision the work was done. Some Departments are willing to loan their copy to libraries, through the inter-library loan service of the University of Alberta Library.

These theses and dissertations are to be used only with due regard to the rights of the author. Written permission of the author and of the Department must be obtained through the University of Alberta Library when extended passages are copied. When permission has been granted, acknowledgement must appear in the published work.

This thesis or dissertation has been used in accordance with the above regulations by the persons listed below. The borrowing library is obligated to secure the signature of each user.

Please sign below:



THE UNIVERSITY OF ALBERTA

A STUDY OF ROUGHNESS
IN OPEN CHANNELS

by

DAVID LEONARD ROY CRONIN



A THESIS
SUBMITTED TO THE FACULTY OF GRADUATE STUDIES
IN PARTIAL FULFILMENT OF THE REQUIREMENTS FOR THE DEGREE OF
MASTER OF SCIENCE

DEPARTMENT OF CIVIL ENGINEERING

EDMONTON, ALBERTA

May 1968

UNIVERSITY OF ALBERTA
FACULTY OF GRADUATE STUDIES

The undersigned certify that they have read, and
recommend to the Faculty of Graduate Studies for acceptance,
a thesis entitled

A STUDY OF ROUGHNESS
IN OPEN CHANNELS

submitted by David Leonard Roy Cronin in partial fulfilment
of the requirements for the degree of Master of Science.



ABSTRACT

The resistance to flow caused by artificial bed forms in a flume was investigated. Curves were developed to relate the roughness to the flow depth, and to the dune shape. Roughness was expressed in terms of non-dimensional forms of Chezy's C, and the equivalent sand grain roughness, k_s .

Tests were performed on five different dune shapes which had wavelength to height ratios of 40, 32, 24, 16, and 8, which are of the same order of magnitude as the dunes and ripples found in nature.

The range of depth of flow to dune height ratios used in the experiments was from 4.75 to 2.25, which is also comparable to the values found under field conditions.

The effect of surface roughness was investigated by coating the original dunes with sand, and then repeating the tests. The difference in resistance to flow due to the surface roughness was reported.

The results of these tests were compared to results of previous studies performed in flumes which had mobile sand beds, and to theoretical formulae advanced in the literature.

ACKNOWLEDGEMENTS

The author wishes to extend his appreciation to Professor A.W. Peterson for his guidance and constructive criticism throughout this investigation.

Thanks are also due to the staff of the Hydraulic Laboratory for their efforts in the manufacture of the artificial bed forms, and for the maintenance of the electrical equipment used in the testing procedure.

TABLE OF CONTENTS

	Page
TITLE PAGE	i
APPROVAL SHEET	ii
ABSTRACT	iii
ACKNOWLEDGEMENTS	iv
LIST OF TABLES	vii
LIST OF FIGURES	viii
LIST OF PLATES	xi
GLOSSARY OF SYMBOLS	xii

Chapter

I	INTRODUCTION	1
	The Problem	
	Purpose and Scope	
	Review of Previous Research	
II	THEORY OF OPEN CHANNEL FLOW	10
	General	
	Chezy's Relation	
	Velocity Distribution	
	Dimensional Considerations	
III	THE EXPERIMENTAL INVESTIGATION	23
	The General Approach	
	The Test Flume	
	The Velocity Meter	
	The Bed Forms	
	The Experimental Procedure	



Chapter		Page
IV	EXPERIMENTAL RESULTS General Equivalent Sand Grain Roughness Chezy's Roughness Coefficient	40
V	DISCUSSION OF RESULTS General Equivalent Sand Grain Roughness Chezy's Roughness Coefficient Possible Sources of Error Comparison with Results of Other Studies The Logarithmic Velocity Formula Comparison with Regime Methods	58
VI	CONCLUSIONS AND RECOMMENDATIONS Conclusions Recommendations	84
LIST OF REFERENCES		87
Appendix		
A	EXPERIMENTAL OBSERVATIONS	A-1
B	DETAILED EXPERIMENTAL RESULTS	B-1



LIST OF TABLES

Table	Title	Page
5.1	Possible Percentage Errors in k_s	68
5.2	Possible Percentage Errors in C/\sqrt{g}	69
5.3	Comparison with Other Experimental Results	71
5.4	Comparison of Results with Published Formulae	75
5.5	Comparison with Regime Method	82
A-1	Experimental Data for Dune Shape $k/L = 1/8$	A-2
A-2	Experimental Data for Dune Shape $k/L = 1/16$	A-8
A-3	Experimental Data for Dune Shape $k/L = 1/24$	A-14
A-4	Experimental Data for Dune Shape $k/L = 1/32$	A-21
A-5	Experimental Data for Dune Shape $k/L = 1/40$	A-28
A-6	Experimental Data for Dune Shape $k/L = 1/8R$	A-33
A-7	Experimental Data for Dune Shape $k/L = 1/16R$	A-39
A-8	Experimental Data for Dune Shape $k/L = 1/24R$	A-45
A-9	Experimental Data for Dune Shape $k/L = 1/32R$	A-51
A-10	Experimental Data for Dune Shape $k/L = 1/40R$	A-57



LIST OF FIGURES

Figure	Title	Page
2.1	Development of Chezy's Equation	12
2.2	Shear Stress Distribution in Open Channel	14
2.3	Experimental Values of B	17
3.1	Experimental Equipment - General Layout	25
3.2	Bed Form Profiles and Construction	32
3.3	Layout of Experimental Observations	37
4.1	Variation of Roughness with Flow Depth for Smooth Dunes	42
4.2	Variation of Roughness with Flow Depth for Rough Dunes	43
4.3	Variation of Roughness with Dune Shape for Smooth Dunes	44
4.4	Variation of Roughness with Dune Shape for Rough Dunes	45
4.5	Change in Roughness Due to Sand Grains	46
4.6	Variation of Roughness with Flow Depth for Smooth Dunes (Based on Mean Velocity)	47
4.7	Variation of Roughness with Flow Depth for Rough Dunes (Based on Mean Velocity)	48
4.8	Variation of Roughness with Flow Depth for Smooth Dunes	52
4.9	Variation of Roughness with Flow Depth for Rough Dunes	53



Figure	Title	Page
4.10	Variation of Roughness with Dune Shape for Smooth Dunes	54
4.11	Variation of Roughness with Dune Shape for Rough Dunes	55
4.12	Change in Roughness Due to Sand Grains	56
B-1	Variation of Roughness with Flow Depth $L/k = 8$	B-2
B-2	Variation of Roughness with Flow Depth $L/k = 16$	B-3
B-3	Variation of Roughness with Flow Depth $L/k = 24$	B-4
B-4	Variation of Roughness with Flow Depth $L/k = 32$	B-5
B-5	Variation of Roughness with Flow Depth $L/k = 40$	B-6
B-6	Variation of Roughness with Flow Depth $L/k = 8R$	B-7
B-7	Variation of Roughness with Flow Depth $L/k = 16R$	B-8
B-8	Variation of Roughness with Flow Depth $L/k = 24R$	B-9
B-9	Variation of Roughness with Flow Depth $L/k = 32R$	B-10
B-10	Variation of Roughness with Flow Depth $L/k = 40R$	B-11
B-11	Variation of Roughness with Flow Depth $L/k = 8$	B-12
B-12	Variation of Roughness with Flow Depth $L/k = 16$	B-13
B-13	Variation of Roughness with Flow Depth $L/k = 24$	B-14
B-14	Variation of Roughness with Flow Depth $L/k = 32$	B-15

Figure	Title	Page
B-15	Variation of Roughness with Flow Depth $L/k = 40$	B-16
B-16	Variation of Roughness with Flow Depth $L/k = 8R$	B-17
B-17	Variation of Roughness with Flow Depth $L/k = 16R$	B-18
B-18	Variation of Roughness with Flow Depth $L/k = 24R$	B-19
B-19	Variation of Roughness with Flow Depth $L/k = 32R$	B-20
B-20	Variation of Roughness with Flow Depth $L/k = 40R$	B-21



LIST OF PLATES

Plate	Title	Page
3.1	General Layout of Laboratory Equipment	26
3.2	Mini-Flowmeter and Counter Unit	26
3.3	Bed Forms and Flowmeter in Flume	27

GLOSSARY OF SYMBOLS

A	- Cross section area of channel
A_1	- Simplifying term in velocity profile equation
A'	- Constant in velocity profile equation
B	- Constant in velocity profile equation
B'	- Constant in velocity profile equation
b	- Breadth of channel
C	- Chezy's roughness parameter
ΔC	- Change in Chezy's roughness parameter
D	- Diameter of bed material
d	- Depth of flow
f''	- Friction factor due to bed forms
g	- Acceleration due to gravity
K	- Constant of proportionality
k	- Height of bed form
k_s	- Equivalent sand grain roughness
L	- Wavelength of bed form
l	- Lower limit of region in which $\tau \approx \tau_t$
Q	- Discharge
R	- Hydraulic radius
S	- Slope of channel



u'	- Lateral component of turbulent velocity fluctuations
V	- Mean velocity of flow
v'	- Transverse component of turbulent velocity fluctuations
v_*	- Shear velocity = \sqrt{gRS}
W	- Weight of a given portion of flow
X	- Representative roughness parameter
x	- Simplifying term in velocity profile equation
y	- Elevation above datum
γ	- Unit weight of flow
δ	- Lower limit of region in which $\tau \approx \tau_t$
κ	- Von Karman's coefficient
μ_t	- Turbulent or eddy viscosity
ν	- Kinematic viscosity of flow
ρ	- Unit mass of flow
τ	- Shear stress at given elevation above datum
τ_b	- Shear stress at bed
τ_v	- Shear stress due to viscous effects
τ_t	- Shear stress due to turbulent effects
ϕ	- Angle of repose of bed material
χ	- Representative roughness spacing parameter



CHAPTER I

INTRODUCTION

1.1 The Problem

Many of the rivers with which man is concerned flow in deposits of natural alluvium. The slope, width, depth, and trace of the river are a consequence of the normal sequence of river flows, the characteristics of the material in which the channel is formed and the type of sediment, if any, transported by the flow. In most rivers of this description the bed is in motion at least during peak flows.

Depending on the geology of the surrounding area, and on that of the regions upstream, the grains of the bed material may be classified as sand, gravel, cobbles, or boulders. In a typical case it might be found that a river had a bed composed of a mixture of different sizes of material with the greatest percentage falling in the sand size range. This material would be in almost constant motion, except at very low flows, with the larger bed material moving only during peak floods.

The sand grain particles move most commonly by rolling or saltation. As a consequence of this transport, during tranquil flows, irregular ripples or dunes are

formed from the bed material.

Previous studies have indicated that the resistance to flow offered by the river bed is a function of both the grain size of the particles on the surface of the bed, and of the shapes into which the material is moulded. That is, there is a frictional drag on the flow due to the surface roughness, and an additional resistance due to the form drag of the bed forms.

Some studies have roughly indicated the percentage of the total resistance to the flow due to grain roughness, bed forms and other factors. However, due to the limited extent of previous work, or the preoccupation of these studies with other facets of the phenomenon, little is known about the actual relation between the form drag caused by the dunes, and the shape of the bed forms themselves. In fact, little research has been done to estimate open channel roughness, or resistance to flow, whether from natural or artificial elements.

It was this lack of knowledge of open channel roughness in general, and a particular desire to investigate the dependency of bed form drag on dune shape, which prompted this present investigation.

1.2 Purpose and Scope

The purpose of this investigation was to initiate a study into the form drag produced by bed forms in alluvial

channels. The present work was conceived as a pilot project to briefly investigate the practicability of such research, to determine if reasonable results could be obtained by the methods used herein, and to yield a rough idea as to the type of relation which existed between the dune shape and the drag produced.

In order to facilitate the investigation, the research was conducted in a laboratory flume, using idealized dune shapes produced from an artificial material, rather than using a natural movable sand bed, or observing a stream bed under field conditions. This allowed a correlation of roughness results with specific dune shapes, and made possible an exact control of the distribution of experimental data, rather than being limited by the multitude of shapes produced under normal conditions.

In order to make the results of the investigation comparable to field conditions the dune shapes chosen for study were of the same range as those found under natural conditions, in rivers or canals, and under laboratory conditions in flumes which have mobile beds. That is, the wavelength to dune height ratios, L/k , were within the range of values to be expected under natural conditions.

In addition, the ratios of depth of flow to dune height, d/k , used throughout the experiments were approximately equal to those which might be expected under field conditions, or in a mobile bed flume.



Typical data which show the range of values of L/k and d/k ratios under field conditions are shown in Yalin (16). Similar data relating to laboratory flume experiments are contained in Vanoni and Hwang (5), or Guy, Simons, and Richardson (15).

The use of artificial dunes in a laboratory flume simplified the problem by creating flow conditions that were close to those of an ideal two dimensional flow, and by eliminating sediment transport, and resistance to flow due to the meandering and channel irregularities which would be found in a natural situation.

The artificial bed forms extended the full width of the flume, and had straight crests perpendicular to the flow. This presented a more regular pattern than a natural channel, where discontinuous and curved crests are the rule.

The height of the experimental bed forms was held constant during the investigation, while the wavelength of the recurring shapes was varied. In addition, the depth of the uniform flow was varied throughout the testing procedure to assess the change in roughness due to the changes in flow depth.

The initial inquiry was performed on smooth bed forms. Then, in an effort to discover the order of resistance due to surface or grain roughness, the original dunes were coated with sand, and the test series repeated, noting the change in the total drag.



Tests were conducted for five different dune shapes, both smooth and roughened, giving a total of ten test series. In each test series, the depth of flow was varied from roughly four to ten times the height of the bed forms. In every case the slope and discharge were varied to give the required uniform flow conditions at the desired depth.

Measurements of the above parameters, plus velocity profiles taken at a number of points along each type of bed form allowed calculation of Chezy's C, and the Equivalent Sand Grain Roughness, k_s , for each flow condition. Observation of changes in these values then permitted comparisons of the performance of each dune shape.

1.3 Review of Previous Research

A review of the applicable literature on this topic indicates that, as far as can be determined, no similar research has previously been undertaken on rigid open channels. Numerous studies have been made of the channel resistance resulting from various types and spacings of artificial roughness elements, however, in no case, did these shapes approximate dunes or ripples.

Suryanarayana (1) reported an investigation using curved corrugations, on a flume bed, at various spacings. The results shown in this work are of the form:

$$\sqrt{\frac{C}{g}} = f \left(\log \frac{y}{a}, \log \frac{y}{L} \right)$$

where: a = average roughness height
 C = Chezy's roughness coefficient
 g = acceleration due to gravity
 L = longitudinal roughness spacing
 y = depth of flow

In addition, it was reported that in this study Von Karman's coefficient, κ , was found to vary from 0.1885 to 0.19.

Mirajgaoker and Charlu (2), and Chithambaran and Mirajgaoker (3), reported similar relations for roughness patterns consisting of natural stones placed at various spacings. In the latter paper Von Karman's coefficient was reported to have remained fixed at 0.38.

Sayre and Albertson (4), among others, have reported studies conducted using baffles of various sizes, shapes, and spacings as roughness elements. They reported similar logarithmic relations, and, in addition, introduced a parameter χ to describe spacing. In this study, Von Karman's coefficient was found to be approximately 0.38 and constant for all spacings.

The applicability of these results to the problem dealt with in this present investigation is somewhat limited, however. There is bound to be a significant difference in the values of roughness due to isolated baffles, rocks, or other artificial elements, and those values due to undulations in the channel bed such as are presented by dunes or ripples. These previous studies serve, however, to illustrate the



factors on which total resistance depends, and to indicate the rough trend of results which may be expected.

A few investigations have been done on channels having a mobile sand bed, and sediment transport, in order to determine the amount of resistance due to sediment transport, surface roughness, and form drag due to bed forms.

Vanoni and Hwang (5) indicated that the resistance to flow caused by dune shapes was:

$$\frac{1}{f^*} = 3.3 \log \frac{LR}{k} - 2.3$$

where: f^* = friction coefficient due to the form drag
 k = average dune height
 L = average dune length
 R = bed hydraulic radius

Considerable data is presented in this paper, both from the authors' experiments, and from other sources. In addition, data is presented concerning the effect of the surface roughness of the bed.

Simons and Richardson (6) do not consider the effect of charge on resistance, but state that the total roughness, C/\sqrt{g} , of a channel may be evaluated by determining the C'/\sqrt{g} of a plane bed of the same material, and then multiplying by a factor C_* to account for form drag. Their study indicates:

$$C_* = f(d, D, S)$$

where: d = depth of flow
 D = particle diameter of bed material
 S = channel slope

In another paper (7) the same authors do not go so

far as to present a relation relating roughness to bed profiles, however, they present a collection of data from which comparisons may be made.

Richardson and Simons (8) present equations relating various bed profiles and channel resistance:

$$\text{for ripples: } \frac{C}{\sqrt{g}} = (7.66 - \frac{0.3}{v_*}) \log d + \frac{0.13}{v_*} + 11.0$$

$$\text{for dunes: } \frac{C}{\sqrt{g}} = 7.4 \log \frac{d}{D_{85}} \sqrt{1 - \frac{\Delta RS}{RS}}$$

where: R = hydraulic radius of flow

$v_* = \sqrt{gRS}$ = shear velocity

ΔRS = resistance to flow due to dunes

Criteria are also presented for predicting the type of profile which will form under given conditions. The sand used in part of the research for this paper, 0.93mm, was roughly similar to that available for the present investigation.

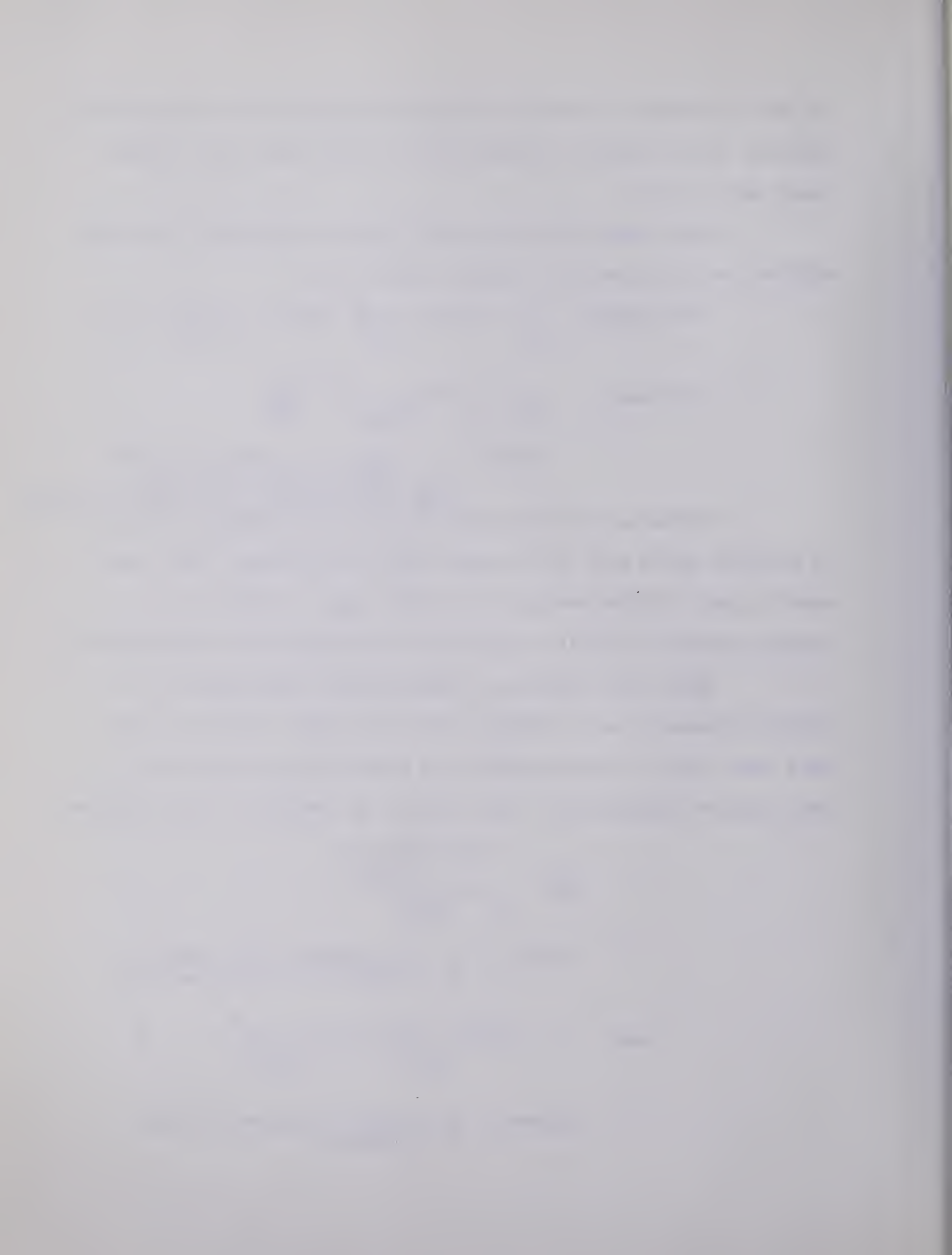
Yalin (9) presents a theoretical development of a relation between bed roughness and dune shape, based on the head loss due to the expansion and contraction of the flow over the bed undulations. The formula he presents is as follows:

$$\frac{C}{\sqrt{g}} = \frac{2.5 \ln \left(\frac{11d}{k_s} \right)}{\sqrt{1 - \left(\frac{k}{L} \right) \sigma^2}}$$

where: k_s = equivalent sand grain roughness of bed material

$$\text{and } \sigma^2 = \tan \phi - \frac{k}{2L} \left(2.5 \ln \frac{11d}{k_s} \right)^2$$

where: ϕ = angle of repose of bed material



Regarding the velocity distribution to be expected in an alluvial channel with an undular bed, Garde and Paintal (10) present data from various sources which indicate that Von Karman's coefficient, κ , is not constant. It is shown that it varies considerably, depending on the sediment concentration, dune shape, and relative roughness. Plots of κ against these factors show considerable scatter, but indicate values ranging from 0.15 to slightly greater than 1.0 in alluvial channels.

Thus, most of the studies to date have dealt with artificial roughness patterns of discrete elements. These are not of great value to this work, except to indicate the trend of results, and important parameters.

The most valuable work in channel roughness has concerned the resistance found in alluvial channels. However, only a few attempts have been made to directly relate roughness to form drag and the shape of the dunes present, and these have been largely theoretical.

CHAPTER II

THEORY OF OPEN CHANNEL FLOW

2.1 General

Due to the complexity of the mechanics of fluid flow, especially that found in open channel applications, many simplifying assumptions must be made when proposing theories to explain observed behavior. A standard assumption, commonly used, is that steady, two-dimensional flow exists.

However, numerous studies, such as those of Keleugan (11), Tracy and Lester (12), or Cruff (13), have demonstrated that, due to sidewall effects, flow in an open channel may be considered to approach the ideal two-dimensional conditions only in a relatively narrow region about the channel centre line.

Cruff demonstrates that within the width to depth ratios to be used in this investigation, 0.111 to 0.246, the shear stress distribution on the channel bed approaches a uniform condition only in a region about the centre line of the channel, approximately ten percent to twenty percent of the channel width.

Thus, it should be carefully noted that implicit



in the discussion that follows is the assumption that measurements are to be taken within a suitable region in which the flow conditions can be considered to approximate those of a two-dimensional flow.

2.2 Chezy's Relation

The uniform flow relation developed by French engineer Antoine Chezy about 1769 was probably the first such formula. It is still widely used, the empirical constant being estimated through experience. No suitable means has been found for calculating the constant from roughness measurements or other factors. The observations of this study may, however, present a somewhat clearer idea of the manner in which certain factors affect the final result.

Chezy based his mathematical derivation on two assumptions:

- 1) That the force resisting the flow, per unit area of stream bed, was proportional to the square of the mean velocity, and
- 2) That in uniform flow the resistance of the bed is exactly equal to the component of the gravity force which causes flow down the slope of the channel.

The Chezy relation is usually expressed as follows:

$$V = C\sqrt{RS}$$

where: V = mean velocity of flow
 C = Chezy's constant
 R = hydraulic radius of flow
 S = slope of the energy line



The formula may be derived in the following manner:
(see fig. 2.1)

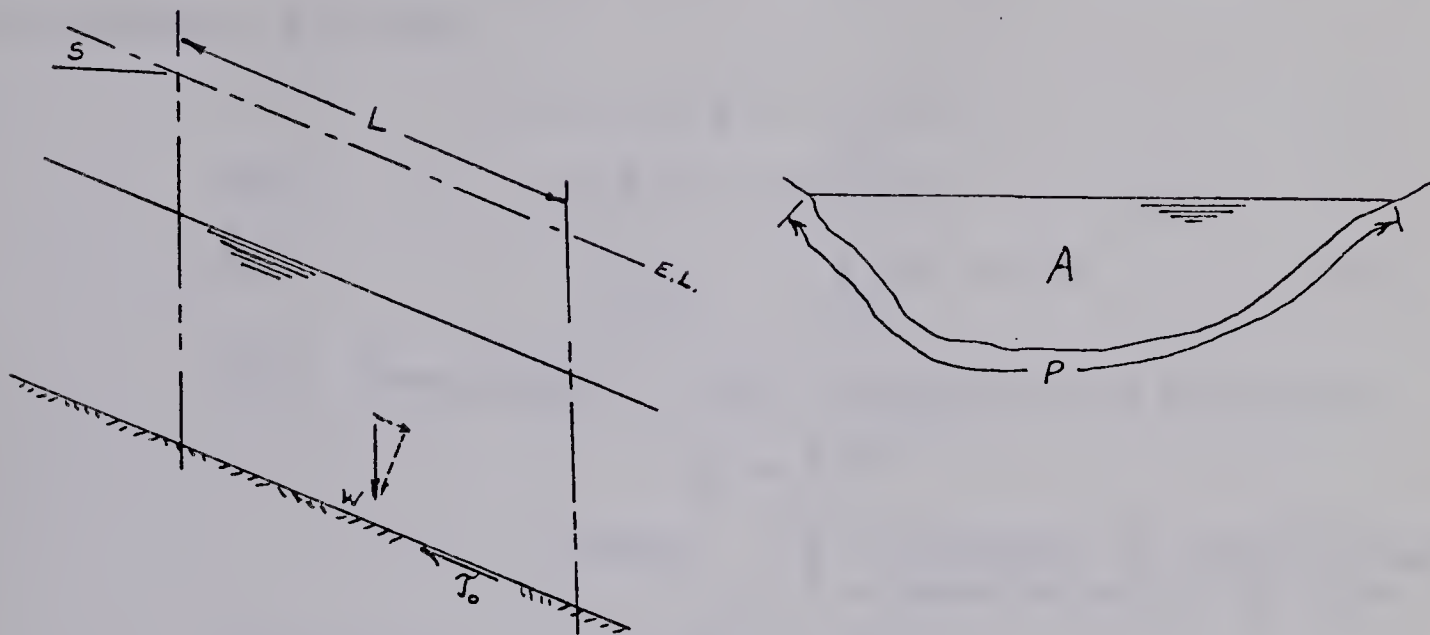


Fig. 2.1: Development of Chezy's Equation

The total weight W of the flow between the two sections shown is:

$$W = \gamma L A$$

where: γ = unit weight of flow
 L = length of section
 A = cross section area of flow

The component of the weight which is causing flow down the slope is:

$$W \sin S = \gamma L A S$$

where: S = slope of energy line or channel

If we assume a unit resisting force T_0 on the bed of the channel we find the total resisting force to be:

$$T_0 L P$$

where: P = wetted perimeter of flow

Now, using Chezy's assumption that accelerating and resisting forces are equal, and assuming, in addition, that S is small, we have:

$$\gamma L A \sin S = \tau_o L P$$

or: $\gamma A S = \tau_o P$

$$\frac{\tau_o}{\gamma} = \frac{A}{P} \cdot S = RS \quad (2.1)$$

Now, from Chezy's other assumption, we may write:

$$\tau_o = K V^2$$

where: K = constant of proportionality
 V = mean velocity of flow

Therefore: $\frac{K V^2}{\gamma} = RS$

or: $V = \sqrt{\frac{\gamma}{K}} \cdot \sqrt{RS}$

Replacing the constants γ and K by a single constant named "Chezy's C " we write:

$$V = C \sqrt{RS} \quad (2.2)$$

Thus the Chezy relation relates the mean velocity of flow, the channel geometry, and the slope. The constant is dependent upon fluid properties, and the shape, distribution, and size of the roughness elements on the channel boundary.

2.3 Velocity Distribution

It is possible to develop an expression for the velocity distribution in a steady, uniform, two-dimensional flow having a free surface. Then, using this type of expression, a relation may be obtained between the bed roughness



and flow parameters.

From the previous development of the Chezy equation we obtained the following relation:

$$\tau_0 = \gamma S R \quad (2.1)$$

Generalizing this expression for any depth within a flow, and for the case of a wide channel, we could write:

$$\tau = \gamma S d$$

which would generate a shear stress distribution as shown in fig. 2.2:

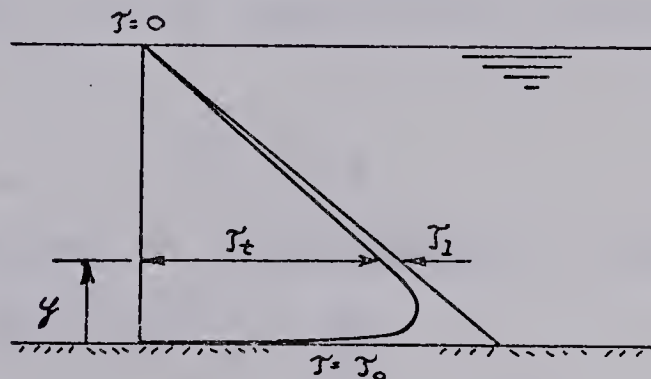


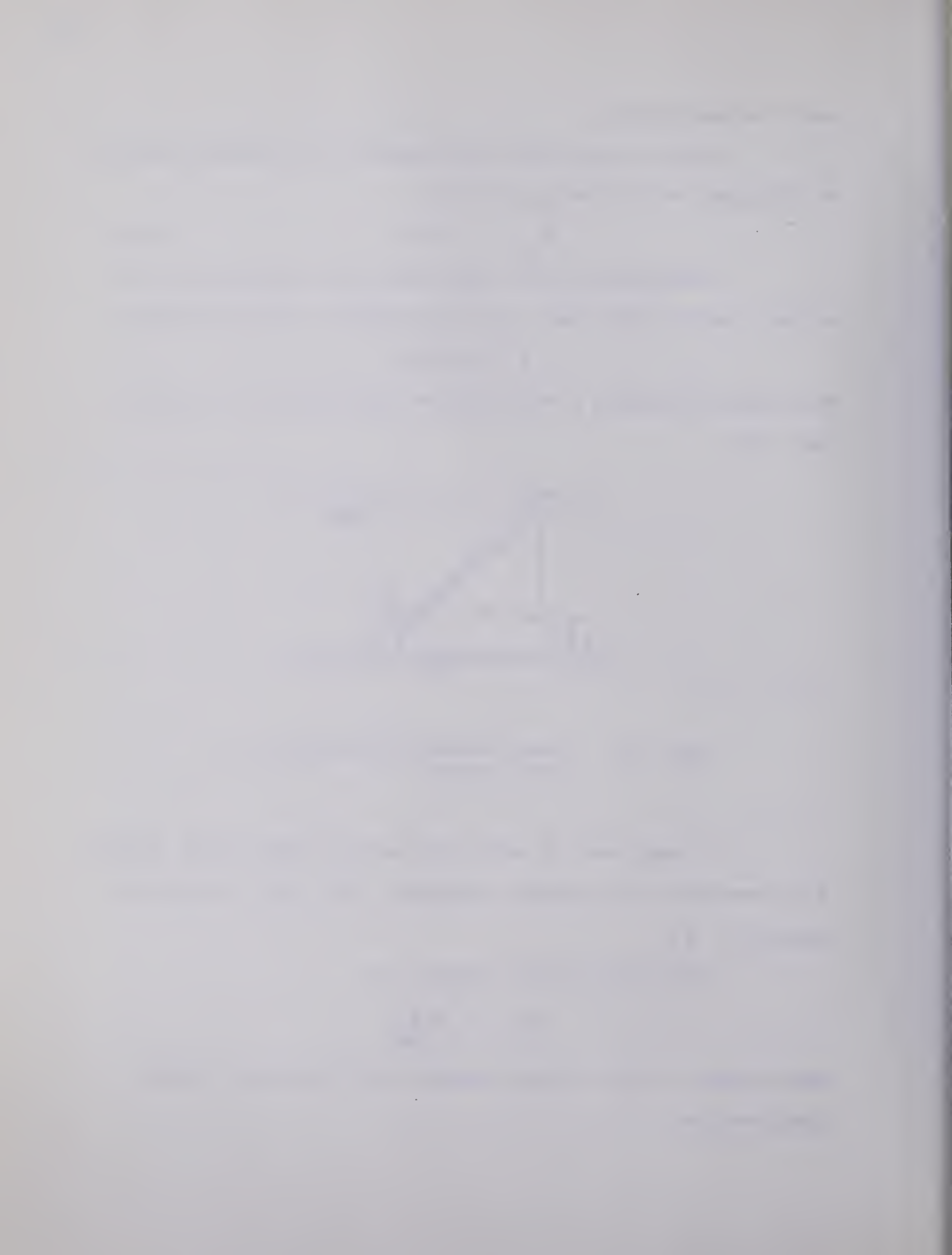
Fig. 2.2: Shear Stress Distribution in Open Channel

At any level y above the bed the total shear stress τ is composed of a viscous component, τ_1 , and a turbulent component, τ_t .

The viscous shear stress is:

$$\tau_1 = \mu \frac{dv}{dy}$$

where dv/dy is the velocity gradient at the level y under consideration.



The turbulent shear stress is:

$$\tau_t = \rho \overline{u'v'}$$

where $\overline{u'v'}$ is the long term average product of the lateral (u') and transverse (v') components of the turbulent velocity fluctuations. Thus, for a turbulent flow:

$$\tau = \tau_l + \tau_t$$

However, as can be seen from fig. 2.2, the contribution of the viscous shear forces is significant only within a small region relatively close to the bed.

Therefore, at any appreciable distance above the bed we could write:

$$\tau \approx \tau_t$$

As an analogy to laminar flow we could write:

$$\tau \approx \tau_t = \mu_t \frac{dv}{dy} \quad (2.4)$$

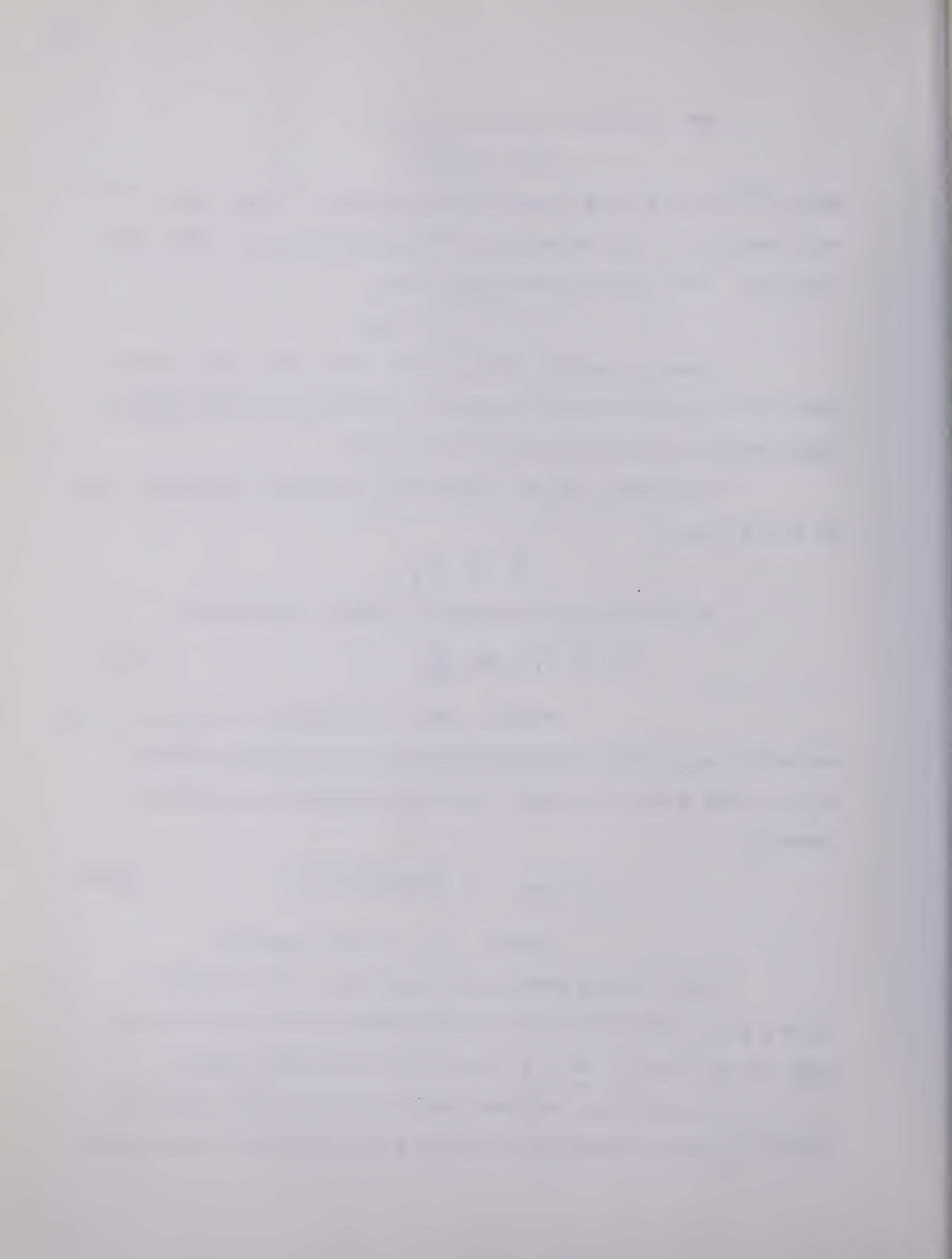
where: μ_t = turbulent or eddy viscosity and where μ_t varies as some function of y . This variation of μ_t with y is not known, but we may say as we approach the boundary:

$$\lim_{(y \rightarrow 0)} \mu_t = (\text{const}) \rho v_* y \quad (2.5)$$

where: v_* = shear velocity

Now, as was previously mentioned, the assumption $\tau \approx \tau_t$ is only valid above some certain depth in the flow, that is, say when $y \geq \delta$, where δ is the lower limit.

In addition, expressions (2.4) and (2.5) are only valid in a space completely occupied by fluid, and can not be



valid in the region of roughness, $0 < y < k_s$, where space is occupied partly by fluid and partly by boundary material.

Thus k_s also constitutes a lower limit of validity.

Therefore, we can say that:

$$\mu_t = (\text{const}) \rho v_* y \quad (2.6)$$

is valid if:

$$d \gg y \gg 1$$

where: $l = \text{larger of } \delta \text{ or } k_s$.

$y = \text{elevation in question}$

Now when $y \rightarrow 0$, then $\tau \rightarrow \tau_0$. So, considering that $\tau_0 = \rho v_*^2$, then by combining equations (2.6) and (2.4) we obtain:

$$v_* = (\text{const}) \cdot y \cdot \frac{dv}{dy} \quad (2.7)$$

Integrating (2.7) in the region l to y , we obtain:

$$\frac{v}{v_*} - \frac{v_l}{v_*} = (\text{const}) \ln \frac{y}{l}$$

where: v_l is the value of v at $y = l$.

Now, if $\delta > k_s$, i.e. if $l = \delta$, we have:

$$\frac{v}{v_*} = (\text{const}) \ln \frac{y}{\delta} + \frac{v_s}{v_*} \quad (2.8)$$

and if $k_s > \delta$, i.e. if $l = k_s$ we have:

$$\frac{v}{v_*} = (\text{const}) \ln \frac{y}{k_s} + \frac{v_{k_s}}{v_*} \quad (2.9)$$

Both expressions (2.8) and (2.9) can be simplified into the form:

$$\frac{v}{v_*} = (\text{const}) \ln \frac{y}{k} + B \quad (2.10)$$

where: $B = (\text{const}) \ln \frac{k}{\delta} + (\text{const})_{\delta}$ if $k/\delta \rightarrow 0$ (2.10)'
 $B = (\text{const})_k$ if $k/\delta \rightarrow \infty$ (2.10)''

Expressions (2.10)' and (2.10)'' may be shown in terms of v_* and v instead of δ as follows:

$$B = (\text{const}) \ln \frac{v_* k_s}{v} + (\text{const})_v \quad \text{if } \frac{v_* k_s}{v} \rightarrow 0$$

$$B = (\text{const})_{k_s} \quad \text{if } \frac{v_* k_s}{v} \rightarrow \infty$$

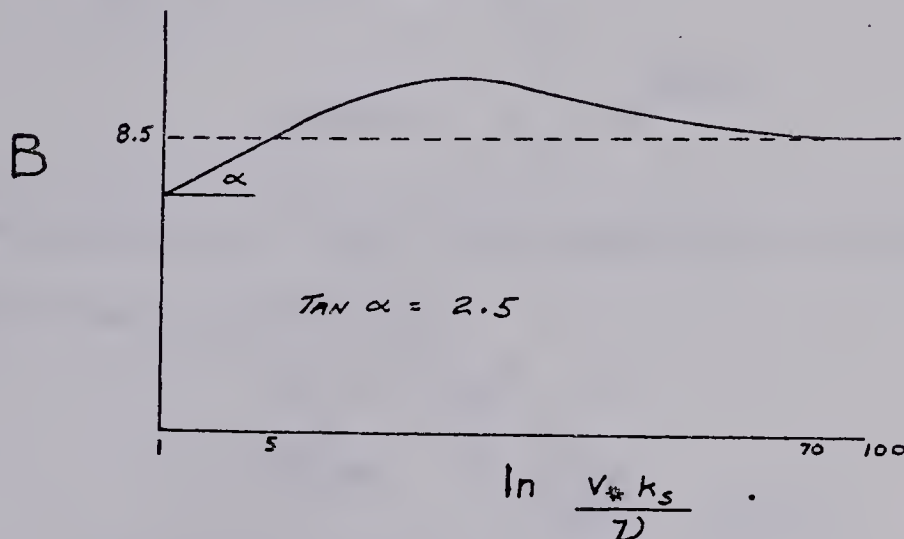


Fig. 2.3: Experimental Values of B

The form of experimental data is shown in fig. 2.3. Using this data, the following can be deduced:

$$B = 2.5 \ln \frac{v_* k_s}{v} + 5.5 \quad \text{if } \frac{v_* k_s}{v} < 5$$

$$B = 8.5 \quad \text{if } \frac{v_* k_s}{v} \geq 70$$

and equation (2.10) now becomes:

$$\frac{v}{v_*} = 2.5 \ln \frac{y}{k_s} + B \quad (2.11)$$

The case when $(v_* k_s / \nu) < 5$ corresponds to hydraulically smooth flow where $\delta \gg k_s$. The case where $(v_* k_s / \nu) > 70$ corresponds to fully developed turbulent flow. In between these cases, the flow is transitional and values of B must be estimated from the experimental graph.

It is useful to note that the expression (2.11) may be simplified to:

$$\frac{v}{v_*} = 2.5 \ln A_1 \frac{y}{k_s} \quad (2.12)$$

$$\text{where: } A_1 = e^{B/2.5}$$

For purposes of this investigation, the above expression was solved for k_s yielding:

$$k_s = y \cdot e^x \quad (2.13)$$

$$\text{where: } x = \left(\frac{B}{2.5} - \frac{v}{2.5 v_*} \right)$$

Thus, using this relation, the equivalent sand grain roughness of any given boundary configuration may be found if the viscosity, slope, depth of flow, and flow velocity at a given elevation above the bed are known.

In a similar manner it is possible to derive an equation relating the equivalent sand grain roughness to the mean velocity of the flow:

$$\frac{v}{v_*} = 2.5 \ln \frac{11.0 d}{k_s} \quad (2.14)$$

Equation (2.11) may also be written in the following manner:



$$\frac{v}{v_*} = 5.75 \log \frac{y}{k_s} + B$$

With regard to the assumption of two-dimensional flow in the central portion of a channel, Tracy and Lester (12) have shown that some variation may be found in the factor 5.75, which is really $2.3/\kappa$, where κ is Von Karman's coefficient, depending on the width to depth ratio of the channel. The possible variation of this factor in the present study will be discussed in a later section.

2.4 Dimensional Considerations

Since expressions relating the flow properties have been developed, it is appropriate to examine the relationships between the parameters involved, in order to devise methods of experimental investigation. By varying various parameters while holding others constant, it is possible to devise appropriate experimental procedures which will yield information concerning the physical laws underlying the behavior of the system under study.

The mean velocity observed in a steady uniform flow can be said to depend on both the properties of the fluid, and those of the channel. In general, we could write:

$$V = f_1(\rho, \mu, d, k_s, gS)$$

where: ρ = unit mass of fluid
 μ = dynamic viscosity of fluid
 d = flow depth
 k_s = equivalent sand grain roughness of channel
 g = acceleration of gravity
 S = slope of channel

Note that in the above expression there is no term describing the channel width or shape. This, therefore, assumes that the flow considered is in a wide channel, where it may be considered two-dimensional, and unaffected by any sidewall effects.

Here we have used one term, k_s , to describe the ultimate channel roughness. However, this term may be broken down as follows:

$$k_s = f_2(L, k, \phi, x) \quad (2.15)$$

where: L = length of bed forms
 k = height of bed forms
 X = some measure of surface roughness
 ϕ = angle of repose of bed material, or slope of dune face

Again, we have used one term, X , to cover all the effects of surface roughness. This term could, in turn, be broken down, and replaced by others describing the roughness spacing, height, shapes, size distribution, and other factors. However, since in this investigation we will not consider the manner in which roughness depends upon these characteristics, we may drop the parameter X from our analysis.

Similarly, the parameter ϕ is constant throughout our tests, and need not be considered. Therefore, we may write:

$$k_s = f_3(L, k)$$

Combining this with our previous expression, we obtain:

$$V = f_4(\rho, \mu, d, L, k, gS)$$



Rearranging these terms to form non-dimensional parameters yields:

$$\sqrt{\frac{V}{gdS}} = f_5 \left(\frac{d}{k}, \frac{L}{k}, \frac{\sqrt{gdS}}{\mu/\rho} \right)$$

$$\frac{V}{v_*} = f_5 \left(\frac{d}{k}, \frac{L}{k}, \frac{v_* d}{\nu} \right)$$

If it is assumed that in these investigations fully developed turbulent flow will exist, then the term $v_* d / \nu$ may be ignored. Thus, we have:

$$\frac{V}{v_*} = f_6 \left(\frac{d}{k}, \frac{L}{k} \right)$$

now, recall that:

$$\frac{V}{v_*} = \sqrt{\frac{C}{g}}$$

Therefore, the expression becomes:

$$\sqrt{\frac{C}{g}} = f_6 \left(\frac{d}{k}, \frac{L}{k} \right) \quad . \quad (2.16)$$

Again, equation (2.15) yields:

$$k_s = f_1(L, k, \phi, X)$$

or, we could write:

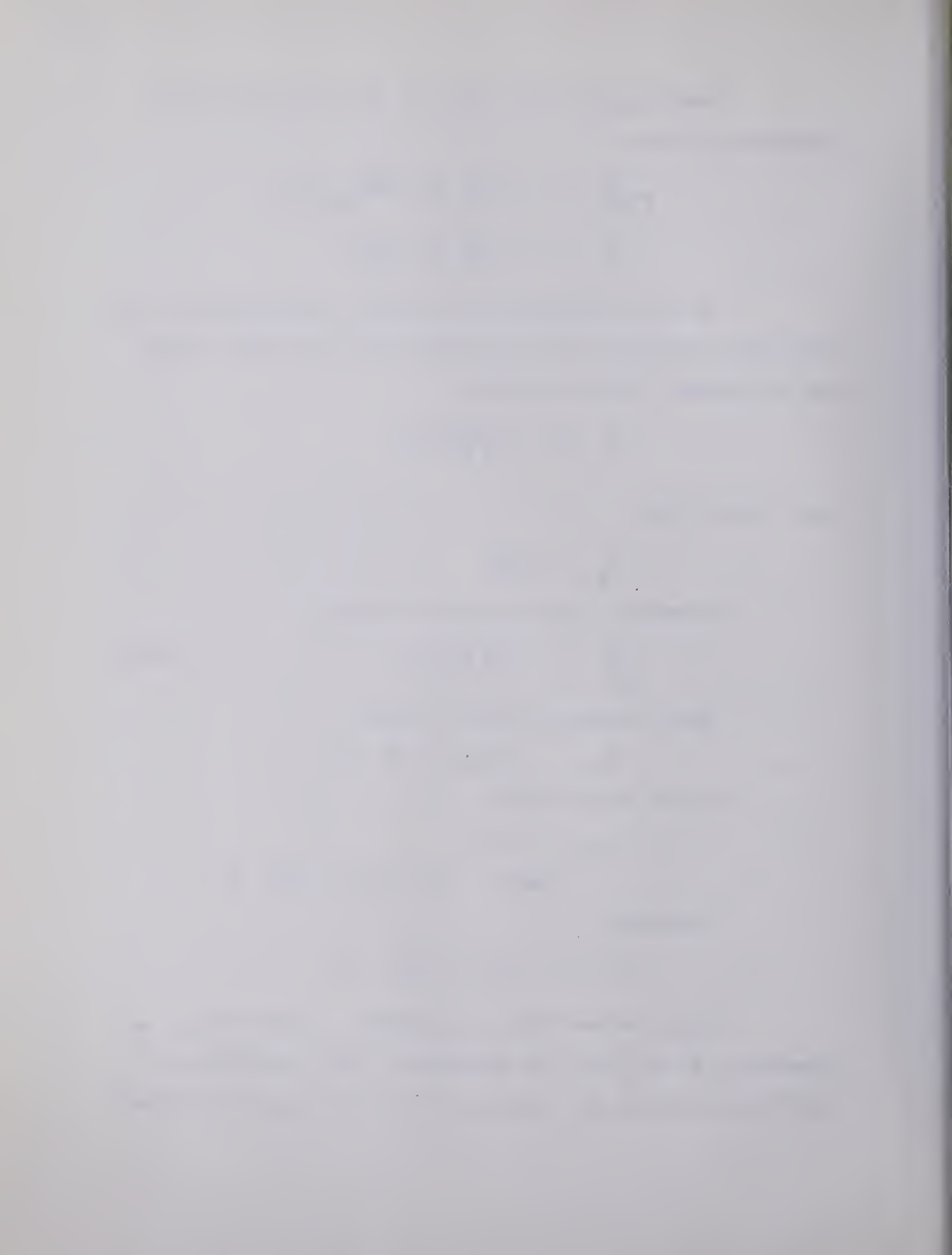
$$k_s = n \cdot k$$

$$\text{where: } n = f_2(k, L, \phi, X)$$

Therefore:

$$k_s = f_2(k, L, \phi, X)k$$

Again, since they are constant in this study, the parameters ϕ and X may be neglected. Also, as before, it will be noted that the presence of a wide channel is assumed



since no channel geometry terms are included.

The expression therefore reduces to:

$$k_s = f_3(k, L)k$$

Therefore:

$$\frac{k_s}{d} = f_4(k, L) \frac{k}{d}$$

$$\text{or: } k_s = f_5(l, k, d)$$

Rearranging these terms gives:

$$\frac{k_s}{k} = f_6\left(\frac{L}{k}, \frac{d}{k}\right) \quad (2.17)$$

Examination of relations (2.15) and (2.17) suggests forms of results which would most appropriately demonstrate the laws governing the resistance of bed forms to uniform flow.



CHAPTER III

THE EXPERIMENTAL INVESTIGATION

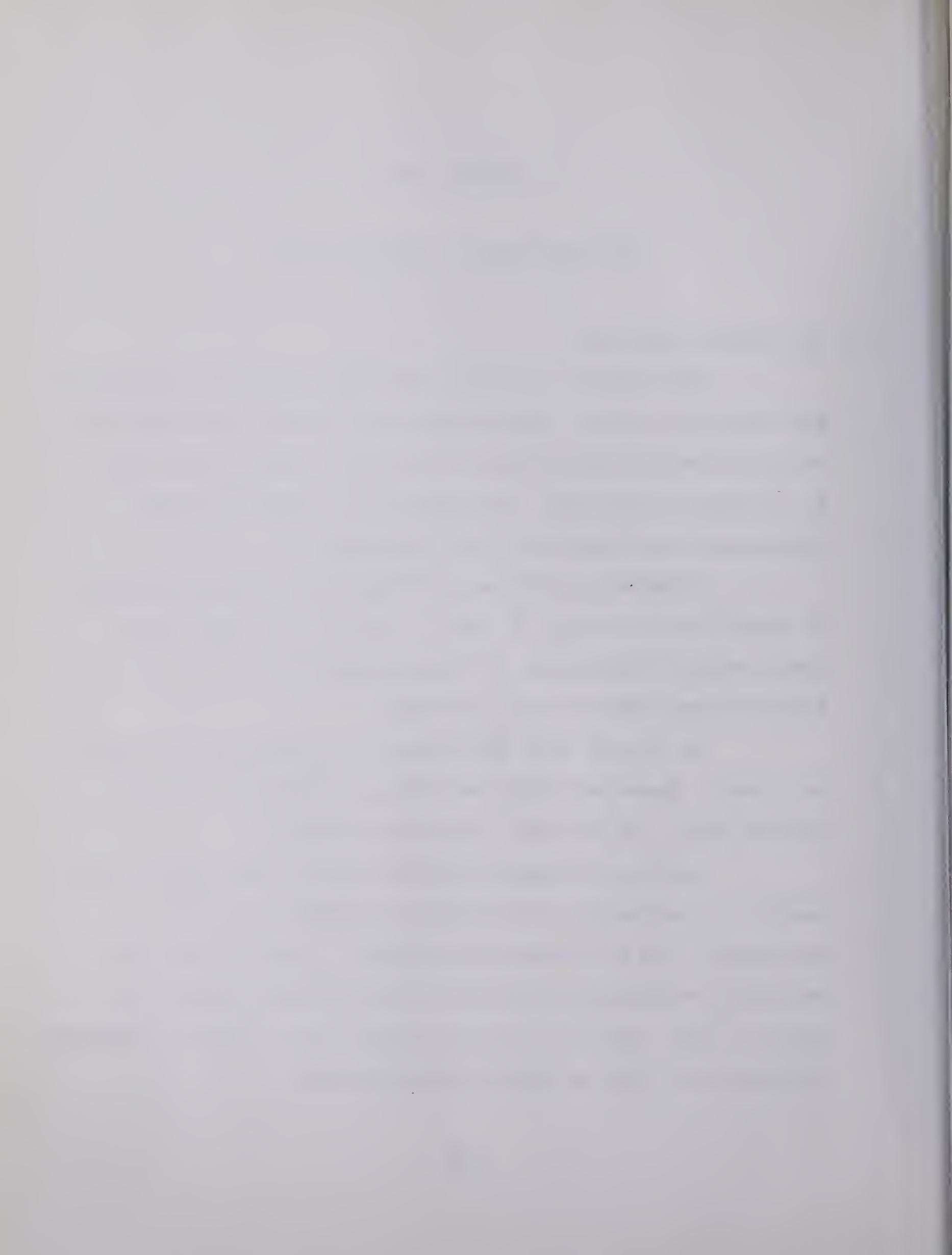
3.1 The General Approach

The testing procedure consisted of placing artificial bed forms in a flume, and establishing uniform flow over them. Velocity profiles were taken at the centre line of the flume at a number of sections. In addition, the depth of flow, discharge, and flume slope were recorded.

Tests were performed for bed forms having wavelength to height ratios of 40, 32, 24, 16, and 8. For each shape tests were run for depths of flow ranging from 4.5 to 9.5 times the amplitude of the bed forms.

An initial test series was run using smooth concrete bed forms. These bed forms were then roughened by adding a coat of sand, and the test series was repeated.

By using the data observed during these tests it was possible to calculate the roughness parameters as outlined previously, and to determine the manner in which this characteristic roughness varied with the bed form shape and the depth of flow. Details of the equipment used, and the procedure followed are given in the following sections.



3.2 The Test Flume

The flume used for this investigation was of the recirculating type, having its own reservoir and pump. In addition, provision was made for the addition or release of water from the system to a larger sump within the building. Thus, although each day's operation was normally performed using only the water in the flume system, it was possible at any time to discharge this water into the larger sump where it could be filtered, or to add fresh water from the larger system to make up for evaporation or leakage losses in the flume.

The flume was of aluminum frame construction, having plexiglass walls, a teak tailgate, and a steel headbox, reservoir, and piping. It was pivoted at the headbox outlet, and had a vertical screw adjustment near the tailgate to allow simple adjustment of the slope. The slope was read directly from a graduated scale at this point on the side of the flume.

The inside dimensions of the flume were as follows: width 19.625 inches, depth 29.0 inches, length 16.25 feet. A layout diagram of the flume is shown in fig. 3.1.

The downstream gate was formed of two sets of vertical fingers which could be raised independently, allowing reasonably easy control over the depth of flow, although some warping of the wood caused occasional sticking of the gate.

A one piece aluminum undershot gate was provided at the headbox outlet, but this was not used during the tests.



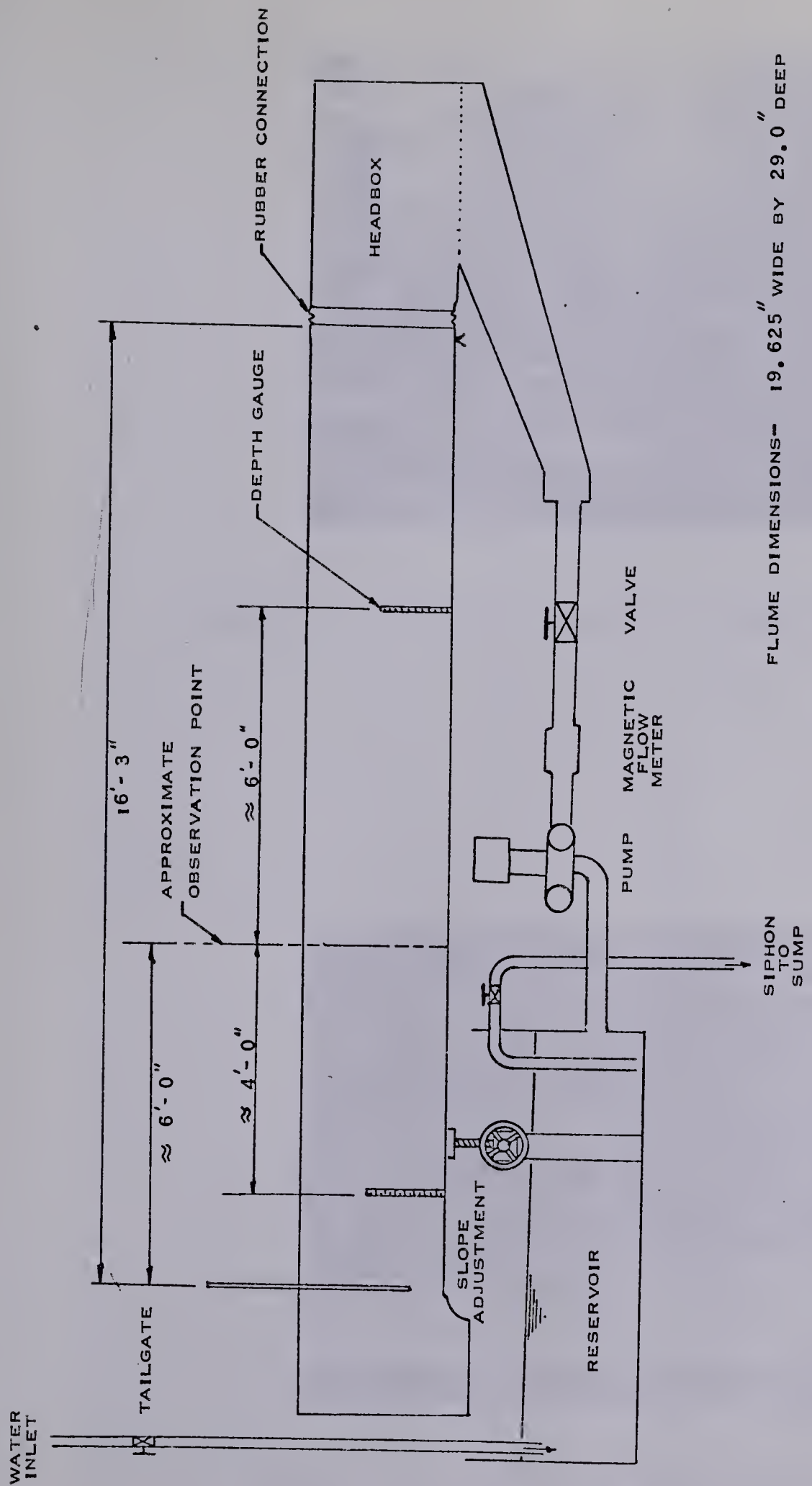


FIG. 3-1 EXPERIMENTAL EQUIPMENT - GENERAL LAYOUT





Plate 3.1 : General Layout of Laboratory Equipment

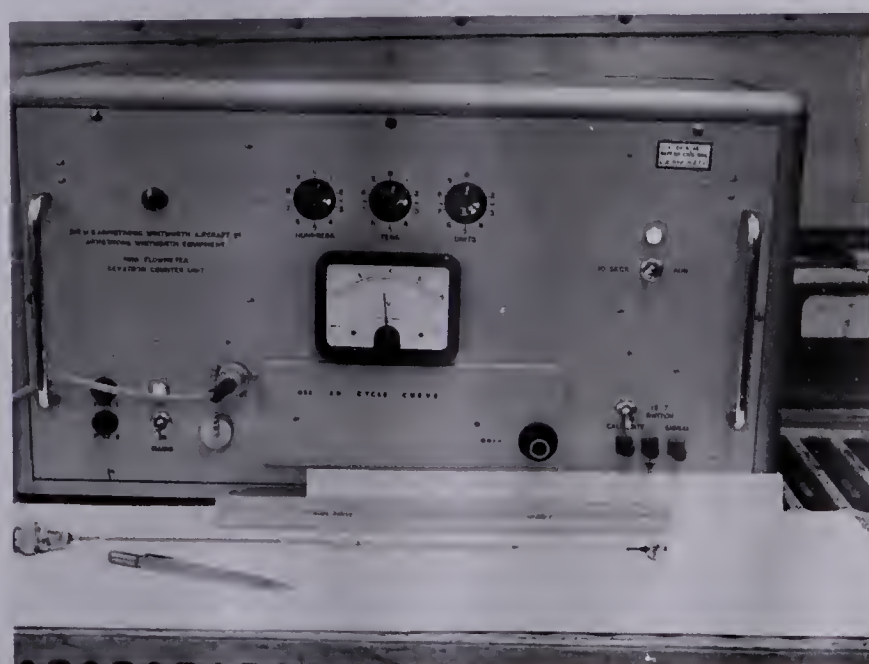


Plate 3.2 : Mini-Flowmeter and Counter Unit





Plate 3.3 : Bed Forms and Flowmeter in Flume



Control of the discharge was accomplished by a valve downstream of the constant speed centrifugal pump.

Expanded metal mesh was installed at the entrance to the headbox to prevent concentration of the flow. In addition, during the test series conducted with the smooth concrete bed forms, about the first four feet of the flume bed were covered with the same material to aid in the quick development of fully developed turbulent flow, and the establishment of a logarithmic velocity profile.

To effect small changes in the tailgate setting it was occasionally found to be better to place similar sheets vertically in front of the tailgate than to tamper with the gate setting. The slight reduction in flow area thus achieved served for minor adjustments in the flow depth.

It was found that after standing idle for a number of days considerable rust sediment collected in the system pipes. This residue was deposited on the plexiglass sides of the flume, and on the velocity measuring probe, and contributed an unpleasant odor. In such a case the flume system was repeatedly flushed with clear water from the main building sump, and the waste water filtered. The build-up of such deposits occasionally necessitated the cleaning of the velocity probe and the flume sides.

The general arrangement of the flume is shown in Plate 3.1.

The discharge was measured by means of a magnetic



flow meter installed just downstream from the pump. This device produced an electrical potential proportional to the discharge, and was attached to a sensitive voltmeter. For each test run the reading of the voltmeter was recorded, and the discharge was read from a calibration curve.

Depth of flow was measured by means of two transparent scales affixed to the sides of the flume. The water surface in the flume could be observed through the scales and the flume sides, and the depth read directly. During the course of the investigation all depths were measured relative to the minimum point of the bed form profile. However, in order to allow a more realistic approximation to natural river conditions the datum for all elevation and depth measurements was later moved to a point midway between the high and low points of the dunes. That is, the average elevation of the bed was adopted as the elevation datum. The tables of observations in Appendix A, and all plots of results are based on this datum.

3.3 The Velocity Meter

The velocity profiles were measured by a Gloster Mini-Flowmeter, and a Dekatron Counter Unit. The flowmeter, or probe, was 1 cm. in diameter, and hence it was possible to obtain velocities relatively accurately at a number of elevations above the bed. Readings were taken at half-inch intervals, generally from an elevation of three quarters of an inch



above datum, to within one quarter of an inch of the surface.

In a number of cases it was found that when the probe was very close to the water surface, say within one inch, the readings obtained were somewhat less than expected. This was due to the fact that the flowmeter was designed to operate under a certain depth of water to ensure proper functioning. When the depth over the probe was less than this specified depth, the propeller occasionally did not register the correct number of revolutions for the incident velocity.

This defect was overcome by plotting each velocity profile taken. In the case of those profiles which showed abnormal curvature near the water surface the top portion of the profile was disregarded, and observed values within that region were not used in subsequent calculations. Those values so neglected are indicated by an asterisk in the data tables in Appendix A.

It was found that unless the water in the flume system was exceptionally clear a coating of rust residue was deposited on the propeller and guard of the probe. In order to avoid any retarding of the meter from this effect, it was necessary to wash the probe in a weak solution of Hydrochloric acid, and to rinse it in distilled water. This was generally done at the end of each day's test run.

In addition, slight trouble was encountered due to the tendency of the probe to collect bits of hair or lint which were present in the water. Any build-up of such material

tended to foul the propeller, and necessitated a tedious cleaning. However, in general, the ease of operation of the flowmeter unit outweighed any disadvantages, and this method proved most satisfactory for velocity measurements.

Some electrical trouble was encountered with the Dekatron Counter unit but, in general, it provided a satisfactory method for controlling the flowmeter.

It was noticed, however, that the length of coaxial cable used to connect the probe to the counter unit had an effect on the number of revolutions registered. In order to minimize this resistance the shortest possible length of cable was used throughout virtually all tests.

The flowmeter and counter unit used are shown in Plate 3.2, and may be seen in operation in Plates 3.1, and 3.3.

A recalibration was performed on the mini-flowmeter after the laboratory tests were completed. The velocities calculated from the original manufacturer's calibration curve were found to vary from six percent low at velocities of one half foot per second, to three percent low at velocities of one and one quarter feet per second.

3.4 The Bed Forms

The bed forms, or dunes, were cast in concrete as shown in fig. 3.2. The height of the individual dunes was held constant at one half an inch, and the wavelength was varied to produce the desired shapes. The dunes were cast either singly, or in multiple units, depending on their size,



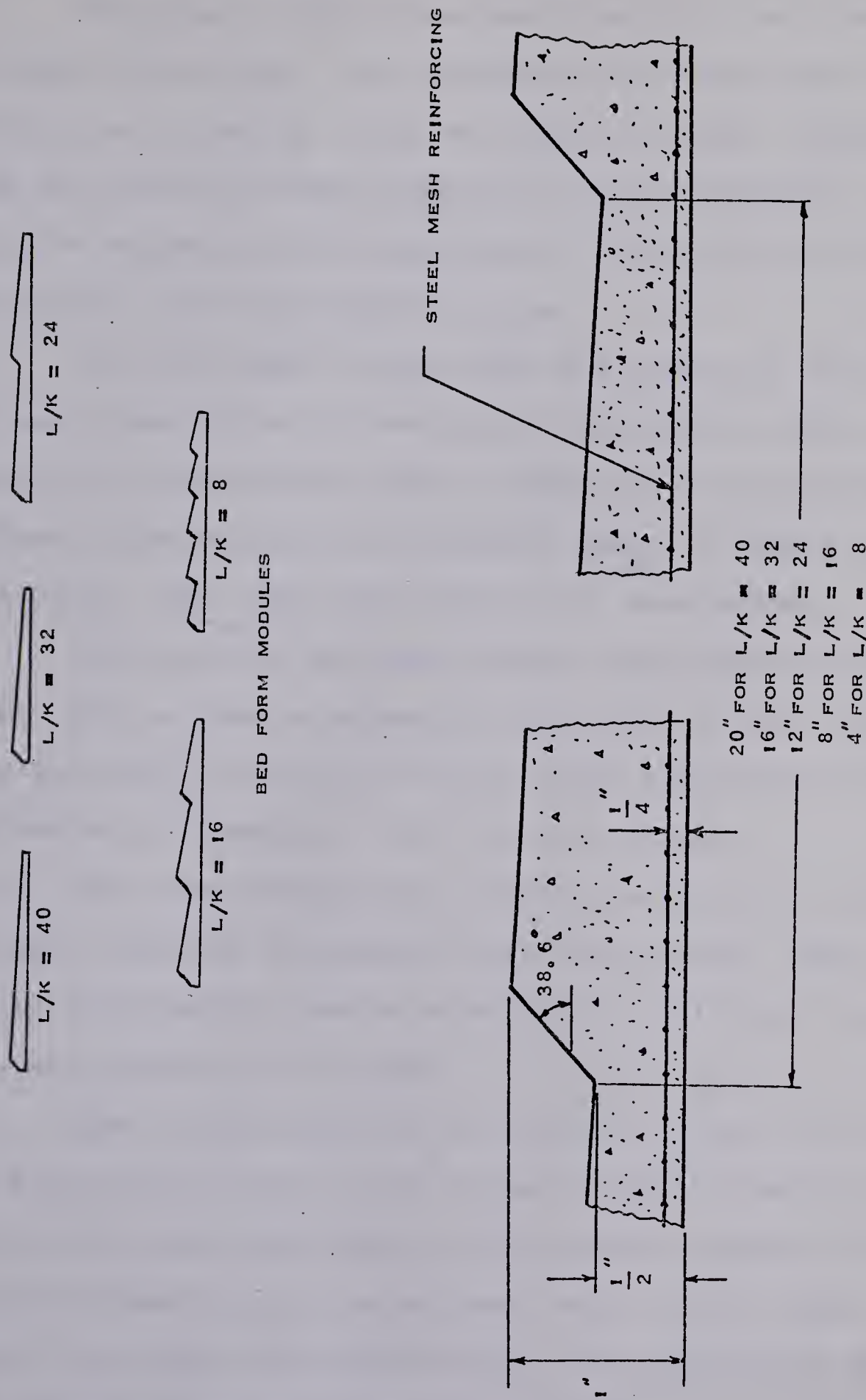


FIG. 3-2 BED FORM PROFILES AND CONSTRUCTION



so as to provide easily handled units.

The shape of the dunes was somewhat idealized to facilitate fabrication. All surfaces on the dune were plane surfaces, not curved as would be found in nature. However, it was felt that for the purpose of the investigation, and within the accuracy of the experiment, little actual error would result from this simplification.

The lee slope of the dunes was chosen as 38.6°. This angle was chosen since it was easy to manufacture when making the forms for the concrete dunes (rise over run equal to 4/5) and since it was close to the natural angle of repose of submerged sand. This angle was used in all dune shapes.

The width of the dune modules was chosen as 19.5 inches. This allowed a reasonably tight fit in the flume, having only 1/16 of an inch on each side, but allowed easy installation and removal of the bed form blocks.

The dune modules were simply placed on the floor of the flume, and held in place by their own weight. This proved entirely satisfactory, and no movement or shifting of the blocks was observed at any time.

The actual length of the portion of the flume bed covered by the bed form blocks varied slightly from one test series to the next, depending on the integral number of blocks which most closely approximated the length of the flume. However, in no case was the covered portion less than the 16'-3" distance from entrance gate to tailgate. Any excess



block length was allowed to project into the headbox.

After the first test series using the smooth concrete dunes, each set of bed forms was coated with sand, and the test runs were repeated. The sand used was white Ottawa sand having an average diameter of 0.0282 inches, or 0.716 mm. A description of a grain size analysis performed on this material is contained in Appendix A.

The procedure followed in coating the dunes with sand was as follows: The dunes were first given a light coat of varnish, and allowed to dry. Each module was then heavily coated with varnish and was buried in a box filled with the Ottawa sand. The varnish was allowed to set, for twenty minutes, then the bedform block was carefully unearthed, and allowed to dry overnight. All excess sand was then brushed off, and any bare spots were patched with a light coat of varnish and sprinkled sand. At the same time, any lumps on the surface were smoothed out as well as possible. When all the blocks were dry and evenly coated that set was deemed ready for its repeat test series.

The final appearance of the blocks after coating was of a rough, but generally uniform, layer of sand usually two to three grains thick. The contours of the original bed forms were closely followed, and there was no noticeable tendency for the sand to be thicker in the low points of the bed profile. That the varnish was reasonably waterproof is shown by the fact that very little sand was observed to wash



off the dunes. The sprinkling that was found in the flume reservoir at the end of the investigation was most likely loose sand that had not been brushed off the blocks before testing, or sand knocked loose during installation or removal of the dune modules from the flume.

3.5 The Experimental Procedure

The test procedure for all runs was as follows: The chosen bed form blocks were set into the flume, and the depth scales zeroed on the low points of the bed form profile. A desired depth of flow was then chosen, and the discharge, tailgate setting, and the slope of the flume were adjusted until uniform flow was achieved at the desired depth. The discharge and slope for that run were then noted. Using the mini-flowmeter probe a velocity profile was then taken at the centre line of the flume at three different sections along a dune. (See fig. 3.3.)

In order to obtain velocity profiles observations were taken at increments of one half inch above the observation datum. At each point an average was taken from five ten-second counts of the probe revolutions. Thus, in effect, each value was the mean over fifty seconds of the velocity at that point.

This procedure was repeated for depth increments of one quarter inch, from two and one half inches to five inches above the observation datum.

By using the observations recorded the required results were then determined by calculation.



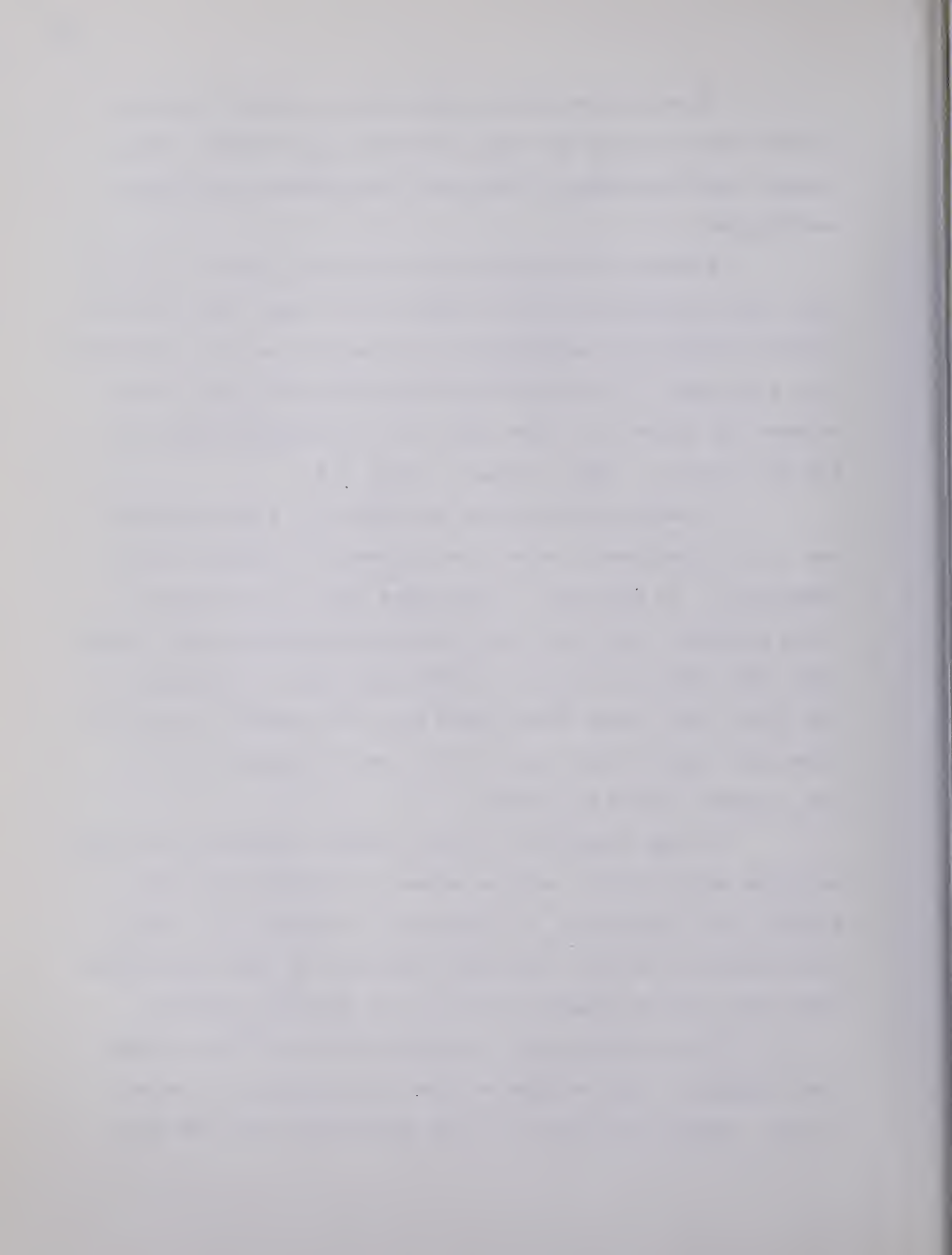
It should be noted, again, that a change was made at this point between the datum used for experimental observations, and the datum to which all calculations and graphs are related.

For ease of operation the elevation datum during all test runs was taken as the low point of the dune shape profile. However, during the calculations one quarter inch was subtracted from all depths of flow and elevations above the bed, so as to move the datum to a level equal to the average height of the bed profile. This is shown in fig. 3.3.

It was felt that this new datum was a more natural one if the experiments were to be compared to natural field conditions. In addition, if the tests were to be repeated using a mobile sand bed, then this new calculation datum would equal the original elevation of the plane bed at the start of the test, after which dunes would form, the amount of material above this datum being equal to the amount required to fill the "valleys" below the datum.

In the calculation of the results, first all velocity profiles were plotted, and low values of velocity near the surface were eliminated, as explained in section 3.3. Then, using equation (2.13), individual values of k_s were calculated from each velocity reading taken in the velocity profiles.

In performing this calculation it was first assumed that $(v_* k_s / \nu)$ would be greater than 70, yielding a B value of 8.5. Using this value of B the calculation was then per-



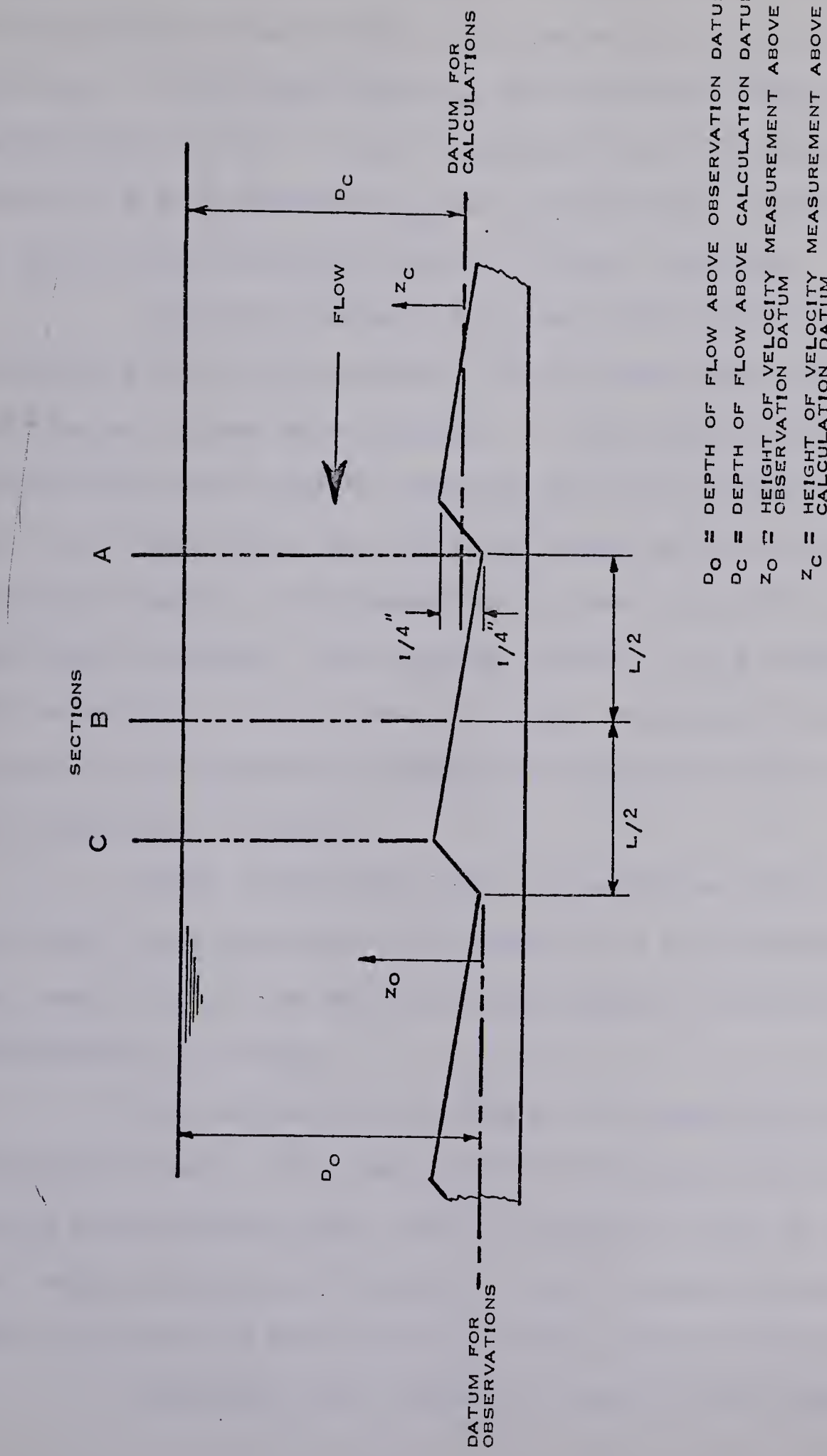


FIG. 3-3 LAYOUT OF EXPERIMENTAL OBSERVATIONS



formed, and the value of $(v_* k_s / \nu)$ was checked. If, in fact, it was greater than 70 the calculation was allowed to stand. However, if the check value of this term was less than 70, meaning that B had a value different from 8.5, then the new value of B was found and k_s was recalculated. This new value of k_s was then accepted without further checking.

After all values of k_s were found for a particular velocity profile (or section) the results were inspected and extraneous values were rejected. Often such values were those calculated from velocity readings near the surface, or near the bed, where there was room for doubt in the accuracy of the observed reading. The remaining values of k_s for that profile were then averaged. The average values of all three sections for each depth of flow were, in turn, averaged to yield a final value of the equivalent sandgrain roughness of the bed form for that depth of flow.

After completing these calculations for all depths of flow, the results were converted to a non-dimensional form and used to plot the desired characteristic curves for that particular dune shape.

The calculation of Chezy's C values was somewhat more straight forward. For each depth of uniform flow the recorded slope and discharge were used in equation (2.2) to calculate the required value of Chezy's C . No iterative procedure was used. This was done for each depth of flow, and each dune shape.

Similarly, the values of C were then converted to



non-dimensional form, and used to plot the required curves for that dune shape.

The observations recorded during all tests are presented in Appendix A. These readings have been adjusted for the change in elevation datum, and are all with reference to the new calculation datum.

Note that the readings recorded on the laboratory data sheets, and the I.B.M. punched data cards, on file in the Department of Civil Engineering, are not adjusted, and are with relation to the observation datum. The detailed calculation sheets for each velocity profile produced by the computer also on file, are adjusted to the new datum, however, and all readings appearing therein are with reference to the calculation datum.

The readings shown in Appendix A are all identified as to test run by showing the dune shape to which they belong. Those readings taken from tests run on sand coated dunes are identified by an R after the dune shape in the table heading. (For example: $L/k = 16$ indicates tests done on the smooth dune shape having a length to height ratio equal to 16. But $L/k = 16R$ indicates tests done on the same dunes after extra roughness in the form of a sand coating had been added.)

CHAPTER IV

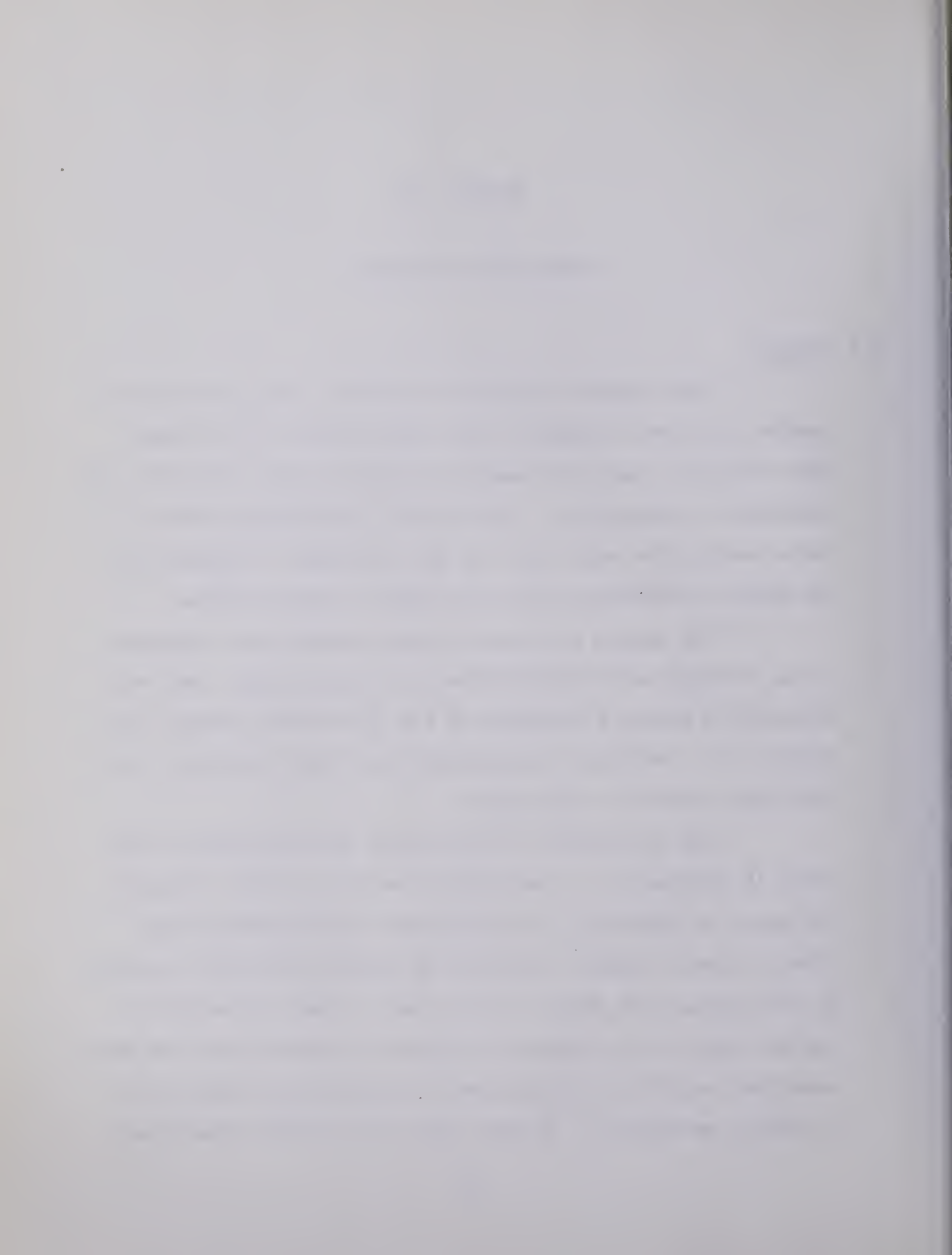
EXPERIMENTAL RESULTS

4.1 General

This chapter contains a summary of the experimental results obtained throughout the investigation. The actual data collected, and the results calculated from that data, are tabulated in Appendix A. In addition, individual plots of these results for each test run are contained in Appendix B. The actual calculated points are shown on these graphs.

The graphs contained in this chapter are composite plots, showing all related tests on a single sheet, and were obtained by merely superimposing the appropriate sheets from Appendix B. Individual calculated points are not shown, only the final curves are reproduced.

The calculation of all points was performed as outlined in section 3.5. The graphs contained in this chapter, and those in Appendix B, were plotted from non-dimensional forms of these results, obtained by simple arithmetic division by the appropriate factor in each case. These calculations are not shown here, however the manner of conversion from the tabulated results to the plotted non-dimensional values may be easily recognized. In most cases the plotted values may



be found simply by inspection of the calculated results in Appendix A. In the case of the k_s values, however, each plotted point is the result of averaging all calculated values, except the disregarded ones, for a given depth.

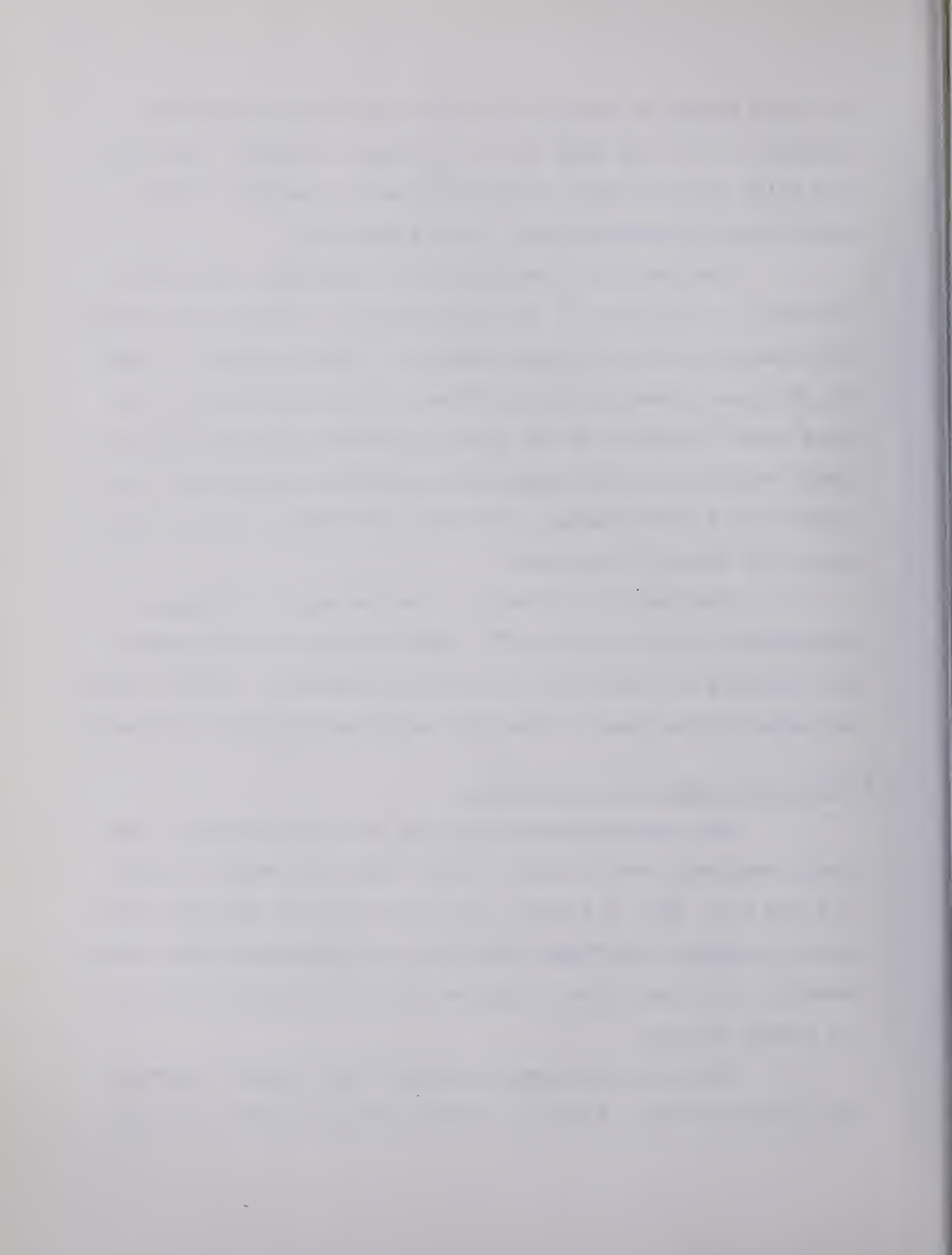
The method of presentation in general follows that outlined in section 2.4. The calculated k_s values were rendered non-dimensional by dividing them by k , the dune height. Thus, (k_s/k) gives a measure of the effective roughness due to the dune shape, compared to the actual physical height of the dune. These values are plotted against a non-dimensional depth, d/k , found in a similar manner, which may be thought of as an indication of relative roughness.

Similarly, the Chezy's C values were rendered non-dimensional by dividing by \sqrt{g} . Again, this may be thought of as a measure of resistance to flow, or roughness. These values are also plotted against the d/k , relative roughness, parameter.

4.2 Equivalent Sand Grain Roughness

The non-dimensional results for the equivalent sand grain roughness versus depth of flow have been shown in figs. 4.1 and 4.2. Fig. 4.1 deals with those results obtained using smooth concrete bed forms, while fig. 4.2 presents those results obtained after additional roughness had been added in the form of a sand coating.

Each of these graphs contains five plots, covering all the dune shapes tested. The dune shape for each curve is



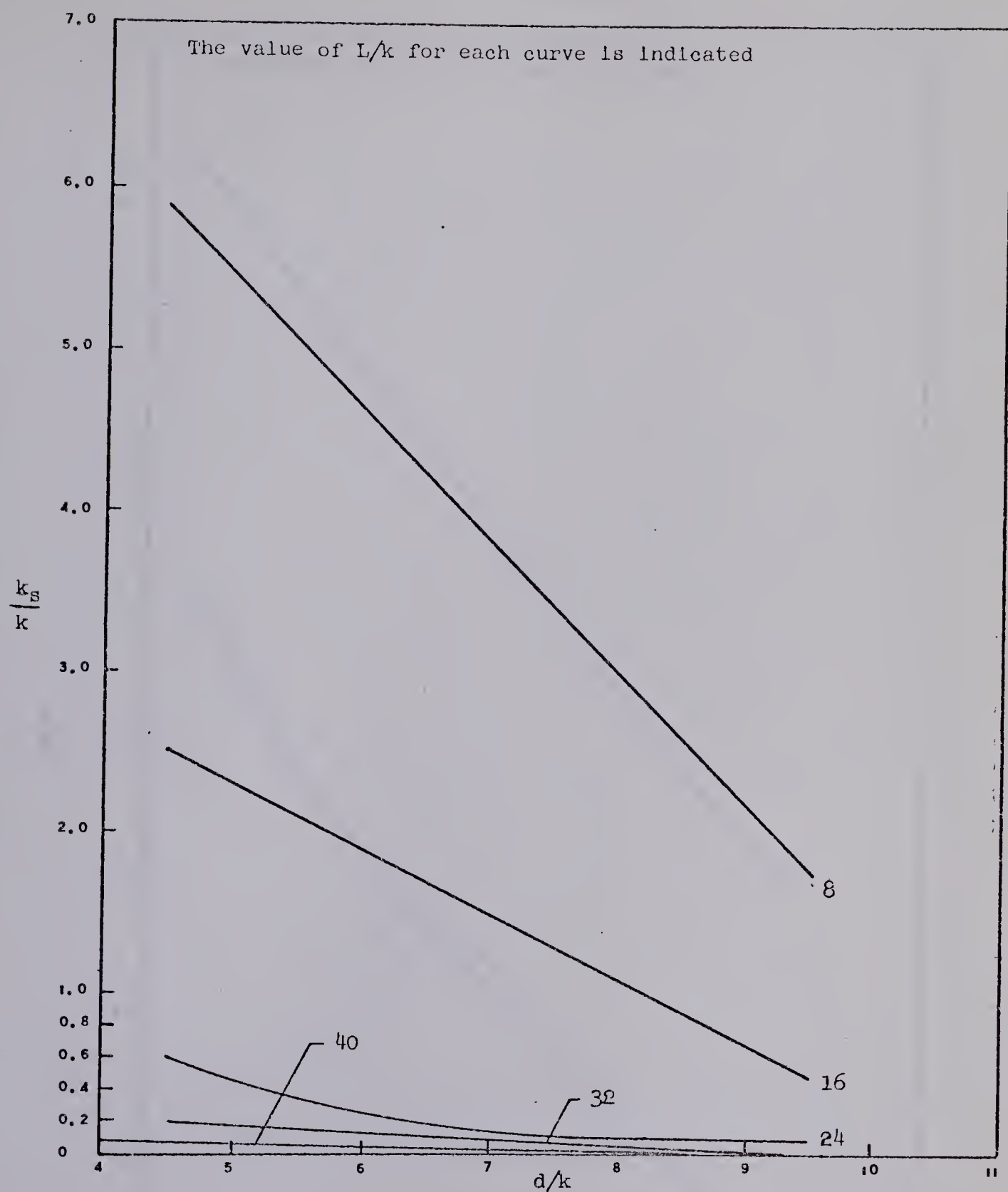


FIG. 4-1 VARIATION IN ROUGHNESS WITH FLOW DEPTH FOR SMOOTH DUNES



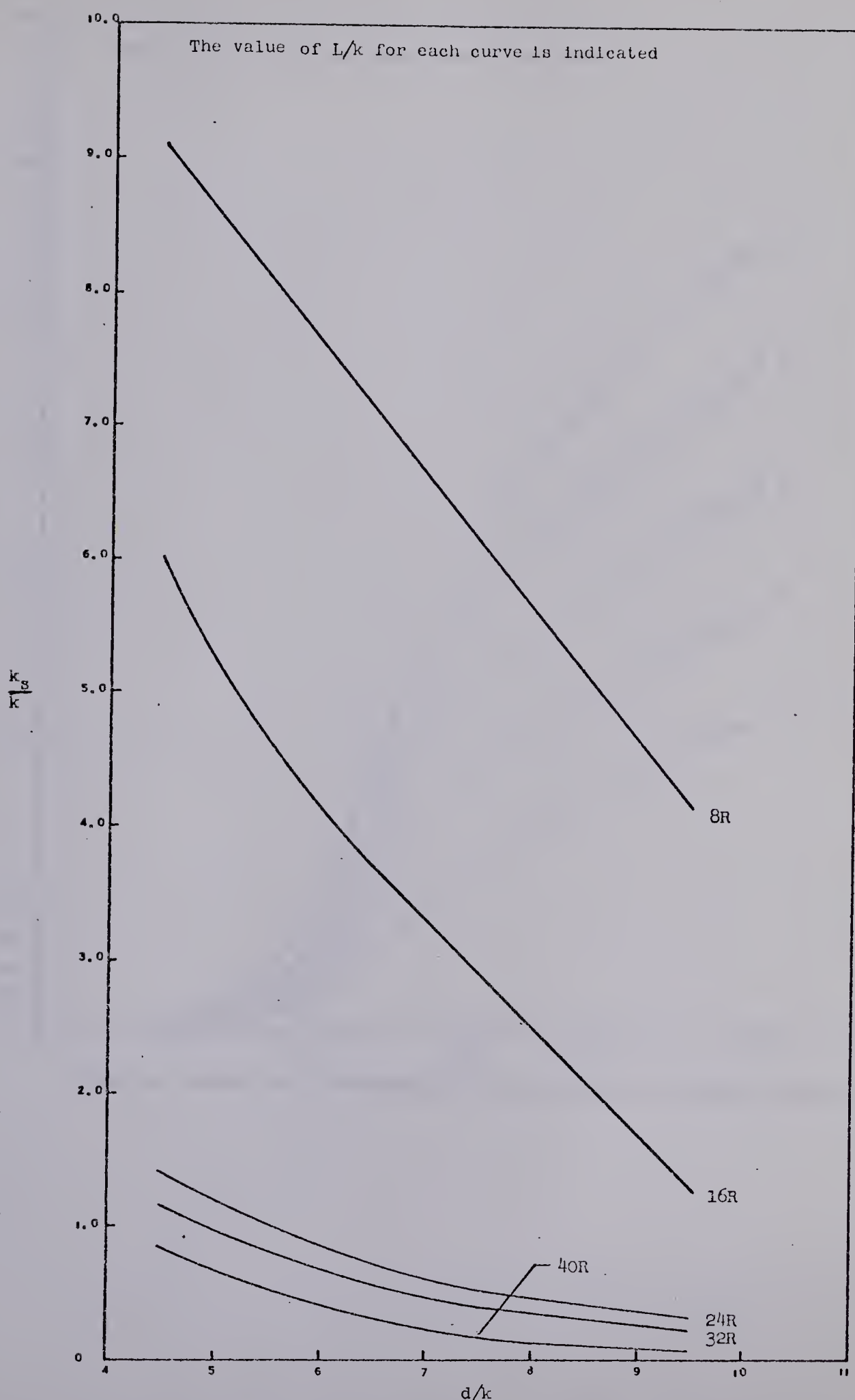
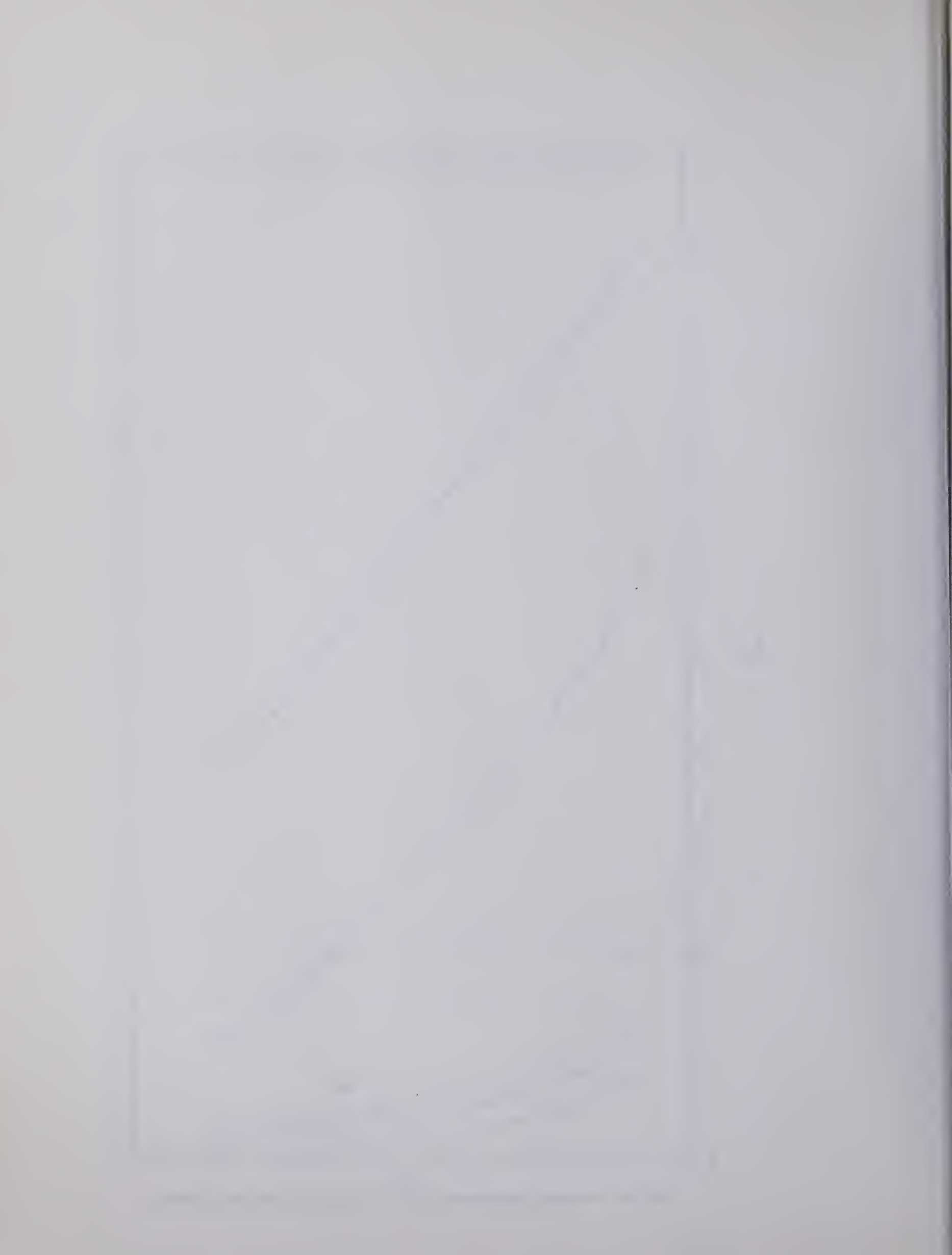


FIG. 4-2 VARIATION IN ROUGHNESS WITH FLOW DEPTH FOR ROUGH DUNES



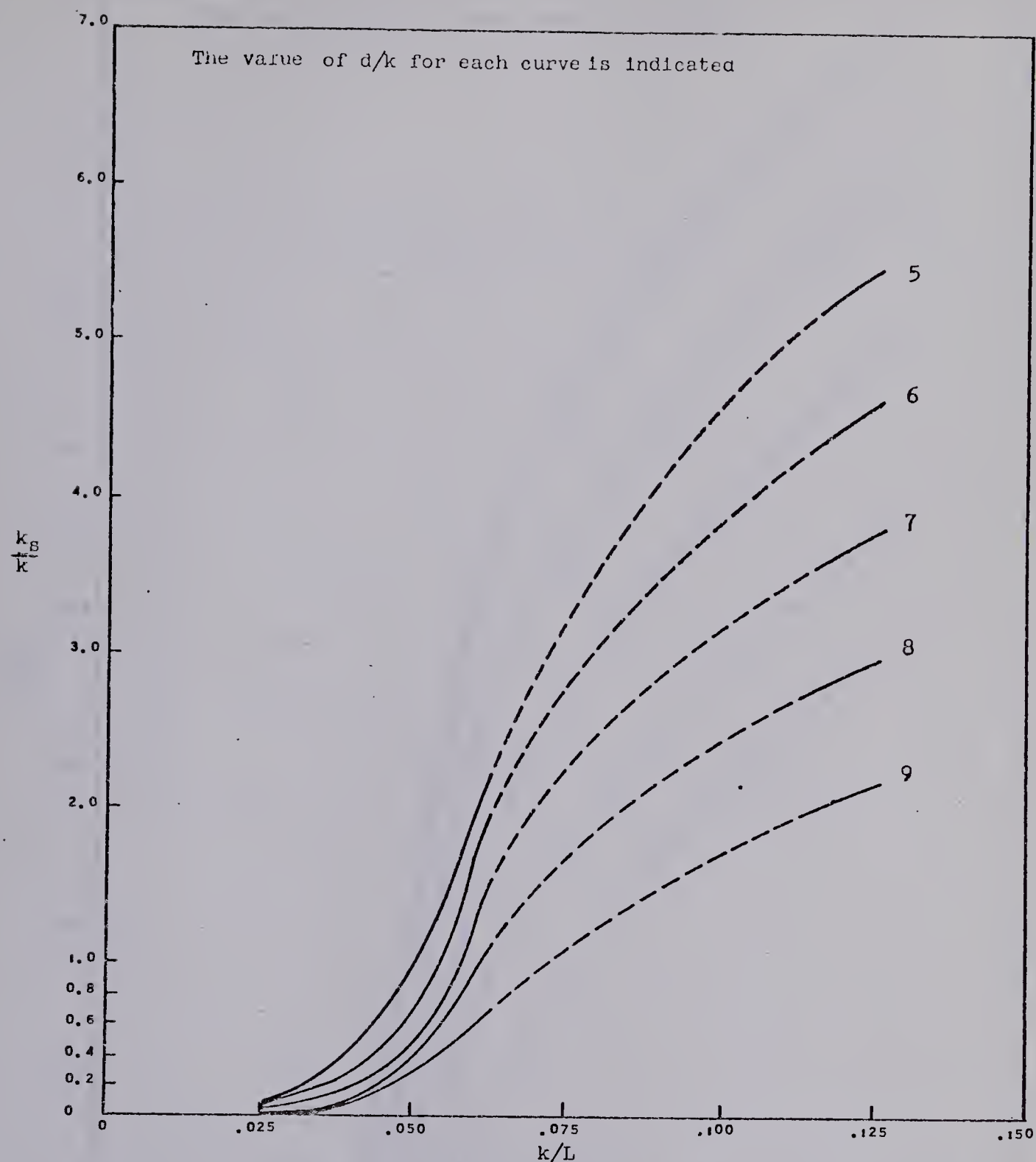


FIG. 4-3 VARIATION IN ROUGHNESS WITH DUNE SHAPE FOR SMOOTH DUNES



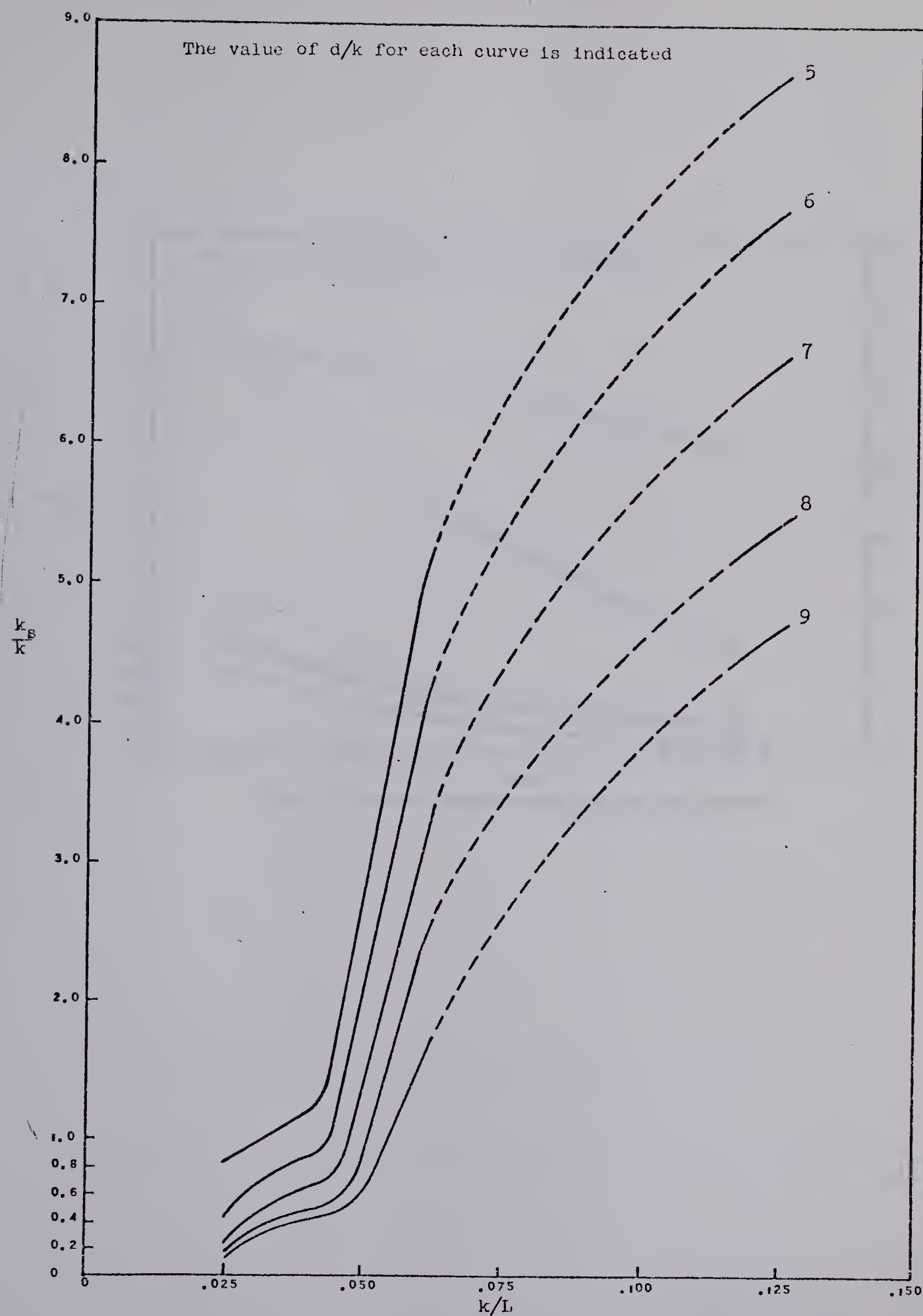


FIG. 4-4 VARIATION IN ROUGHNESS WITH DUNE SHAPE FOR ROUGH DUNES

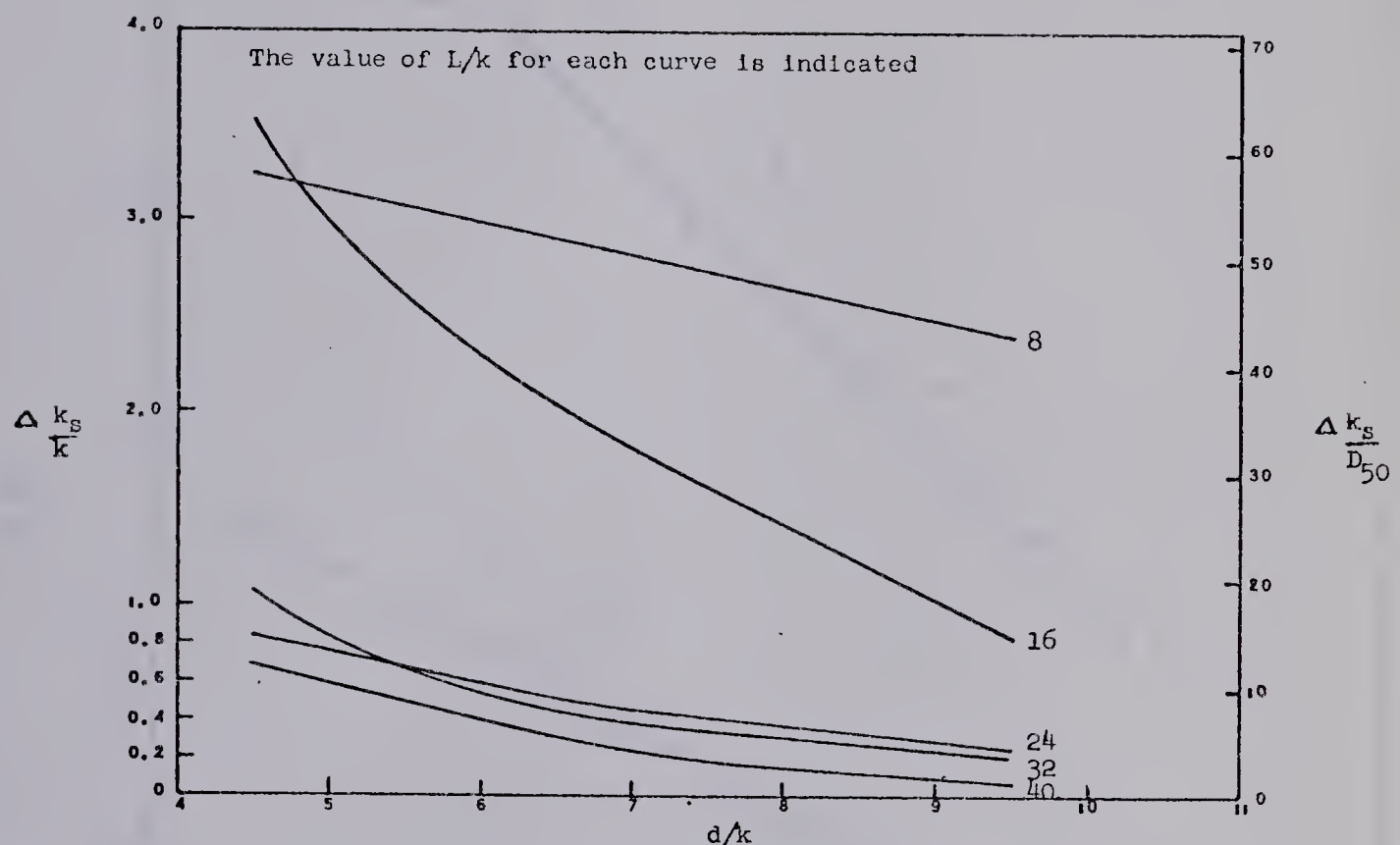


FIG. 4-5 CHANGE IN ROUGHNESS DUE TO SAND GRAINS

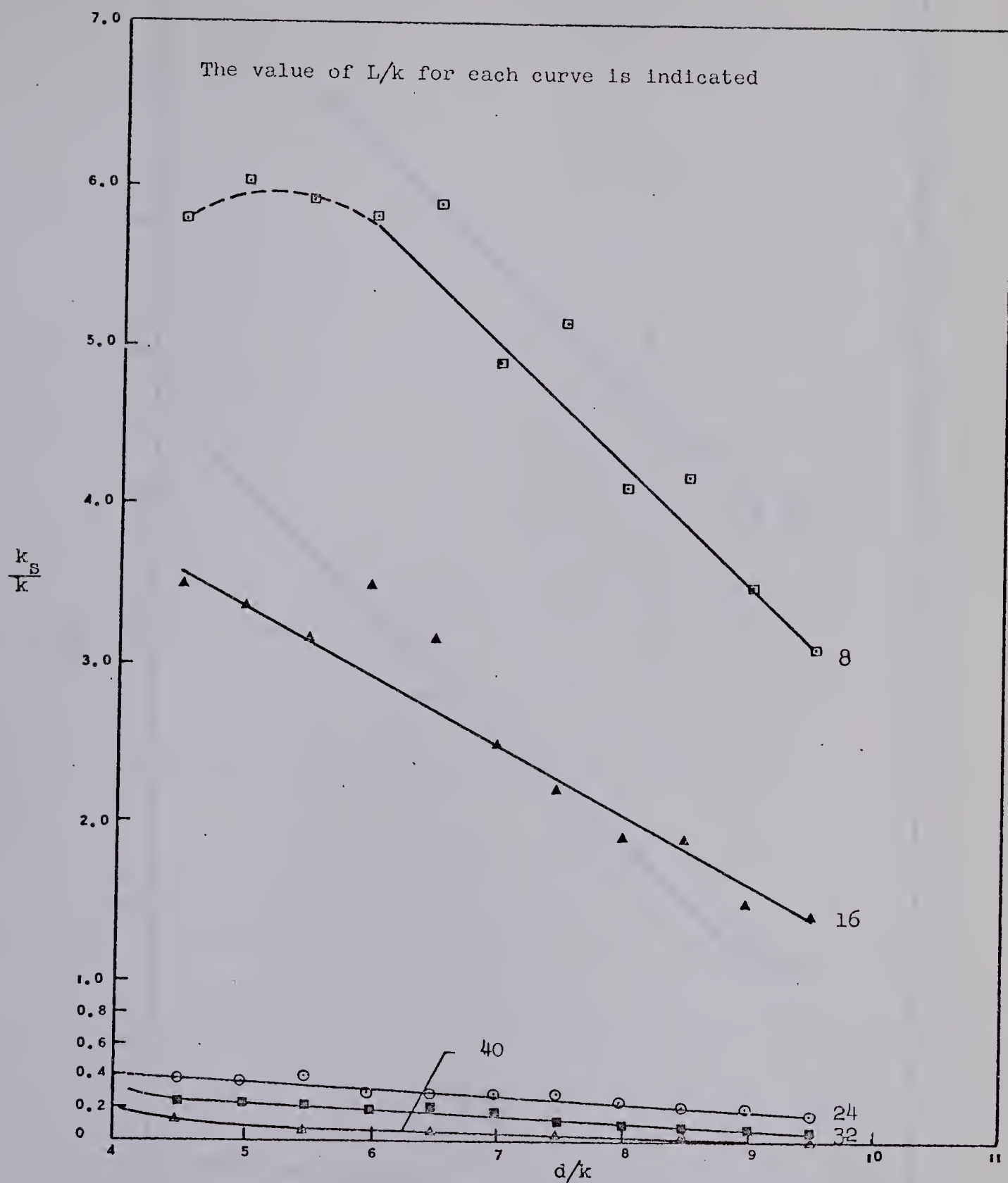


FIG. 4-6 VARIATION OF ROUGHNESS WITH FLOW DEPTH FOR SMOOTH DUNES
[BASED ON MEAN VELOCITY]

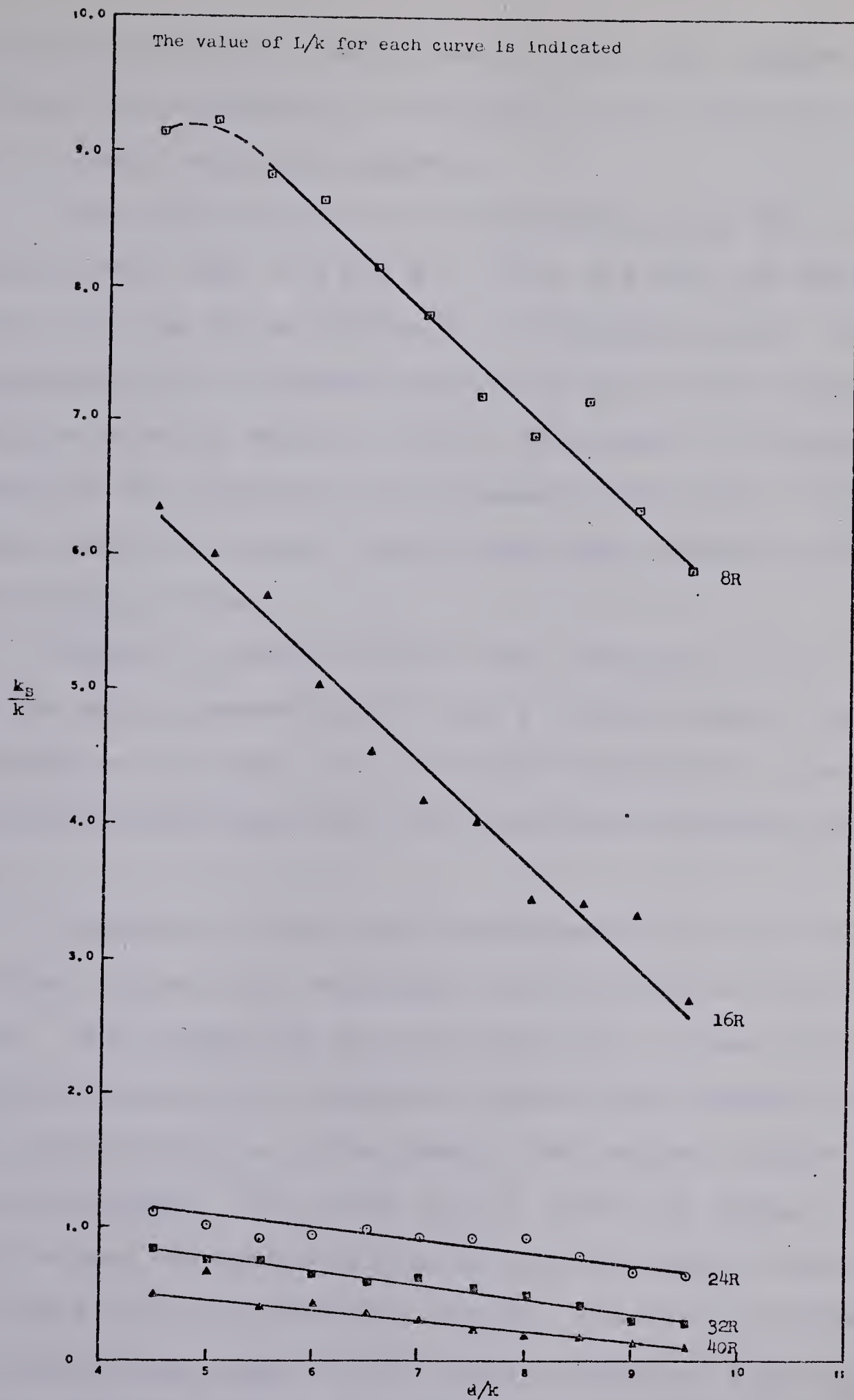


FIG. 4-7 VARIATION OF ROUGHNESS WITH FLOW DEPTH FOR ROUGH DUNES
[BASED ON MEAN VELOCITY]

indicated on the graph. The purpose of both these figures is to indicate the dependence of roughness on flow depth, and, in fact, marked trends are apparent.

The same data used in the foregoing plots are reconstructed to form figs. 4.3 and 4.4. Fig. 4.3 uses the data from fig. 4.1, but it is plotted in a different manner. Here the roughness k_s/k is plotted against the dune shape ratio, for various relative depths of flow. This graph is intended to point out the dependence of roughness on the shape of the bed forms which are present, while also taking account of the relative depth of flow.

Figure 4.3 deals with the data obtained in the tests run on the smooth concrete dunes. In a similar manner, fig. 4.4 was derived from fig. 4.2, and shows the results of tests run on the same bed forms after the additional roughness was added.

The effect on the total equivalent sand grain roughness of the addition of a coating of uniform sand is shown in fig. 4.5. This figure was derived from figs. 4.1 and 4.3, and presents the increase in roughness caused by the change in the surface characteristics of the dunes. Two ordinate scales are shown on this graph. The first, $\Delta k_s/k$, shows the change in the k_s/k values associated with each relative depth. Plots are included for each dune shape tested. The second ordinate scale converts the change in k_s/k into a multiple of the D_{50} size of the grains used in the sand coating. That is, it

demonstrates the effective size of the added sand grains compared with their actual size.

Figures 4.6 and 4.7 are of the same type as figs. 4.1 and 4.2, however, they were arrived at in a somewhat different way.

Figures 4.1 and 4.2 were plotted from values calculated, as was previously mentioned, from equation (2.13). Thus they represent values of roughness derived from individual readings of velocity at given elevations in the flow. However, figs. 4.6 and 4.7 were derived from calculations based on equation (2.14), that is, on the observed mean velocity of the entire flow.

The plots of figs. 4.6 and 4.7 do not coincide exactly with their counterparts in figs. 4.1 and 4.2. This should be expected due to their different methods of calculation, and is easily explainable. However, a similar relationship between roughness and relative depth is apparent. Again, plots are shown for each dune shape tested.

The individual plots for these dune shapes are not included in Appendix B, since they were shown only for purposes of comparison. Hence the original points calculated are shown on these graphs.

Thus the relationship between the non-dimensional equivalent sand grain roughness, and the relative depth of flow, and the dune shape, is summarized in a variety of forms in figs. 4.1 through 4.7.

4.3 Chezy's Roughness Coefficient

The non-dimensional values of Chezy's C were treated in exactly the same manner as the values for the equivalent sand grain roughness.

Figures 4.8 and 4.9 deal with the results for the smooth dunes, and the roughened dunes respectively. The non-dimensional C/\sqrt{g} term is a measure of the roughness, or of the resistance to flow. It is shown here plotted against the non-dimensional depth, d/k , which could be called a relative depth, or a measure of the relative roughness of the boundary. These plots demonstrate the dependence of the resistance of the bed forms on the depth of the flow in the channel. Similar marked trends may be seen in figures 4.8 and 4.9. In each figure curves are shown for all dune shapes tested. The individual calculated points are not shown since these graphs are meant only as a summary of results. Individual graphs for each dune shape, with the calculated points shown, may be found in Appendix B.

The curves shown in these graphs were assumed to be straight lines, and are best-fit lines obtained by using a least-squares curve fitting technique.

Figures 4.10 and 4.11, dealing with results from the smooth and roughened dunes respectively, show the dependence of the resistance to flow on the dune shape, for various depths of flow. These figures were derived from figures 4.8 and 4.9, and show the data plotted in a different manner.

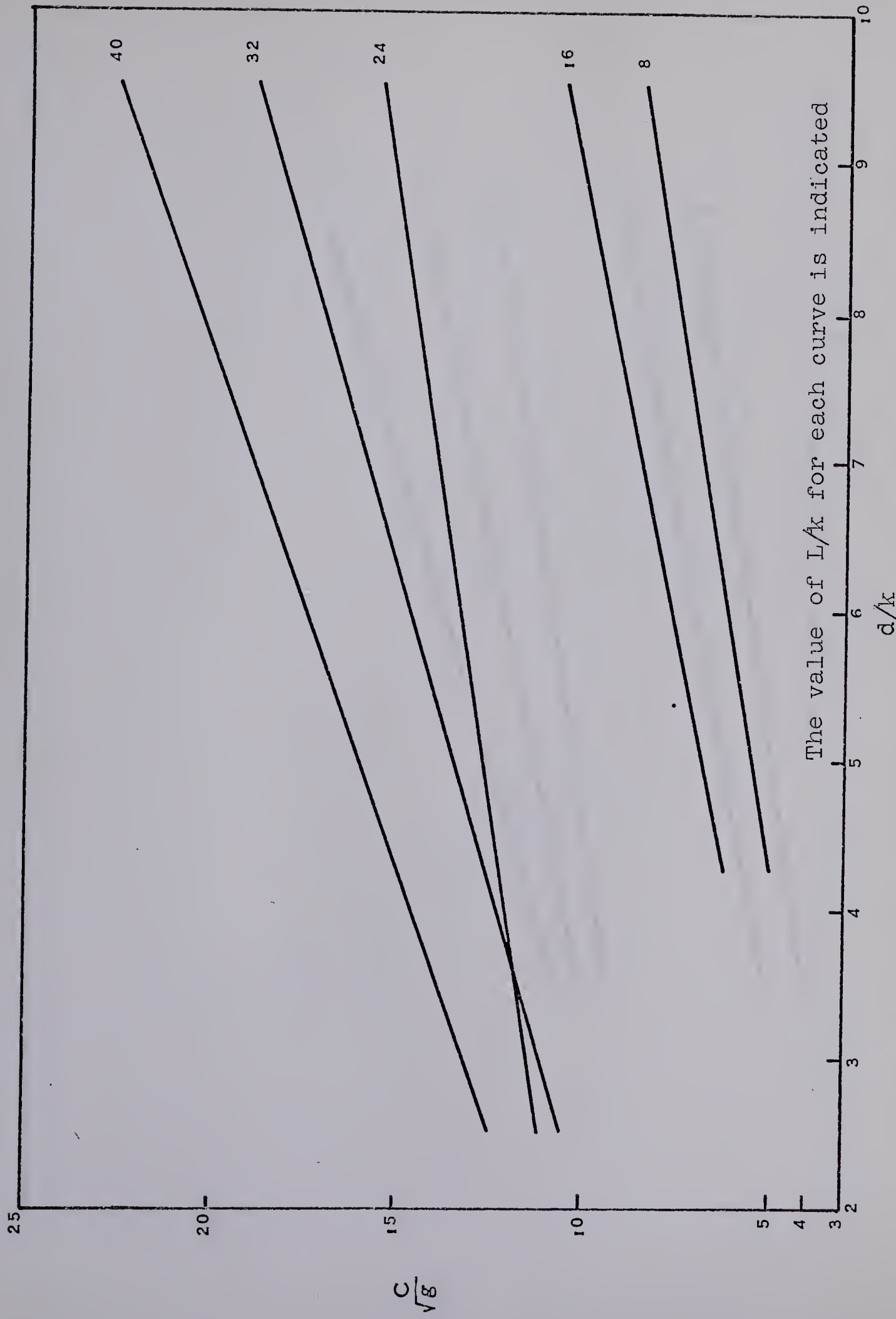


FIG. 4-8 VARIATION OF ROUGHNESS WITH FLOW DEPTH FOR SMOOTH DUNES

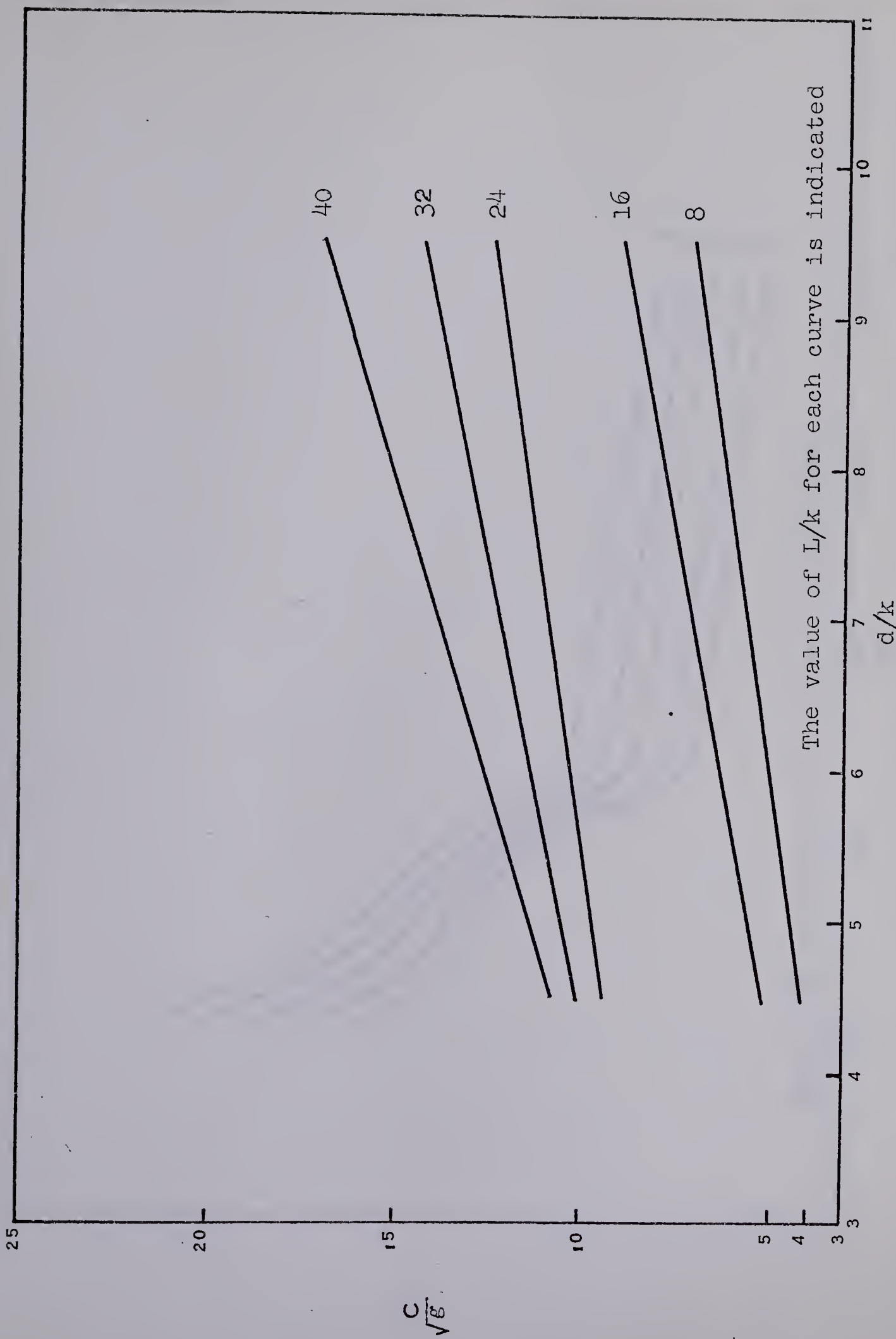


FIG. 4-9 VARIATION OF ROUGHNESS WITH FLOW DEPTH FOR ROUGH DUNES

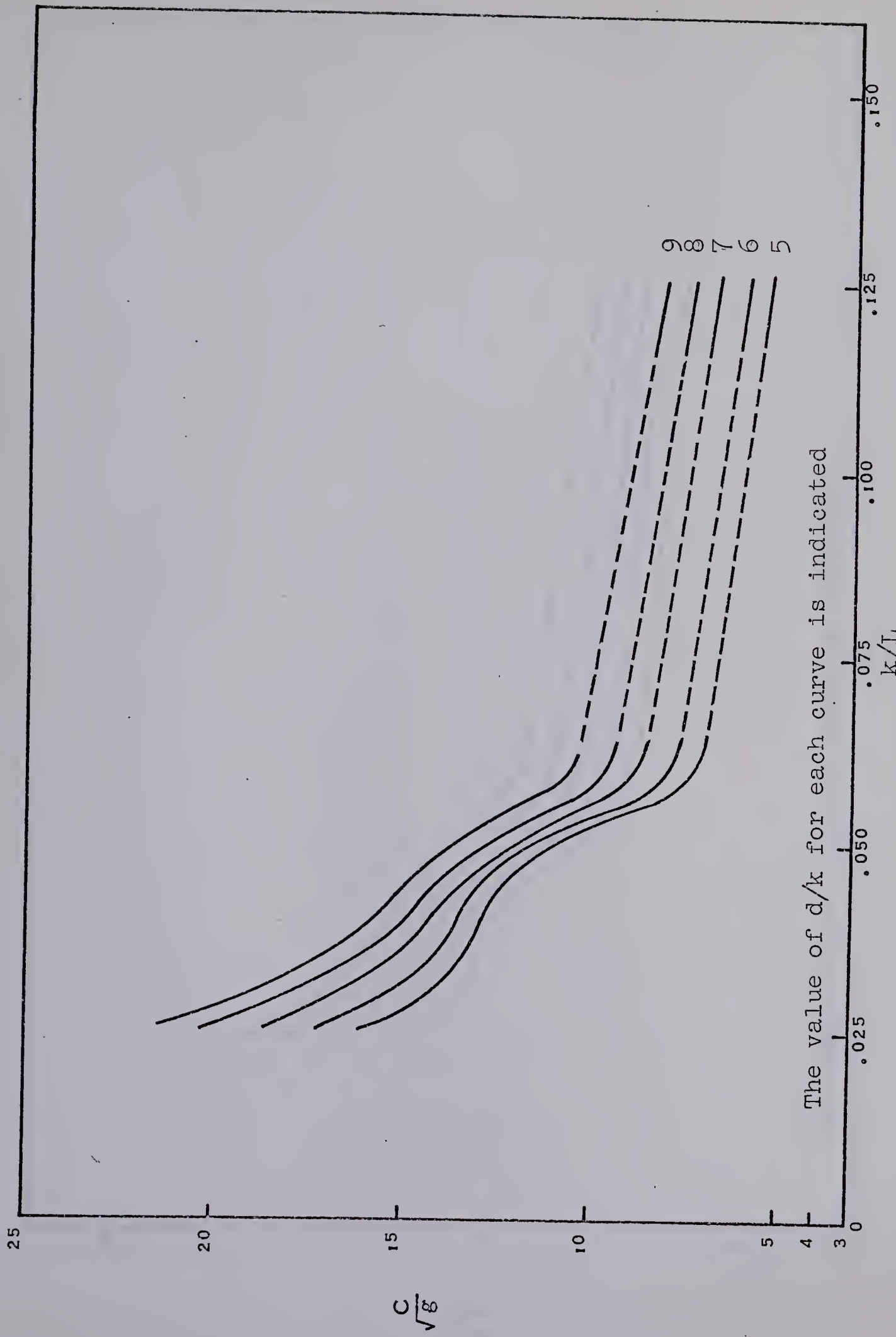


FIG. 4-10 VARIATION OF ROUGHNESS WITH DUNE SHAPE FOR SMOOTH DUNES

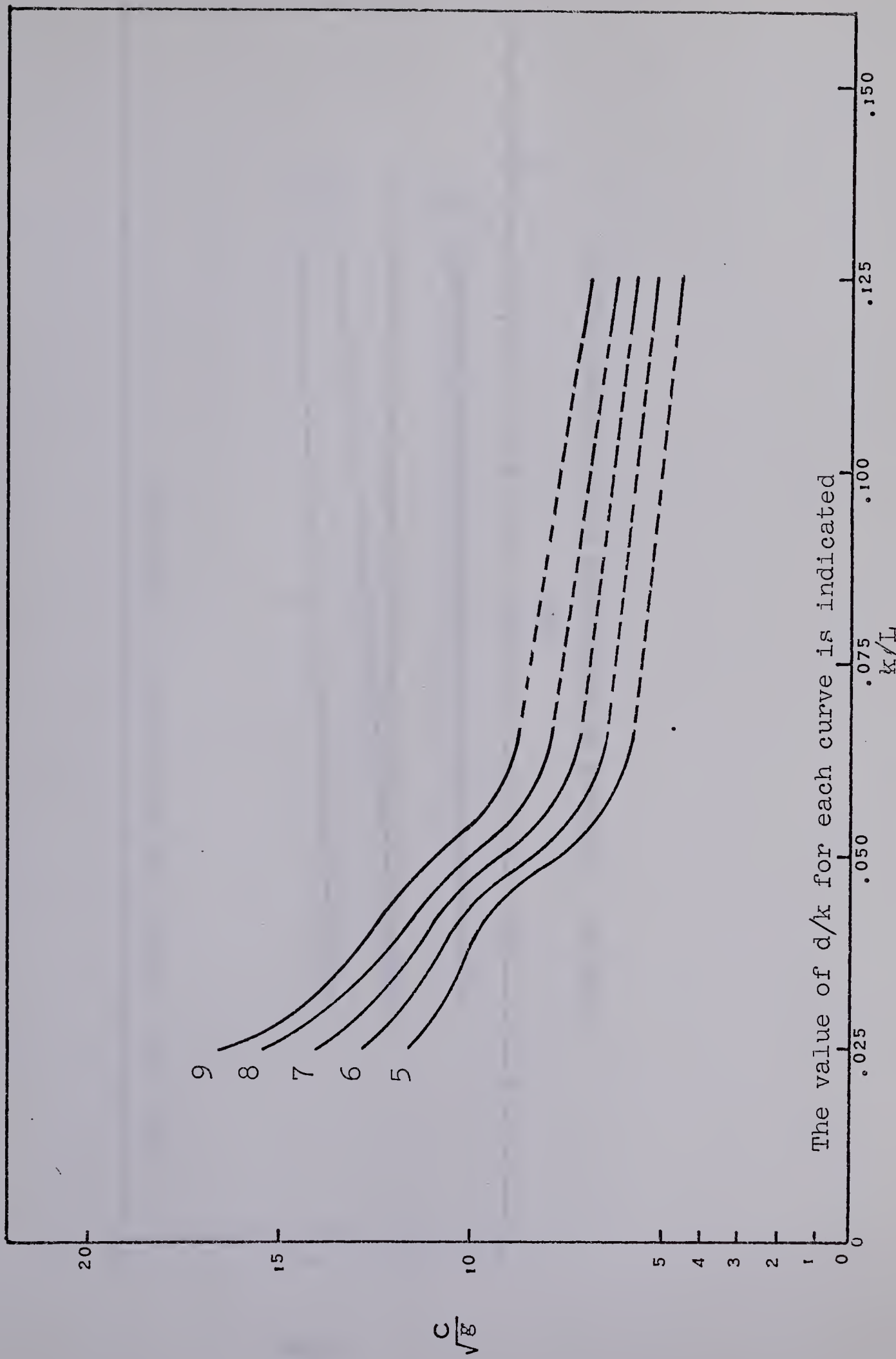


FIG. 4-II VARIATION OF ROUGHNESS WITH DUNE SHAPE FOR ROUGH DUNES

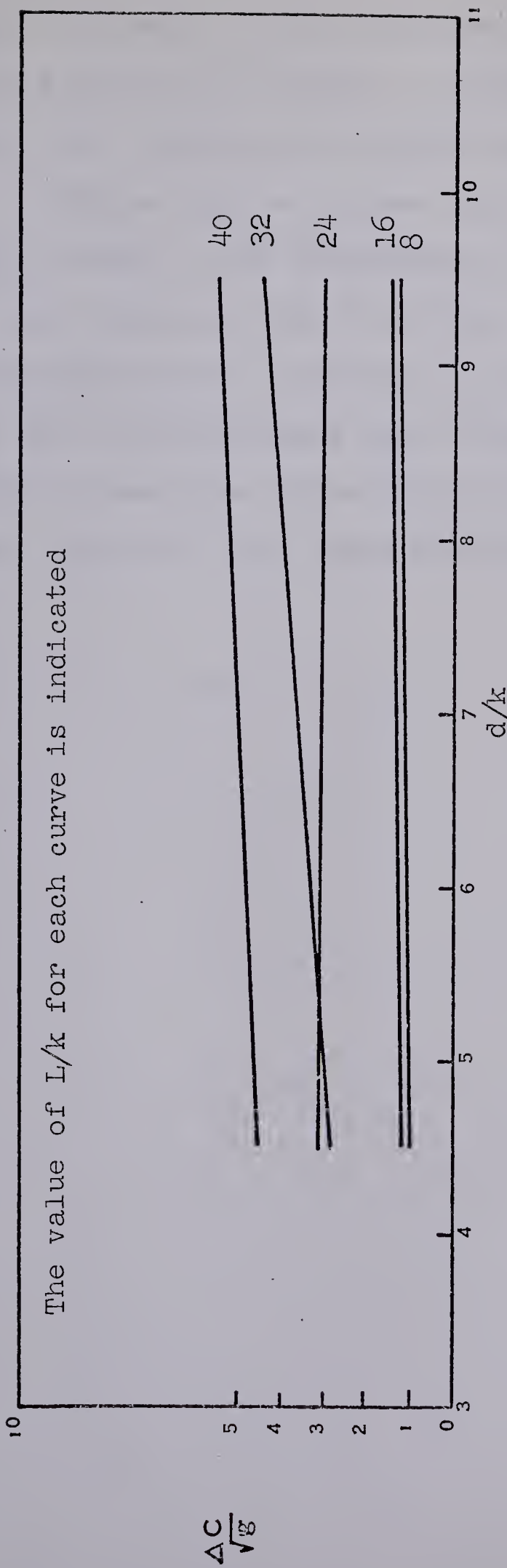


FIG. 4-12 CHANGE IN ROUGHNESS DUE TO SAND GRAINS

In figs. 4.10 and 4.11 the non-dimensional roughness, C/\sqrt{g} , is plotted against the height to length ratio of the dune profiles, k/L . Curves for various relative depths are included.

Figure 4.12 is derived from figs. 4.8 and 4.9, and shows the change in the resistance to flow due to the addition of the sand coating on the bed forms. Here $\Delta C/\sqrt{g}$, the change in the non-dimensional resistance coefficient C/\sqrt{g} , is plotted against the non-dimensional depth parameter d/k . Plots are included for each dune shape tested, and the appropriate length to height ratio for each curve is indicated on the graph.

CHAPTER V

DISCUSSION OF RESULTS

5.1 General

This chapter contains a general discussion of the experimental results which were reported in Chapter IV. The form of the resultant graphs is discussed, and possible sources of error are mentioned.

5.2 Equivalent Sand Grain Roughness

Observation of figs. 4.1 and 4.2 shows a definite relationship between roughness and flow depth. It is seen that an increase in the depth of flow reduces the resistance due to the bed forms. That is, a smaller relative roughness produces less resistance to flow, which is what would be expected.

It is also apparent that a much greater change is effected in the case of bed forms having shorter wavelengths. However, if the numerical values are considered, it will be noted that the percentage change in the resistance to flow between, for example, relative depths of 4.5 and 9.5, though not equal, are roughly of the same order.

It would appear that the resistance of the dunes

with shape ratios of 16 and 8 is very much greater than that of any of the smoother shapes. The reason for this is not immediately apparent. It may be that a change in the flow pattern over the bed forms takes place between the curves of the dunes having shape ratios of 16 and 24, leading to larger eddies and resulting in greater energy dissipation.

Examination of figs. B1 to B10 in Appendix B will show that the scatter of points from which these curves are drawn, though present, is not by any means exceptional. It is felt that within the accuracy of the experimental tests, and for the original purpose of the study, the accuracy of the curves is satisfactory. The general trends of the results are shown clearly.

It will be seen in figs. B1, B6, B8, and B9 that the point or points at the shallow end of the curves drop sharply from the trend indicated by the remainder of the points. This is assumed to be due not to a sudden change in flow conditions, but to the fact that all k_s values were calculated based on the assumption of a logarithmic velocity profile. It is assumed that at these small depths of flow the eddies caused by the flow pattern over the bed forms may disrupt this ideal velocity profile. Yalin (14) suggests that the logarithmic velocity profile may not be valid for d/k values of less than 6 or 7. Thus, these values were assumed to be in error, and were not used in drawing the final curves.

Figure 4.5, showing the change in roughness caused

by the addition of the sand coating to the bed forms is, unfortunately, rather inconclusive. In general, it shows that the sand coating made a greater difference at small depths of flow, which seems reasonable. However, it is also shown that the rougher the original bed form pattern, the more difference that was made by the addition of sand grains. This may be due to the greater surface area of the rougher patterns, allowing more flow contact with the sand grain roughness. Again, a rather distinct difference is noted between the magnitude of the difference found for the 16 and 8 shapes, and that found for the flatter shapes.

The fact that the effective increase in the sand grain roughness is greater than the assumed D_{50} size of the coating material may be explained, in part, by the unevenness of the sand grain layer. Although the coating was made reasonably uniform some irregularities were unavoidable. Thus, the effect of these variations was magnified beyond the size of the individual sand grains, just as the bed forms caused an effective roughness greater than their height.

In fig. 4.5 it will be seen that all plots are roughly parallel, with the exception of that for dune shape 16. This deviation is unexplained, and is likely due to experimental error. The same accounts for the sharp upsweep of the $L/k = 32$ curve at small depths of flow.

Although the effect of dune shape on flow resistance is shown in the previously mentioned figures, it is more

apparent in figs. 4.3 and 4.4. These curves demonstrate that the resistance increases sharply as the wavelength of the bed forms is decreased. The true relation between roughness and shape may not be well represented, however. Unfortunately, only five points were available for plotting each of these curves. In addition, the points are all grouped mostly toward the flatter shapes. Thus a small change in the values, for instance, of $L/k = 16$, or $k/L = 0.0625$, would drastically change the shape of the curves. Since the point derived from the $L/k = 8$ tests, or $k/L = 0.125$, was so far removed from the remainder of the points, and the shape of the curve in this interval was uncertain, this portion of the curve is shown only as a dashed line. The general trend toward increasing roughness with increasing values of k/L is, however, quite obvious. The reason for the concave-up shape of the curves for smooth dunes at low k/L , while the corresponding curves for the roughened bed forms are concave-down, is not immediately explainable. Again, this is possibly due to insufficient data, and/or experimental errors.

Figures 4.6 and 4.7 present the roughness calculated from the mean velocity readings. It will be seen that these curves generally give higher k_s/k values than figs. 4.1 and 4.2 respectively. This may be explained by considering that figs. 4.1 and 4.2 were derived from velocity profiles taken on the flume centre line, largely free of sidewall effects. However, the figs. 4.6 and 4.7 are based on the flow

through the entire cross section, which, especially in a narrow flume such as the one used in this study, contains a large percentage of flow which is retarded due to boundary layer growth on the sidewalls of the flume. Thus the mean velocity calculated by considering the entire cross section would be markedly lower than that observed on a velocity profile on the channel centre line. Since both formulae (2.13) and (2.14) are similarly derived, and make no allowance for sidewall effects, the roughness or resistance calculated by equation (2.14) is bound to be larger. In general, both sets of curves give roughly similar values, and figs. 4.6 and 4.7 provide a good check on the preceding calculations. It will be noted that in both figs 4.6 and 4.7 the plot for the dune shape $L/k = 8$ has a sharp break downward at small depths of flow. This is again assumed to be due to the lack of a logarithmic velocity distribution at these small depths over a very rough boundary.

5.3 Chezy's Roughness Coefficient

The results of the Chezy's C calculations are in some ways more satisfactory than those of the equivalent sand grain roughness. The scatter of the experimental points was less severe, as may be seen in figs. B-11 to B-20, and no untoward breaks were seen in the curves.

Figures 4.8 and 4.9 demonstrate the effect of depth on the Chezy parameter. Again, as with the equivalent sand grain roughness, an unmistakable trend toward decreased

resistance to flow with increased depth is shown. In addition, it would seem that the flatter the dune shape, the more sensitive it is to changes in depth. That is, there is a larger change in roughness for the dune shape having $L/k = 40$ than for the shape $L/k = 8$ when the depth is changed from small to large values.

Again, there seems to be a distinct break between the $L/k = 16$ and $L/k = 24$ shapes, similar to the difference detected in the k_s results. Although it is reasonable to assume that if the difference shows up in one roughness parameter then it should also appear in the other, no satisfactory explanation can be made for this phenomenon.

In fig. 4.8. it will be noted that the results for dune shapes having ratios of 40, 32 and 24 were extended to very shallow depths, as low as $d/k = 2.5$. These were among the first tests performed, and the practice of trying such small depths was later discontinued. This action was taken due to the extreme difficulty of establishing uniform flow at these depths with the equipment used. In addition, it was decided that bed form heights in the order of 40% of the depth flow were not realistic under normal circumstances.

The same degree of confidence should not be placed in these readings, taken at low depths of flow, as those taken in deeper water. The fact that the $L/k = 24$ and the $L/k = 32$ curves cross in this area bears out these suspicions.

With respect to accuracy in the investigation it

should be pointed out that in fig. 4.8, and to a lesser extent in fig. 4.9, the general appearance of the set of curves would be improved if the $L/k = 24$ curves had a slightly steeper slope. Attempts to confirm the original values by re-testing merely duplicated the first results. However, the author is not convinced that the curves shown are correct, and it is possible that experimental error caused a somewhat flatter slope than should actually exist.

The difference in resistance to flow caused by the addition of sand coating to the dunes is presented in fig. 4.12. As with fig. 4.5, the results are not as explicit as might have been hoped. Examination of the figure will show that the change in the non-dimensional Chezy parameter, C/\sqrt{g} , is relatively insensitive to depth of flow. That is, the addition of the sand coating tended to add a certain value to the original roughness coefficient, and this added amount was virtually constant with changes in depth of flow.

The additional roughness was not, however, constant over varying dune shapes. The smoother dunes showed a much greater change in resistance to flow than the more rugged profiles.

The fact that the plot for $L/k = 32$ is not parallel to the remainder of the curves is not immediately explainable. It is probably due to errors in the investigation.

The relation between dune shape and the non-dimensional Chezy parameter is shown in figs. 4.10 and 4.11. As

with figs. 4.3 and 4.4, five points do not adequately define the underlying relation. Therefore the curves, as presented here, may not be correct in detail. However, it would seem that an unmistakable trend exists toward a lower C/\sqrt{g} value with increased k/L values. That is, more resistance to flow with a more rugged bed form profile.

It is apparent that if the C/\sqrt{g} values for a k/L of 0.0416, or $L/k = 24$, could be lowered slightly, and/or the C/\sqrt{g} values for a k/L of 0.0625, or $L/k = 16$, could be raised slightly, then a smooth concave-up curve would result. However, more extensive testing, producing more points to plot, would be necessary to establish whether or not this is the true relation.

5.4 Possible Sources of Error

As was previously mentioned, one possible source of error in the experimental procedure was the application of a roughness formula based on a logarithmic velocity profile. A number of the velocity profiles taken were plotted on logarithmic paper for checking purposes, and they all approximated a straight line. However, slight deviations did occur, especially near the bed and near the water surface. Most of the results derived from doubtful readings were rejected, as was mentioned in section 3.3; however, any dubious value which was overlooked would lead to a greater scatter in the final experimental results.

Another source of error which may be considered is the equation (2.13). This equation is based on the assumption of fully developed turbulent flow. However, during the calculation of some of the results it was found that the parameter $(v_* k_s / \nu)$ was less than 70. This indicates that fully developed turbulent flow had not been reached, and that the flow is only in a transitional state. In a few cases the value of this term dropped below 5, indicating smooth flow. This condition occurred only in the larger d/k region of the smooth dunes having L/k ratios of 32 and 40.

Under these conditions the viscous sub-layer theoretically buries all roughness elements. That is, δ , the thickness of the viscous sub-layer is greater than k_s , the equivalent sand grain roughness height of the roughness elements. Thus the flow does not depend on the roughness characteristics of the boundary, and acts as if the boundary were smooth. Therefore the argument could be made that equation (2.13) is not valid for these calculations. However, rough calculations would show that δ , at its thickest value, is less than one-tenth the actual height of the bed forms. Therefore, while $\delta > k_s$, $\delta \ll k$. Thus it was deemed reasonable to proceed with the original method of calculation.

In these experiments no allowance was made for the resistance to flow due to the walls of the flume. All resistance was attributed to the bed forms. However, since the flume walls were smooth plexiglass, and contributed much less

roughness than the bed forms, it was felt that the resistance from this source could be neglected.

The measurement of depth, which determined whether or not the flow was, in fact, uniform, was another possible source of error. At larger depths of flow the water surface was glassy and the depth could be read fairly accurately. However, when the flow depth was reduced to 2.5 inches or less, small ripples tended to appear on the surface. These tended to make accurate depth determination difficult, so that readings could be taken only to approximately the nearest one-tenth of an inch. Another phenomenon which was observed at small depths of flow was a dip in the water surface over the crest of each dune. This is normal in sub-critical flow, but is not usually apparent. The small depths used in this study, however, magnified this effect. In order to avoid error due to this cause all depths were measured at similar points on the bed forms at each end of the test section.

Minor errors may have been introduced by the equipment used to measure the discharge, or by the mini-flowmeter used for the velocity profile determination. However, since both these systems are normally quite reliable and produce accurate results little error was expected from these sources.

By far the largest errors undoubtedly arose from measurements of slope. The scale from which the slope was read could only be interpolated accurately to the nearest 0.0002. Any closer estimations could have been in error.

TABLE 5.1
POSSIBLE PERCENTAGE ERRORS IN k_s

OBSERVATION ERROR %	S			d			V		
	-10	0	+10	-10	0	+10	-10	0	+10
y	-10	-27.5	-10.0	+8.4	-21.4	-10.0	+0.9	+34.4	-10.0
	0	-19.5	0	+20.5	-12.7	0	+12.2	+49.3	0
	+10	-11.4	+10.0	+32.6	-4.0	+10.0	+23.4	+64.2	+10.0
V	-10	+22.8	+49.3	+76.6	+32.1	+49.3	+65.5		
	0	-19.5	0	+20.5	-12.7	0	+12.2		
	+10	-47.2	-33.0	-17.8	-42.3	-33.0	-24.0		
d	-10	-30.2	-12.7	+5.9					
	0	-19.5	0	+20.5					
	+10	-9.1	+12.2	+34.4					

Example: If error in the observation of $S = +10\%$
error in the observation of $y = -10\%$
Then the resultant error in $k_s = +8.4\%$

TABLE 5.2
POSSIBLE PERCENTAGE ERRORS IN C/\sqrt{g}

OBSERVATION ERROR %	Q			d		
	-10	0	+10	-10	0	+10
S	-10	-5.1	+5.5	+8.4	+10.3	+5.5
	0	-10.0	0	+10.0	+13.8	0
	+10	-15.5	-5.5	+3.3	+8.8	-5.5
d	-10	+2.7	+13.8	+25.0		
	0	-10.0	0	+10.0		
	+10	-20.2	-13.8	-2.6		

Example: If the error in the observation of $S = +10\%$
the error in the observation of $d = -10\%$
Then the resultant error in $C/\sqrt{g} = +8.8\%$

Example: If the error in the observation of $Q = -10\%$
the error in the observation of $d = +10\%$
Then the resultant error in $C/\sqrt{g} = -20.2\%$

Since in many cases the recorded slope was of this order of magnitude, it is possible that some readings could have been in error by as much as 100%. Any such errors in slope estimation would, of course, effect changes in the calculated values of k_s and C .

During all tests the viscosity of the water was assumed to be constant at the value for 70° F. However, the room temperature in the laboratory probably ranged from 65° F. to 85° F. during the course of the study, thereby introducing a slight error. However, considering the magnitude of the errors introduced from other sources, this error was relatively unimportant.

Tables 5.1 and 5.2 summarize the resulting errors in k_s and C/\sqrt{g} respectively, due to errors in the observation of various parameters.

5.5 Comparison with Results of Other Studies

A number of studies have been reported in the literature which have used mobile bed flumes to study the variation of resistance to flow with changes in various parameters. The data presented in these references may be compared with the results obtained in this investigation.

Table 5.3 presents data already published in various references. In each case the original data were analysed to yield C/\sqrt{g} values for the various test runs performed, based on the reported values of slope, depth of flow, channel width

TABLE 5.3
COMPARISON WITH OTHER EXPERIMENTAL RESULTS

REFERENCE		EXPERIMENTAL RESULTS		
REF. NO.	DATA NO.	c/\sqrt{g}	c/\sqrt{g}	% DIFF.
5	2-9	8.14	6.00	+35.6
	9-1	7.40	5.60	+32.2
	9-2	7.16	5.60	+27.8
	9-3	7.11	5.70	+24.7
	9-4	9.84	6.00	+64.0
	9-5	8.00	5.50	+45.5
	9-6	8.00	6.00	+33.3
	9-8	6.90	7.20	-4.2
	9-9	7.85	5.75	+36.6
	9-11	9.20	5.40	+70.4
6	9-12	9.65	5.70	+69.2
	9-15	9.85	6.10	+61.5
	I	12.00	11.30	+6.2
	II	10.60	11.30	-6.2
7	III	9.60	13.00	-26.2
	IV	10.80	11.50	-6.1
	33	11.90	11.50	+3.5
	1a	11.80	11.40	+3.5
	14	12.30	13.10	-6.1
	21	12.60	11.80	+6.8
	19	11.80	11.60	+1.7

TABLE 5.3 (Cont'd)

REFERENCE			EXPERIMENTAL RESULTS	
REF. NO.	DATA NO.	C/√g	C/√g	% DIFF.
7	16a	11.10	10.80	+2.8
	17a	12.30	11.90	+3.4
	3a	12.20	11.60	+5.2
15	2-8	13.70	13.80	-0.7
	2-11	12.60	11.20	+16.2
	2-6	10.40	11.80	-11.9
	2-35	11.50	13.30	-13.5
	2-9	12.00	11.10	+8.1
	3-57	9.50	10.10	-5.9
	3-54	11.50	14.00	-17.8
	3-56	10.60	12.00	-11.7
	3-43	9.40	11.00	-14.5
	3-44	11.30	11.00	+2.7
	4-33	10.60	11.20	-5.4
	4-1	10.70	11.60	-7.8
	4-14	11.40	14.50	-21.4
	4-2	10.50	10.80	-2.8
	4-21	11.20	11.80	-4.2
	4-19	11.40	11.70	-2.6
	4-17	11.40	10.90	+4.6
	4-3	11.00	11.70	-6.0
	4-34	10.70	15.90	-32.7
	5-3	11.20	10.70	+4.7

TABLE 5.3 (Cont'd)

REFERENCE			EXPERIMENTAL RESULTS	
REF. NO.	DATA NO.	C/\sqrt{g}	C/\sqrt{g}	% DIFF.
15	5-9	10.50	9.50	+10.5
	5-1	11.80	12.10	-2.5
	5-11	9.40	7.00	+34.1
	5-8	9.40	8.90	+5.6
	5-6	9.40	6.80	-38.3
	5-12	8.50	6.90	+23.1
	5-4	12.80	12.80	0
	5-29	11.80	11.60	+4.4
	6-16	10.50	13.10	-20.0
	6-17	10.00	10.20	-2.0
	6-10	11.20	12.20	-8.2
	6-7	8.40	11.60	-27.5
	6-8	8.80	12.60	-30.0
	10-47	15.90	13.20	+20.7
	10-43	12.10	13.00	-6.9
	10-51	7.50	11.50	-34.6
21		9.14	9.95	-8.4

and mean velocity. Combining these values with equation (2.2) yields a C/\sqrt{g} value for each particular run. Then, using the values for length of bed form, and height of bed form also reported, L/k , and d/k ratios were calculated, and a value of C/\sqrt{g} was obtained from the experimental results of this study, as shown in Chapter IV.

In this procedure the curves of fig. 4.8 were used exclusively, even though these results were determined for smooth dunes. By using the data reported in the references the D_{50} size of the sand used for the mobile beds was found. In addition, the average length of dune was determined. Combining these two factors gives a measure of the scale of the surface roughness, compared to the bed forms. The average D_{50}/L value for each study was as follows:

Reference	Average D_{50}/L
6	0.000273
7	0.000173
15	0.000268
21	0.000485

The average D_{50}/L value for this present investigation was 0.00235, or about five to fourteen times as large as the values for the reference data. In view of these results, it was assumed that the dunes referred to in the references could be considered "smooth" with respect to the sand coated dunes used in this study, and that a better comparison could

TABLE 5.4
COMPARISON OF RESULTS WITH PUBLISHED FORMULAE

REF. NO.	REFERENCE	EXPERIMENTAL RESULTS						
		FORMULA	C/\sqrt{g}	L/k	d/k	SMOOTH DUNES	ROUGH DUNES	
8	$\frac{C}{g} \frac{(7.66 - 0.3) \log D}{V^*}$ + $\frac{0.13}{V^*} + 11.0$	14.68 14.44 14.28 14.98 $D_{50} = 0.716 \text{ mm.}$	40 7.0 5.0 9.0 7.0 14.60 14.25 15.14 14.69 14.20 15.31 14.79 14.19	9.0 7.0 5.0 9.0 7.0 14.00 13.60 15.30 7.0 5.0 9.0 7.0 5.0 16.00 13.60 15.30 14.00 12.80 10.25 13.55 5.0	21.90 19.00 16.15 18.30 16.00 14.60 13.60 15.30 14.00 12.80 10.25 13.55 6.90	-33.0 -24.0 -11.6 -18.1 -8.7 +4.8 +4.8 -1.0 +4.9 +11.0 +49.4 +71.0 +105.0	16.68 13.95 10.93 14.32 12.03 10.80 12.40 11.00 9.91 8.48 7.28 +103.1 +166.0	-12.0 +3.5 +30.6 +4.6 +21.3 +31.9 +22.1 +33.5 +43.2 +80.6 5.54

TABLE 5.4 (Cont'd)

REFERENCE	EXPERIMENTAL RESULTS							
	REF. NO.	FORMULA	C/\sqrt{g}	L/k	d/k	SMOOTH DUNES C/\sqrt{g}	DUNES C/\sqrt{g}	ROUGH DUNES C/\sqrt{g}
9	$\frac{C}{g} = \frac{2.5 \ln(11d/k_s)}{1 - (k/L)\sigma}$	14.90	32	9.0	18.30	-18.6	14.32	+4.1
	$\sigma = \tan \phi - \frac{k}{2L} \cdot A^2$	13.90		7.0	16.00	-13.1	12.03	+15.5
	$A = 2.5 \ln(11d/k_s)$	12.50		5.0	13.60	-8.5	10.80	+15.7
	$D_{50} = 0.716 \text{ mm.}$	14.10	24	9.0	15.30	-8.0	12.40	+13.7
		13.00		7.0	14.00	-7.1	11.00	+18.2
		11.70		5.0	12.80	-8.6	9.91	+18.1

be made with the results of the tests on the smooth concrete bed forms.

The comparison of the experimental results with the results of Vanoni and Hwang (5) are not as close as those of the other references. In their study Vanoni and Hwang arrived at a dune roughness by subtracting a grain roughness, or surface roughness, from the total resistance to flow. This surface roughness was determined by using a plot of the data of Nikuradse for sand grain roughness in pipes. This data was obtained for smooth walled (i.e. no corrugations) pipes, while Vanoni and Hwang had a surface roughness superimposed on an undulating bed, which may possibly introduce some error and account for the larger difference between their results and those of the present study.

In the case of the above mentioned study, the results were compared with those of fig. 4.8 not because the D_{50}/L ratio was appropriately small, but because the f'' factor calculated by the authors should show only the roughness effects due to the form drag.

Table 5.4 presents a comparison of the experimental results with values calculated by proposed formulae by which resistance to flow may be predicted. Formulae put forward by Richardson (8), and Yalin (9) are examined. The formulae are compared with results from both smooth and rough dunes, of which the former give closer agreement. This is, as before, due to the scale of surface roughness in these tests, compared to that

used to derive the formulae.

5.6 The Logarithmic Velocity Formula

In Chapter II the following expression was developed for the velocity distribution in a wide open channel:

$$\frac{v}{v_*} = A \ln \frac{y}{k_s} + B \quad (2.11)$$

By transforming natural logarithms into logarithms to the base ten, we may write:

$$\frac{v}{v_*} = 5.75 \log \frac{y}{k_s} + B$$

Assuming that k_s and B are constant, we can say:

$$\frac{v}{v_*} = A' \log \frac{y}{k_s} + B' \quad (5.1)$$

where: A' = coefficient (usually 5.75)
 B' = constant

The relation (5.1) was investigated by plotting values of v against $\log y$, and finding the best straight line fit for the points. The value of the coefficient A' was then found from the slope of the curve.

Unfortunately, the results of this analysis were not conclusive. A summary of the results is presented below, and the error with respect to the accepted theoretical value of 5.75 is shown:

Dune Type	A' average	Error
Smooth	5.99	+4.18%
Rough	5.39	-6.25%
Average	5.69	-1.04%

A number of investigators (1), (3), (4), (10), have shown that some variation may be expected in this coefficient. But considerable scatter was evident in the results of the analysis conducted on the present results, and it was difficult to define any firm trends in the results. Individual values of A' ranged from 3.009 to 8.482, indicating a variation of Von Karman's coefficient from 0.768 to 0.271. This is within the range of variation discovered by Garde and Paintal (10) for alluvial channels.

It was originally thought that a slight raising or lowering of the datum might lead to an improvement in the results of the determination of A' . However, there did not seem to be a narrowing of the scatter of A' values when this was attempted.

The complete calculations for the values of A' for each depth and dune shape are not shown here, but are included with the remainder of the thesis data, on file with the Department of Civil Engineering.

It will be seen that the average of the extreme values of A' , as reported above, is 5.746, or close to the theoretical value of 5.75. This may indicate that most of the variation is due to experimental errors. The scatter of the values calculated, along with this possibility, showed that the assumption of a value of A' other than 5.75 for purposes of calculating k_s was unwarranted.

The effect of changing the elevation datum was studied

in some detail by calculating values of A' for each velocity profile taken, while varying the elevation datum and thus all depth measurements. When the results for each dune shape were averaged and then plotted against change in datum, there was no improvement in the scatter of the points, and it was impossible to definitely define any trend in the results. For this reason the elevation datum was left at its original position, midway between the high and low points of the bed form profile.

5.7 Comparison with Regime Methods

An attempt was made by Yalin (16) to relate the parameters of flow and particle size of the bed material to the size and shape of the bed forms which may be expected in a channel. The relations given for the dimensions of the dunes are as follows:

$$\frac{k}{d} = \frac{1}{6} \left(1 - \frac{d_{cr}}{d} \right) \quad (5.2)$$

$$L = 5d \quad (5.3)$$

where: d = depth of flow
 d_{cr} = depth corresponding to competent shear, $T_c = \gamma S d$
 k = height of bed form
 L = length of bed form

By combining these equations with the results given in fig. 4.9 it should then be possible to predict the channel resistance if the flow parameters and the bed material size are known.

To study the validity of this approach the results

are compared to those found by using regime methods.

Table 5.5 shows channel geometry and Chezy's C values calculated for various discharges by the regime method, assuming a bed material diameter of 0.716 mm., (the same size material as was used to produce the roughness coating on the smooth bed forms in this investigation) and a side factor of 0.2, using formulae provided by Blench (17). In addition, another Chezy's C value, to be called C_y , and slope have been calculated by Yalin's method, and are included for comparison. The method of calculating these values will be explained.

Using a Shields diagram for competent tractive force, for the particle size used in this study, we may say:

$$S_{cr} d_{cr} = 0.000133 \quad (5.4)$$

Using equations (5.2) and (5.4) an iterative solution for any given channel may be found. The procedure used is as follows:

- (1) Using (5.2) calculate a value of k .
- (2) Using d , k , equation (5.3), and fig. 4.9, calculate a value of C_y .
- (3) Substitute Q , b , d , and C into Chezy's equation to calculate S_y . If the difference between the new and old values of S_y is significant, continue the procedure.
- (4) From equation (5.4) calculate a new d_{cr} and hence a new value of k for step (1).

Observation of Table 5.5 shows that the agreement between the two methods is not very good. The resistance and slope predicted by the above method increases with increasing

discharge, which would not normally be expected.

TABLE 5.5
COMPARISON OF RESULTS WITH REGIME METHOD

Regime Method						Yalin's Method	
Q	d	b	S	V	C	C _y	S _y
500	3.4	63.4	.00022	2.3 fps	90.8	68.7	.00039
2000	5.4	126.8	.00018	2.9	100.7	65.2	.00042
5000	7.3	200.4	.00015	3.4	108.0	64.1	.00043

Since the agreement of the results of this study with those derived from flume experiments is reasonably good, it is probable that equations (5.2) and (5.3) are at least partly in error.

In a later paper, Yalin (18) proposes that both sand wave height and length can be expressed as:

$$k, L = f \left(\frac{Dv_*}{\nu}, \frac{v_*^2}{\gamma_s D}, \frac{d}{D}, \frac{\rho}{\gamma_s} \right)$$

where: ρ = unit mass of sediment
 ν = unit mass of fluid
 γ_s = submerged weight of sediment

In the derivation of equations (5.2) and (5.3) the factor d/D was not considered. This omission may contribute some of the error between the two sets of results shown in Table 5.5.

The term $(v_* D / \nu)$, a grain size Reynolds number, is mentioned in Yalin's original paper as a criterion for the type

of bed form to be expected. If $(v_* D / \nu) < 20$ ripples will form, but if $(v_* D / \nu) \geq 20$ dunes may be expected.

White and MacMahon (19), and Nordin (20) also criticize Yalin's results, and present data from a number of sources to indicate relationships different from those predicted by equations (5.2) and (5.3).

Thus, while Yalin's equations give results accurate to within a factor of two or three when compared to those predicted by the regime method, the apparent errors may be due to an oversimplification of the problem. Research on the prediction of bed profiles is, however, as yet very limited, and hence any roughness or slope values predicted by the aforementioned means can be regarded only as very rough approximations.

CHAPTER VI

CONCLUSIONS AND RECOMMENDATIONS

6.1 Conclusions

A review of the current literature on the effect of roughness elements on open channel flow showed a lack of knowledge of the effects of shape and spacing on the resistance to flow. This was particularly evident in the case of river channel bed forms. In the present investigation, the use of idealized dune shapes in a laboratory flume presents a different approach to the problem.

The tests conducted indicated that a definite relationship exists between resistance to flow in an open channel and the shape and height of the bed forms which occur on the channel boundary. In addition, the grain size of the bed material, or the surface roughness of the dunes, was shown to have a considerable effect on the total roughness.

Examination of the results presented suggests a definite increase in the resistance to flow, both in the C/\sqrt{g} and k_s/k parameters, with any decrease in depth for a given bed form pattern, or with any decrease in the L/k shape ratio of the dunes for a given depth.

The addition of a surface roughness caused increases in the total equivalent sand grain roughness up to many times the size of the actual sand grains used.

The results obtained in this investigation were deemed satisfactory for the purposes of the study. The methods used proved suitable in most respects, and, with minor changes, could be used in a more extensive project.

6.2 Recommendations

It is recommended that:

- (a) a more extensive series of tests be conducted utilizing a greater range of dune shapes, and heights, in order to verify or limit the conclusions of this study.
- (b) various sizes of sand be employed for surface roughness in order to more adequately determine the effect of this factor on the total resistance to flow. In addition, a natural river bed gradation of sand grains should be tried, rather than a uniform size. That is, the grain size distribution of the sand used should follow a log-normal distribution.
- (c) In connection with (b) above, an effort should be made to determine the best characteristic size of the bed material to be used in such plots as fig. 4.5, showing the change in total

roughness compared to the actual size of the bed material.

- (d) further investigation be conducted to determine the effect of the breadth to depth ratio of the flow on the calculated values of C/\sqrt{g} , and k_s/k . If changes occur at low values of b/d , then it would be advisable to use a wider flume in future studies. This would permit deeper flows without side wall effects, and would allow extension of the range of d/k values.
- (e) different methods of measuring the depth of flow, and slope should be considered, which would allow less error in the estimation of these values. Greater accuracy in slope measurement is especially important.
- (f) a much longer flume should be used in future studies in order to allow accurate confirmation of the presence of uniform flow.

LIST OF REFERENCES

- 1) Suryanarayana, B.; Natural Roughness Effects in Rigid Open Channels, Journal, Instn. Engrs. (India), vol. 46 No. 9, 1966, p. 435-448
- 2) Mirajaoker, A.G., and Charlu, K.L.N.; Natural Roughness Effects in Rigid Open Channels, Journal of Hyd. Div., ASCE, vol. 89, No. HY5, 1963, p. 29-44
- 3) Chithambaran, V.K., and Mirajaoker, A.G.; Flume Studies on Natural Roughness in Rigid Open Channels, Journal, Instn. Engrs. (India), vol. 45 1964-65, p. 571-585
- 4) Sayre, W.W., and Albertson, M.L.; Roughness Spacing in Rigid Open Channels, Transactions, ASCE, vol. 128 Pt. I, 1963, p. 343-372
- 5) Vanoni, V.A. and Hwang, L.S.; Relation Between Bed Forms and Friction in Streams, Journal of Hyd. Div., ASCE, vol. 93, No. HY3, 1967, p. 121-144
- 6) Simons, D.B. and Richardson, E.V.; Resistance to Flow in Alluvial Channels, U.S.G.S. Prof. Paper 422-J, 1966
- 7) Simons, D.B. and Richardson, E.V.; Forms of Bed Roughness in Alluvial Channels, Transactions, ASCE, vol. 128 Pt. I, 1963, p. 284-323
- 8) Richardson, E.V. and Simons, D.B.; Resistance to Flow in Sand Channels, Proceedings, 12th Congress, I.A.H.R., Fort Collins, U.S.A., 1967, p. 141-150

9) Yalin, M. S.; On the Average Velocity of Flow Over a Movable Bed, La Houille Blanche, vol. 19, No. 1, 1964, p. 45-50

10) Garde, R. J., and Paintal, A. S.; Velocity Distribution in Alluvial Channels, La Houille Blanche, vol. 19, No. 1, 1964, p. 719-725

11) Keulegan, G. H.; Laws of Turbulent Flow in Open Channels, U.S. National Bureau of Stds., Journal of Research, vol. 21, 1938, p. 707-741

12) Tracy, H. J. and Lester, C. M.; Resistance Coefficients and Velocity Distribution, Smooth Rectangular Channel, U.S.G.S., Water Supply Paper 1592-A, 1961

13) Cruff, R. W.; Cross Channel Transfer of Linear Momentum in Smooth Rectangular Channels, U.S.G.S., Water Supply Paper, 1592-B 1965

14) Yalin, M. S.; Notes on Fluid Mechanics, Unpublished, Univ. of Alberta, 1967

15) Guy, H. P., Simons, D. B., and Richardson, E. V.; Summary of Alluvial Channel Data from Flume Experiments 1956-1961, U.S.G.S., Prof. Paper 462-I, 1966

16) Yalin, M. S.; Geometrical Properties of Sand Waves, Journal of Hyd. Div., ASCE, vol. 90 No. HY5, 1964, p. 105-119

17) Blench, T.; Mobile Bed Fluviology, University of Alberta, 1966

18) Yalin, M. S.; Similarity in Sediment Transport Currents, Ministry of Technology, Hydraulics Research Station, Wallingford, England, 1965

- 19) White, C.M. and MacMahon, B.; discussion of: Geometrical Properties of Sand Waves, Journal of Hyd. Div., ASCE, vol. 91 No. HY3, 1965, p. 364
- 20) Nordin, C.F.; discussion of: Geometrical Properties of Sand Waves, Journal of Hyd. Div., ASCE, vol. 91 No. HY3, 1965, p. 367
- 21) Task Force on Bed Forms in Alluvial Channels; Nomenclature for Bed Forms in Alluvial Channels, Journal of Hyd. Div., ASCE, vol. 92 No. HY3, 1966, p. 56

APPENDIX A

EXPERIMENTAL OBSERVATIONS

TABLE A-1
EXPERIMENTAL DATA

DUNE SHAPE KLE = 1/8

DEPTH OF FLOOD (IN.)	SECTION ON DUNE (IN.)	DISCHARGE (CFS)	MEAN VELOCITY (FPS)	PROBE EL. ABOVE DATUM (IN.)	VELOCITY AT PROBE (FPS)	CHARAC- TERISTICS	
						C	S
4.075	A	0.0011	0.591	0.651	4.250	1.153	0.092524
				3.750	1.132	1.059	0.09375
				3.250	1.144	1.073	
				2.750	1.033	0.078377	
				2.250	1.039	0.078549	
				1.750	0.953	0.097053	
				1.250	0.874	0.079072	
				0.750	0.784	0.074723	
	B						
				4.250	1.165	0.08182	
				3.750	1.159	0.079634	
				3.250	1.132	0.077411	
				2.750	1.104	0.073237	
				2.250	1.012	0.087603	
				1.750	0.979	0.077970	
				1.250	0.861	0.090495	
				0.750	0.732	0.092556	
	C						
				4.250	1.163	0.087055	
				3.750	1.153	0.078413	
				3.250	1.132	0.062956	
				2.750	1.039	0.078043	
				2.250	1.032	0.050697	
				1.750	0.930	0.077737	
				1.250	0.902	0.076519	
				0.750	0.770	0.079253	
	D						
				4.250	1.065	0.122603	
				3.750	1.059	0.106494	
				3.250	1.009	0.119375	
				2.750	1.003	0.080057	
				2.250	0.952	0.099426	
				1.750	0.957	0.079554	
				1.250	0.773	0.122804	
				0.750	0.715	0.093319	
	E						
				4.250	1.072	0.109773	
				3.750	1.067	0.107493	
				3.250	1.013	0.076839	

NOTE

THESE VALUES OF S WHICH ARE MARKED WITH AN ASTERISK USED IN PLOTTING THE CHARACTERISTIC SIGNIFICANCE CROVES.

TABLE A-1 [continued]

DUNE SHAPE $K/L = 1/3$

DEPTH (IN.)	SECTION OF FLOOD PLANE	SLOPE OF FLOOD PLANE	DISCHARGE (CFS)	MEAN VELOCITY (FPS)	PROBE ELEV. ABOVE DATUM	VELOCITY AT PROBE (IN.)	CHEZY'S C		KS (FT.)
							(FPS)	(IN.)	
4.050	b	0.0011	0.469	0.798	2.750	1.017	47.43	0.096049	
					2.250	0.967		0.090145	
					1.750	0.916		0.095246	
					1.250	0.857		0.086216	
					0.750	0.661		0.117774 *	
					4.250	1.669		0.122429 *	
					3.750	1.160		0.097403	
					3.250	1.093		0.094707	
					2.750	1.049		0.085309	
					2.250	1.006		0.082301	
					1.750	0.864		0.108272	
					1.250	0.846		0.096257	
					0.750	0.753		0.078457	
4.020	a	0.0011	0.420	0.726	3.750	1.018	44.01	0.121022	
					3.250	0.945		0.115714	
					2.750	1.005		0.093895	
					2.250	0.922		0.109670	
					1.750	0.872		0.105526	
					1.250	0.774		0.114742	
					0.750	0.679		0.103311	
					3.750	1.049		0.106219	
					3.250	0.979		0.123612	
					2.750	0.925		0.102263	
					2.250	0.951		0.096722	
					1.750	0.889		0.098288	
					1.250	0.759		0.121924	
					0.750	0.614		0.136070 *	
					3.750	1.023		0.118514 *	
					3.250	1.010		0.108494	
					2.750	0.997		0.097126	
					2.250	0.950		0.097126	
					1.750	0.941		0.078572	
					1.250	0.791		0.106376	
					0.750	0.678		0.103812	

NOTE
THESE VALUES OF KS WHICH ARE MARKED WITH AN ASTERISK WERE NOT USED IN PLOTTING THE CHARACTERISTIC ROUGHNESS CURVES.

TABLE A-1 [CONTINUED]

DRAIN SHAPE $K/L = 1/8$

ELEV. OF FLOOR (ft.)	SECTION IN FLUKE (ft.)	SLOPE OF FLUKE (ft/ft.)	DISCHARGE VELOCITY (CFS)	MEAN VELOCITY (FPS)	PROBE EL. ABOVE DATUM (IN.)	VELOCITY AT PROBE (FPS)	CHEZY'S C	KS
4.00	A	0.0611	0.382	0.700	3.750 3.250 2.750	0.932 0.960 0.921	43.38	0.16035 0.123021
					2.250 1.750 1.250 0.750	0.868 0.845 0.754 0.672		0.127554 0.10597 0.116142 0.094954
					3.750 3.250 2.750 2.250 1.750 1.250 0.750	0.952 0.966 0.949 0.897 0.821 0.752 0.632		0.143322 0.125222 0.109142 0.112472 0.121798 0.098726 0.116232
					3.750 3.250 2.750 2.250 1.750 1.250 0.750	0.904 0.975 0.914 0.859 0.803 0.757 0.649		0.139421 0.115375 0.127236 0.115853 0.101108 0.110252 0.110513
					3.250 2.750 2.250 1.750 1.250 0.750	0.922 0.887 0.852 0.752 0.729 0.623	30.29	0.151327 0.154626 0.147453 0.148197 0.138339 0.129275
					3.250 2.750 2.250 1.750 1.250 0.750	0.920 0.897 0.857 0.788 0.720 0.617		0.159042 0.148519 0.144395 0.150849 0.144023 0.132933
					3.250	0.947		0.141647

NOTE

THESE VALUES ARE FOR AN ASYMETRICAL DRAIN AND NOT FOR A DRAIN WITH AN ASYMETRICAL DRAIN. THE CHARACTERISTIC DRAINS ARE PLOTTED IN THE PLOTS.

TABLE A-1 [CONTINUED]

DUST SHAPE $M/L = 1/3$

DEFIN LF FLIB FLIB (IN.)	SECTION SH. OF FLIB	SLOPE OF FLIB	DISCHARGE FLIB	MEAN VELOCITY (FPS)	PROBE EL. ABOVE DATUM (IN.)	VELOCITY AT PROBE (FPS)	CHEVIS	
							C	S
3.75	C	0.0012	0.351	0.647	2.750	0.853	39.29	0.150665
					2.250	0.862		0.140945
					1.750	0.773		0.160257
					1.250	0.719	0.144261	
					0.750	0.621	0.131940	
3.50	C	0.0011	0.287	0.801	3.250	0.842	39.07	0.171678
					2.750	0.807		0.170574
					2.250	0.770		0.165709
					1.750	0.713		0.163557
					1.250	0.554		0.15675
					0.750	0.597		0.122046
					3.250	0.852		0.164357
					2.750	0.810		0.161664
					2.250	0.757		0.175219
					1.750	0.714		0.165508
					1.250	0.542		0.165121
					0.750	0.553		0.145865
					3.250	0.887		
					2.750	0.811		0.138289
					2.250	0.757		0.167974
					1.750	0.723		0.149105
					1.250	0.663		0.159748
					0.750	0.560		0.150160
								0.144611
3.25	A	0.0011	0.254	0.529	2.750	0.768	35.35	0.185249
					2.250	0.722		0.168217
					1.750	0.666		0.190716
					1.250	0.623		0.166781
					0.750	0.515		0.166555
								0.144611
					2.750	0.767		0.185907
					2.250	0.728		0.182523
					1.750	0.738		0.135533
					1.250	0.561		0.138912
					0.750	0.522		0.161032

NOTE
THESE VALUES OF SMOOTH AND MARKED WITH AN ASTERISK WERE NOT USED IN PLOTTING THE CHARACTERISTIC SMOOTHNESS CURVES.

TABLE A-1 [continued]

DUNE SHAPE N/L = 1.6

DEPTH IN FEET (IN.)	SECTION OR PIPE NUMBER	DISCHARGE CFS	VELOCITY IN FEET PER SECOND (FPS)	PROBE FL. AT ABOVE DATA PIPE	CHARACTERISTICS	
					VELOCITY AT PIPE	CHARACTERISTICS CFS
3.025	C	0.234	0.525	2.750	0.767	0.185977
				2.250	0.729	0.181973
				1.750	0.695	0.173221
				1.250	0.644	0.181977
				0.750	0.523	0.155969
Bend		0.0010	0.479	2.750	0.675	0.221054 *
				2.250	0.647	0.20362
				1.750	0.620	0.196971
				1.250	0.534	0.206363
				0.750	0.469	0.172963
Bend		0.0010	0.479	2.750	0.677	0.219353
				2.250	0.643	0.212472
				1.750	0.596	0.211352
				1.250	0.500	0.191116
				0.750	0.446	0.193643
Bend		0.0010	0.479	2.750	0.678	0.217655
				2.250	0.647	0.195662
				1.750	0.623	0.184032
				1.250	0.565	0.174964
				0.750	0.464	0.176928
Bend		0.0010	0.541	2.250	0.537	0.255912 *
				1.750	0.558	0.231821
				1.250	0.510	0.213452
				0.750	0.452	0.173887
Bend		0.0010	0.541	2.250	0.591	0.251282 *
				1.750	0.553	0.236353
				1.250	0.505	0.219064
				0.750	0.435	0.192030
Bend		0.0010	0.541	2.250	0.619	0.216397
				1.750	0.573	0.209067
				1.250	0.533	0.186764
				0.750	0.430	0.195492

NOTE

THESE VALUES ARE NOT USED IN PLOTTING THE CHARACTERISTIC COUGHNESS CURVES.

TABLE A-1 [CONTINUED]

DUNE SHAPE $K/L = 1/8$

DEPTH L.F. FLLD (IN.)	SECTION L.H. FLLD (IN.)	SLOPE OF FLLD (FT/FT)	DISCHARGE OF FLLD (CFS)	MEAN VELOCITY (FPS)	PROBE EL. ABOVE DATUM (IN.)	VELOCITY AT PROBE (FPS)	CHARIS	
							KS	C
2.50	a	0.0010	0.138	0.404	2.250	0.562	31.3;	0.260319
					1.750	0.548	—	0.216427
					1.250	0.513	—	0.186227
					0.750	0.428	—	0.183355
					2.250	0.570	—	0.246327
					1.750	0.539	—	0.230052
					1.250	0.479	—	0.220556
					0.750	0.403	—	0.237512 *
					2.250	0.581	—	0.236774
					1.750	0.553	—	0.213615
					1.250	0.512	—	0.190522
					0.750	0.437	—	0.172362 *
					1.750	0.613	30.45	0.229324
					1.250	0.581	—	0.190351
					0.750	0.482	—	0.184175
					1.750	0.621	—	0.212977
					1.250	0.555	—	0.214150
					0.750	0.470	—	0.196254
					1.750	0.636	—	0.204365
					1.250	0.502	—	0.172227
					0.750	0.481	—	0.185182

NOTE
THESE VALUES OF KS WHICH ARE MARKED WITH AN ASTERISK WERE NOT USED IN PLOTTING THE CHARACTERISTIC COUGHNESS CURVES.

TABLE A-2
EXPERIMENTAL DATA

DUNE SHAPE $K/L = 1/16$

DEPTH OF FLUID (IN.)	SECTION NUMBER ON DUNE (IN.)	SLOPE OF FLUME (FT/FT)	DISCHARGE (CFS)	MEAN VELOCITY (FPS)	PROBE EL. ABOVE DATUM (IN.)	VELOCITY AT PROBE (FPS)	CHEZY'S C	KS
4.75	A	0.0007	0.537	0.830	4.250	1.131	60.76	0.031140 *
					3.750	1.153		0.024595
					3.250	1.140		0.022772
					2.750	1.082		0.025941
					2.250	1.083		0.021183
					1.750	1.019		0.022838
					1.250	0.913		0.028165
					0.750	0.829		0.026066
					4.250	1.079		0.040719 *
					3.750	1.122		0.028844
					3.250	1.122		0.024998
					2.750	1.107		0.022863
					2.250	1.034		0.027219
					1.750	1.025		0.022138
					1.250	0.930		0.025907
					0.750	0.811		0.028615
					4.250	1.093		0.037894 *
					3.750	1.132		0.027370
					3.250	1.136		0.023219
					2.750	1.059		0.029206
					2.250	1.046		0.025628
					1.750	1.036		0.020925
					1.250	0.934		0.025359
					0.750	0.822		0.027152
4.00	A	0.0007	0.475	0.775	4.250	1.006	57.78	0.053919 *
					3.750	1.080		0.032276 *
					3.250	1.098		0.025487
					2.750	1.066		0.025518
					2.250	1.005		0.028715
					1.750	0.948		0.030115
					1.250	0.870		0.032470
					0.750	0.767		0.033379 *
					4.250	1.006		0.054025 *
					3.750	1.084		0.031581 *
					3.550	1.066		0.032811

NOTE
THOSE VALUES OF KS WHICH ARE MARKED WITH AN ASTERISK WERE NOT USED IN PLOTTING THE CHARACTERISTIC ROUGHNESS CURVES.

TABLE A-2 [CONTINUED]

DUNE SHAPE $K/L = 1/16$

SECTION UN D.L.	SLOPE OF FLUME (FT/FT)	DISCHARGE (CFS)	MEAN VELOCITY (FPS)	PROBE EL. ABOVE DATUM (IN.)	VELOCITY AT PROBE (FPS)	CHEZY'S C	KS
4.00	B	0.0007	0.475	0.775	2.750	1.018	57.78
				2.250	0.963	0.032812	0.035843
				1.750	0.950	0.029760	
				1.250	0.882	0.030416	
				0.750	0.722	0.042329 *	
				4.250	1.011	0.052549 *	
				3.750	1.094	0.030056 *	
				3.250	1.101	0.025037	
				2.750	1.011	0.034002	
				2.250	1.034	0.024656	
				1.750	0.945	0.030656	
				1.250	0.890	0.029178	
				0.750	0.791	0.029407	
4.25	A	0.0007	0.420	0.726	3.750	1.033	55.17
				3.250	1.034	0.037018	
				2.750	1.005	0.031888	
				2.250	0.993	0.031649	
				1.750	0.922	0.027622	
				1.250	0.835	0.031340	
				0.750	0.740	0.035688	
						0.035688	
	b						
				3.750	0.998	0.044664	
				3.250	0.982	0.042220	
				2.750	0.967	0.038729	
				2.250	0.966	0.031880	
				1.750	0.886	0.038120	
				1.250	0.841	0.034623	
				0.750	0.702	0.043761	
	c						
				3.750	0.983	0.048519 *	
				3.250	0.994	0.039658	
				2.750	0.983	0.035509	
				2.250	0.965	0.032074	
				1.750	0.927	0.030528	
				1.250	0.848	0.033253	
				0.750	0.751	0.033659	

NOTE
THESE VALUES OF KS WHICH ARE MARKED WITH AN ASTERISK WERE NOT USED IN PLOTTING THE CHARACTERISTIC ROUGHNESS CURVES.

TABLE A-2 [CONTINUED]

DUNE SHAPE $K/L = 1/16$

DEPTH L_f FLU. (IN.)	SECTION UN DUNE (IN.)	SLOPE OF FLUME	DISCHARGE	MEAN VELOCITY	PROBE EL. ABOVE DATUM	VELOCITY AT PROBE	CHEZY'S C	KS
4.00								
	A	0.0007	0.382	0.706	3.750	0.935	54.39	0.056393 *
					3.250	0.964		0.041697
					2.750	0.954		0.037225
					2.250	0.902		0.040403
					1.750	0.920		0.028521 *
					1.250	0.812		0.036748
					0.750	0.699		0.040938
	B				3.750	0.912		0.063954 *
					3.250	0.957		0.043184
					2.750	0.921		0.044451
					2.250	0.899		0.041075
					1.750	0.870		0.037446 *
					1.250	0.780		0.043700
					0.750	0.692		0.042574
	C				3.750	0.856		0.086785 *
					3.250	0.953		0.044085
					2.750	0.941		0.040012
					2.250	0.947		0.031544 *
					1.750	0.915		0.029296 *
					1.250	0.800		0.039337
					0.750	0.718		0.036850
3.75								
	A	0.0007	0.331	0.647	3.250	0.828	51.44	0.078796 *
					2.750	0.819		0.069990
					2.250	0.773		0.074242 *
					1.750	0.745		0.067364
					1.250	0.712		0.058062
					0.750	0.656		0.047714
	B				3.250	0.829		0.078134 *
					2.750	0.808		0.074409 *
					2.250	0.782		0.070426
					1.750	0.764		0.060617
					1.250	0.707		0.059804
					0.750	0.621		0.057818
	C				3.250	0.792		0.096497 *

NOTE
THOSE VALUES OF KS WHICH ARE MARKED WITH AN ASTERISK WERE NOT USED IN PLOTTING THE CHARACTERISTIC ROUGHNESS CURVES.

TABLE A-2 [CONTINUED]

DUNE SHAPE $K/L = 1/16$

DEPTH OF FLUME (IN.)	SECTION OR CURE	SLOPE OF FLUME (FT/FT)	DISCHARGE (CFS)	MEAN VELOCITY (FPS)	PROBE EL. ABOVE DATUM (IN.)	VELOCITY AT PROBE (FPS)	CHEZY'S C		KS (FT.)
							PROBE EL. ABOVE DATUM (IN.)	VELOCITY AT PROBE (FPS)	
3.75	C	0.0007	0.647	2.750	0.798	51.44	0.078773	*	0.053701
				2.250	0.809	0.060496	0.073299		
				1.750	0.730	0.064798	0.053701		
				1.250	0.692	0.064798	0.053701		
3.00	A	0.0007	0.285	0.598	3.250	0.805	48.75	0.079709	*
				2.750	0.809	0.066002	0.066002		
				2.250	0.758	0.072488	0.072488		
				1.750	0.747	0.059903	0.059903		
3.00	B	0.0007	0.285	0.598	1.250	0.690	0.059588	0.059588	*
				0.750	0.612	0.055724	0.055724	*	
				3.250	0.779	0.092952	0.092952	*	
				2.750	0.809	0.065859	0.065859		
3.00	C	0.0007	0.234	0.529	2.250	0.659	0.128093	*	0.080766
				1.750	0.743	0.061346	0.061346		
				1.250	0.713	0.051991	0.051991		
				0.750	0.609	0.056698	0.056698		
3.25	A	0.0007	0.234	0.529	3.250	0.778	0.093355	*	0.071781
				2.750	0.807	0.066720	0.066720		
				2.250	0.791	0.060044	0.060044		
				1.750	0.755	0.057364	0.057364		
3.25	B	0.0007	0.234	0.529	1.250	0.715	0.051655	0.051655	A-II
				0.750	0.641	0.047168	0.047168	*	
				2.750	0.710	0.103827	0.103827	*	
				2.250	0.682	0.100379	0.100379		
3.25	C	0.0007	0.234	0.529	1.750	0.673	0.082172	0.093688	0.095041
				1.250	0.607	0.086834	0.086834		
				0.750	0.533	0.080766	0.080766		
				0.750	0.553	0.071781	0.071781		

NOTE
THESE VALUES OF KS WHICH ARE MARKED WITH AN ASTERISK WERE NOT USED IN PLOTTING THE CHARACTERISTIC ROUGHNESS CURVES.

TABLE A-2 [CONTINUED]

DUNE SHAPE $K/L = 1/16$

DEPTH OF FLUME (IN.)	SECTION NUMBER C	SLOPE OF FLUME (FT/FT)	DISCHARGE (CFS)	MEAN VELOCITY (FPS)	PROBE EL. ABOVE DATUM (IN.)	VELOCITY AT PROBE (FPS)	CHEZY'S C	KS
3.25	C	0.0007	0.234	0.529	2.750	0.699	44.32	0.111242 *
					2.250	0.700	0.090210 *	0.090210 *
					1.750	0.668	0.084773	0.084773
					1.250	0.636	0.073160	0.073160
3.00	A	0.0007	0.157	0.482	2.750	0.635	41.63	0.144338 *
					2.250	0.664	0.092201 *	0.092201 *
					1.750	0.637	0.091012 *	0.091012 *
					1.250	0.596	0.083476	0.083476
3.00	B	0.0007	0.157	0.482	2.750	0.612	0.166398 *	0.166398 *
					2.250	0.613	0.135210 *	0.135210 *
					1.750	0.578	0.130171 *	0.130171 *
					1.250	0.518	0.133901 *	0.133901 *
3.00	C	0.0007	0.157	0.482	2.750	0.629	0.150078 *	0.150078 *
					2.250	0.659	0.102204 *	0.102204 *
					1.750	0.600	0.113433 *	0.113433 *
					1.250	0.556	0.105967 *	0.105967 *
2.75	A	0.0006	0.163	0.434	2.250	0.588	41.86	0.103179 *
					1.750	0.541	0.110549 *	0.110549 *
					1.250	0.513	0.095696	0.095696
					0.750	0.457	0.083897	0.083897
2.75	B	0.0006	0.163	0.434	2.250	0.591	0.101604 *	0.101604 *
					1.750	0.543	0.109142 *	0.109142 *
					1.250	0.492	0.110179 *	0.110179 *
					0.750	0.446	0.090601	0.090601
2.75	C	0.0006	0.163	0.434	2.250	0.606	0.091706	0.091706
					1.750	0.552	0.102895	0.102895
					1.250	0.485	0.115973	0.115973
					0.750	0.438	0.095366	0.095366

NOTE
THOSE VALUES OF KS WHICH ARE MARKED WITH AN ASTERISK * WERE NOT USED IN PLOTTING THE CHARACTERISTIC ROUGHNESS CURVES.

TABLE A-2 [CONTINUED]

DUNE SHAPE $K/L = 1/16$

DEPTH OF FLUM	SECTION ON DUNE	SLOPE OF FLUME	DISCHARGE FLUME	MEAN VELOCITY	PROBE EL. ABOVE DATUM	VELOCITY AT PROBE	CHEZY'S C		KS
							(IN.)	(FPS)	
2.56	A	0.0000	0.135	0.396	2.250	0.525	39.71	0.138026 *	*
					1.750	0.516		0.11433 *	
					1.250	0.490		0.098733	
					0.750	0.432		0.089241	
E					2.250	0.519		0.144413 *	*
					1.750	0.496		0.132114 *	
					1.250	0.475		0.109821 *	
					0.750	0.403		0.109241 *	
L					2.250	0.529		0.134402 *	*
					1.750	0.518		0.112920 *	
					1.250	0.484		0.102754	
					0.750	0.434		0.088062	
2.25	A	0.0000	0.110	0.360	1.750	0.497		0.112563	*
					1.250	0.480		0.091353	
					0.750	0.426		0.081522	
b					1.750	0.472		0.135949	*
					1.250	0.455		0.109418	
					0.750	0.403		0.096565	
C					1.750	0.497		0.112876	*
					1.250	0.480		0.091353	
					0.750	0.423		0.083585	

NOTE
THESE VALUES OF KS WHICH ARE MARKED WITH AN ASTERISK WERE NOT USED IN PLOTTING THE CHARACTERISTIC ROUGHNESS CURVES.

TABLE A-3
EXPERIMENTAL DATA

DUNE SHAPE $K/L = 1/24$

DEPTH OF FLUX (IN.)	SECTION OF FLUME (IN.)	DISCHARGE (CFS)	MEAN VELOCITY (FPS)	PROBE EL. ABOVE DATUM (IN.)	VELOCITY AT PROBE (FPS)	CHEZY'S C (FT.)	KS
4.75	A	0.0005	0.043	4.250	1.288	90.32	0.005844 *
				3.750	1.320		0.004530
		0.005	1.043	3.250	1.329		0.003780
				2.750	1.300		0.003832
				2.250	1.274		0.003675
				1.750	1.241		0.003497
				1.250	1.123		0.004808
				0.750	1.063		0.004366
				0.250	0.724		0.014221 *
4.20	A	0.0005	0.613	4.250	1.277		0.006164 *
				3.750	1.311		0.004725
		0.005	1.613	3.250	1.295		0.004563
				2.750	1.285		0.004168
				2.250	1.256		0.004072
				1.750	1.185		0.004748
				1.250	1.084		0.005938
				0.750	1.010		0.005665
4.00	A	0.0005	0.613	4.250	1.302		0.005460 *
				3.750	1.329		0.004313
		0.005	1.613	3.250	1.326		0.003846
				2.750	1.315		0.003501
				2.250	1.287		0.003398
				1.750	1.216		0.004044
				1.250	1.158		0.004109
				0.750	1.033		0.005080 *
3.50	A	0.0005	0.613	4.250	1.178	88.19	0.011393 *
				3.750	1.267		0.005245 *
		0.005	1.613	3.250	1.260		0.004856
				2.750	1.245		0.004550
				2.250	1.226		0.004240
				1.750	1.201		0.003881
				1.250	1.097		0.005082
				0.750	1.024		0.004846
				0.250	0.697		0.018157 *

NOTE
THOSE VALUES OF KS WHICH ARE MARKED WITH AN ASTERISK WERE NOT USED IN PLOTTING THE CHARACTERISTIC ROUGHNESS CURVES.

TABLE A-3 [CONTINUED]

DUNE SHAPE $K/L = 1/24$

DEPTH OF FLU DUNE (IN.)	SECTION UN DUNE (IN.)	SLOPE OF FLUME (FT/FT)	DISCHARGE (CFS)	MEAN VELOCITY (FPS)	PROBE EL. ABOVE DATUM (IN.)	VELOCITY AT PROBE (FPS)	CHEZY'S C	KS	PROBE EL. ABOVE DATUM (IN.)	
									(IN.)	(FT.)
4.026	E	0.00005	0.613	1.000	3.750	1.233	88.19	0.006207	*	*
					3.250	1.276		0.004472		
					2.750	1.220		0.005173		
					2.250	1.224		0.004293		
					1.750	1.141		0.005338		
	C				1.250	1.111		0.004727		
					0.750	0.939		0.007570	*	
					4.250	1.179		0.011211	*	
					3.750	1.250		0.005713	*	
					3.250	1.261		0.004819		
4.025	A	0.00005	0.551	0.952	3.750	1.176	85.61	0.007514	*	*
					3.250	1.168		0.006848	*	
					2.750	1.205		0.004966		
					2.250	1.207		0.004142		
					1.750	1.132		0.005003		
	B				1.250	1.080		0.004975		
					0.750	1.000		0.004958		
					0.250	0.773		0.006496	*	
					3.750	1.188		0.006951	*	
					3.250	1.208		0.005583		
4.024	C				2.750	1.172		0.005870		
					2.250	1.160		0.005320		
					1.750	1.078		0.006555		
	B				1.250	1.035		0.006244		
					0.750	0.903		0.008747	*	
					3.750	1.209		0.006207	*	
4.023	A				3.250	1.216		0.005379		
					2.750	1.237		0.004160		
					2.250	1.201		0.004279		
4.022	C				1.750	1.126		0.005179		

NOTE

THESE VALUES OF KS WHICH ARE MARKED WITH AN ASTERISK WERE NOT USED IN PLOTTING THE CHARACTERISTIC ROUGHNESS CURVES.

TABLE A-3 [continued]

DUNE SHAPE $K/L = 1/24$

DEPTH OF FLU. (IN.)	SECTION OR DUNE (IN.)	SLOPE OF FLURE (FT/FT)	DISCHARGE (CFS)	MEAN VELOCITY (FPS)	PROBE EL. ABOVE DATUM (IN.)	VELOCITY AT PROBE (FPS)	CHEZY'S C		KS (FT.)
							PROBE EL. ABOVE DATUM (IN.)	VELOCITY AT PROBE (FPS)	
4.25	C	6.0005	0.551	0.952	1.250 0.750	1.065 0.976	95.61	0.005370 0.005616	
4.000	A	0.0005	0.489	0.897	3.750 3.250 2.750 2.250 1.750 1.250 0.750 0.250	1.089 1.156 1.169 1.146 1.121 1.071 0.945 0.777	82.47	0.015713 0.006426 0.005274 0.005068 0.004690 0.004633 0.005942 0.005874	*
	B				3.750 3.250 2.750 2.250 1.750 1.250 0.750	1.077 1.138 1.150 1.085 1.044 0.984 0.874	0.020873 0.007086	*	
	C				3.750 3.250 2.750 2.250 1.750 1.250 0.750	1.110 1.157 1.183 1.167 1.108 1.065 0.933	0.011009 0.006376 0.004900 0.004495 0.005028 0.004810 0.006292	*	
3.75	A	0.0005	0.434	0.849	3.250 2.750 2.250 1.750 1.250 0.750 0.250	1.125 1.128 1.110 1.047 1.092 0.912 0.636	79.88	0.006611 0.005700 0.005336 0.006089 0.006236 0.006340 0.024055	*
	B				3.250 2.750	1.091 1.091	0.008146 0.006950	*	

NOTE
THOSE VALUES OF KS WHICH ARE MARKED WITH AN ASTERISK WERE NOT USED IN PLOTTING THE CHARACTERISTIC ROUGHNESS CURVES.

TABLE A-3 [CONTINUED]

DUNE SHAPE K/L = 1/24

DEPTH OF FLOW (IN.)	SECTION NUMBER L	SUCTION OF FLUME (FT/FT)	DISCHARGE (CFS)	MEAN VELOCITY (FPS)	PROBE EL. ABOVE DATUM (IN.)	VELOCITY AT PROBE (FPS)	CHEZY'S C	KS
3.75	b	0.0005	0.434	0.849	2.250 1.750 1.250 0.750	1.051 0.990 0.954 0.860	79.88 0.007326 0.008719 0.007765 0.008890	
					3.250 2.750 2.250 1.750 1.250 0.750	1.121 1.122 1.106 1.092 1.008 0.924	0.006761 0.005880 0.005478 0.004786 0.005737 0.005946	
3.00	A	0.0005	0.395	0.829	3.250 2.750 2.250 1.750 1.250 0.750 0.250	1.009 1.086 1.048 1.036 1.024 0.875 0.592	79.97 0.016749 0.006176 0.006539 0.005663 0.005740 0.006871 0.002873 *	
	b				3.250 2.750 2.250 1.750 1.250 0.750	1.007 1.058 1.033 0.977 0.920 0.811	0.017479 0.007193 0.007017 0.007890 0.008355 0.012127 *	
3.25	A	0.0005	0.349	0.787	3.250 2.750 2.250 1.750 1.250 0.750	1.033 1.078 1.055 1.024 1.057 0.907	0.011100 0.006439 0.006209 0.006025 0.006626 0.005804	
							0.005804	

NOTE

THOSE VALUES OF KS WHICH ARE MARKED WITH AN ASTERISK WERE NOT USED IN PLOTTING THE CHARACTERISTIC ROUGHNESS CURVES.

TABLE A-3 [CONTINUED]

DUNE SHAPE $N/L = 1/24$

DEPTH OR FLDN (IN.)	SECTION UN UNIT	SLOPE OF FLDN (FT/FT)	DISCHARGE (CFS)	MEAN VELOCITY (FPS)	PROBE EL. ABOVE DATUM (IN.)	VELOCITY AT PROBE (FPS)	CHEZY'S C	KS	DUNE SHAPE $N/L = 1/24$	
									(IN.)	(FT.)
2.25	A	0.0005	0.349	0.787	0.750 0.250	0.816 0.582	78.04	0.008724 0.042675 *		
	B				2.750 2.250 1.750 1.250 0.750	0.936 0.941 0.883 0.846 0.782		0.027544 *		
	C				2.750 2.250 1.750 1.250 0.750	0.976 0.989 0.954 0.891 0.794		0.011502 0.007752 0.007706 0.008566 0.010916		
3.00	A	0.0005	0.306	0.748	2.750 2.250 1.750 1.250 0.750 0.250	0.933 0.959 0.919 0.862 0.770 0.566	76.47	0.013896 *		
	E				2.750 2.250 1.750 1.250 0.750	0.904 0.921 0.898 0.825 0.734		0.028570 *		
	C				2.750 2.250 1.750 1.250 0.750	0.942 0.962 0.940 0.869 0.787		0.012008 * 0.007669 0.007092 0.008285 0.008995		
2.75	A	0.0006	0.278	0.743	2.250 1.750 1.250 0.750	0.909 0.909 0.846 0.794	71.67	0.086389 * 0.020307 0.030904 0.016276		

NOTE
THOSE VALUES OF KS WHICH ARE MARKED WITH AN ASTERISK ARE NOT USED IN PLOTTING THE CHARACTERISTIC ROUGHNESS CURVES.

TABLE A-3 [CONTINUED]

DUNE SHAPE K/L = 1/24

WEPln C _r FLin (IN.)	SECTION OR DUNE	STURF OF FLUID	DISCHARGE	MEAN VELOCITY	PROBE EL. ABOVE DATUM	VELOCITY AT PROBE	CHEZY'S C	KS
			(LFS)	(FPS)	(IN.)	(FPS)	(FT.)	
2.75	A	0.0006	0.278	0.743	0.250	0.541	71.67	0.015793
	E				2.250	0.674		0.014830
					1.750	0.857	0.212778 *	
					1.250	0.799	0.013649	
					0.750	0.721	0.013919	
	C				2.250	0.926	0.040009 *	
					1.750	0.932	0.012686	
					1.250	0.662	0.012818	
					0.750	0.789	0.018356	
2.056	A	0.0007	0.265	0.777	2.250	0.935	72.03	0.223349 *
	E				1.750	0.961		0.016011
					1.250	0.659	0.096389 *	
					0.750	0.810	0.027945	
					0.250	0.559	0.016220	
	C				2.250	0.895	0.016219	
					1.750	0.882	0.013751	
					1.350	0.837	0.014221	
					0.750	0.759	0.013188	
	b				2.250	0.952	0.081710 *	
					1.750	0.562	0.015506	
					1.250	0.914	0.014541	
					0.750	0.813	0.025134	
2.025	A	0.0009	0.248	0.809	1.750	1.001	69.04	0.097520 *
	E				1.250	0.958		0.053536
					0.750	0.868		0.068114 *
					0.250	0.652	0.012379	
	b				1.750	0.937	0.015618	
					1.250	0.869	0.016814	
					0.750	0.790	0.016201	
	C				1.750	1.005		0.080986 *

Note

THESE VALUES OF KS WHICH ARE MARKED WITH AN ASTERISK WERE NOT USED IN PLOTTING THE CHARACTERISTIC ROUGHNESS CURVES.

TABLE A-3 [CONTINUED]

DUNE SHAPE $K/L = 1/24$

DRAIN LF F.L.	SECTION ON DRAIN F.L.	SLOPE LF FLUME (IN/FT)	DISCHARGE (CFS)	MEAN VELOCITY (FPS)	PROBE EL. ABOVE DATUM (IN.)	VELOCITY AT PROBE (FPS)	CHEZY'S C	KS
2.25	C	0.0005	0.248	0.809	1.250 0.750	0.977 0.875	69.04	0.027120 0.050787 *

NOTE
THOSE VALUES OF KS WHICH ARE MARKED WITH AN ASTERISK WERE NOT USED IN PLOTTING THE CHARACTERISTIC ROUGHNESS CURVES.

TABLE A-4
EXPERIMENTAL DATA

CUNAE SHAPE $K/L = 1/32$

DEPTH L/F FL/L	SECTION UN LINE	SLOPE L/F FL/UN	DISCHARGE CFS	MEAN VELOCITY FT/FT	PROBE ABOVE DATUM IN.	VELOCITY AT PROBE FPS	CHEZY'S C	KS	(FT.)	
									(CFS)	(IN.)
4.0/15	A	0.0003	0.027	0.909	4.250	1.185	108.28	0.001214 *		
					3.750	1.221		0.000808		
					3.250	1.219		0.000713		
					2.750	1.221		0.000593		
					2.250	1.191		0.000613		
					1.750	1.167		0.000580		
					1.250	1.096		0.000722		
					0.750	1.026		0.000755		
					0.250	0.754		0.002442 *		
					4.250	1.175		0.001442 *		
					3.750	1.185		0.001171		
					3.250	1.214		0.000805		
					2.750	1.163		0.001023		
					2.250	1.170		0.000794		
					1.750	1.135		0.000811		
					1.250	1.056		0.001001		
					0.750	1.017		0.000878		
					4.250	1.170		0.001549 *		
					3.750	1.213		0.000935 *		
					3.250	1.254		0.000611		
					2.750	1.227		0.000638		
					2.250	1.227		0.000522		
					1.750	1.179		0.000594		
					1.250	1.144		0.000561		
					0.750	1.080		0.000554		
					4.250	1.093		0.002396 *		
					3.750	1.085	104.90	0.002641 *		
					3.250	1.156		0.002118 *		
					2.750	1.132		0.001485		
					2.250	1.156		0.001544		
					1.750	1.159		0.001233		
					1.250	1.126		0.001251		
					0.750	1.078		0.001316		
					0.250	1.034		0.001125		
					0.750	0.765		0.001952 *		
					4.250	1.075		0.002396 *		

NOTE: THOSE VALUES OF KS WHICH ARE MARKED WITH AN ASTERISK WERE NOT USED IN PLOTTING THE CHARACTERISTIC ROUGHNESS CURVES.

TABLE A-4 [CONTINUED]

DUNE SHAPE $K/L = 1/32$

DEPTH (IN.)	SETTLEMENT CH. FLUID LEVEL (IN.)	SLURRY OF FLUID (FL/FT)	DISCHARGE VELOCITY (CFS)	MEAN VELOCITY (CFS)	DISCHARGE VELOCITY (FPS)	PROBE EL. ABOVE DATUM (IN.)	VELOCITY AT PROBE (FPS)	CHEZY'S C	KS
4.056	b	0.5003	0.505	0.921	3.750	1.160	104.90	0.002223	*
					3.250	1.178		0.001671	
					2.750	1.131		0.002051	
					2.250	1.114		0.001923	
					1.750	1.069		0.002143	
					1.250	1.037		0.001992	
					0.750	0.967		0.002084	
					4.250	1.075		0.002886	*
					3.750	1.156		0.002291	*
					3.250	1.182		0.001612	
					2.750	1.156		0.001675	
					2.250	1.178		0.001153	
					1.750	1.115		0.001478	
					1.250	1.143		0.000845	
					0.750	1.049		0.001078	
4.025	A	0.5003	0.510	0.680	3.750	1.082	102.23	0.001921	*
					3.250	1.123		0.001482	
					2.750	1.099		0.001532	
					2.250	1.093		0.001313	
					1.750	1.054		0.001403	
					1.250	1.029		0.001236	
					0.750	0.978		0.001125	
					0.250	0.742		0.002092	*
					3.750	1.054		0.002490	*
					3.250	1.092		0.002390	
					2.750	1.078		0.002267	
					2.250	1.051		0.002330	
					1.750	0.997		0.001774	
					1.250	1.016		0.001719	
					0.750	0.882		0.001977	*
					3.750	1.085		0.001866	*
					3.250	1.127		0.001406	
					2.750	1.080		0.001749	*
					2.250	1.100		0.001208	
					1.750	1.068		0.001225	

NOTE
THOSE VALUES OF KS WHICH ARE MARKED WITH AN ASTERISK WERE NOT USED IN PLOTTING THE CHARACTERISTIC ROUGHNESS CURVES.

TABLE A-4 [CONTINUED]

DUNE SHAPE $R/L = 1/32$

DEPTH OF FLU. (IN.)	SECTION IN FLU. (IN.)	SLOPE OF FLU. (IN/FT)	DISCHARGE (CFS)	MEAN VELOCITY (FPS)	PROBE EL. ABOVE DATUM (IN.)	VELOCITY AT PROBE (FPS)	CHEZY'S C		KS
							(IN.)	(FT.)	
4.25	C	0.0003	6.510	0.880	1.250 0.750	1.046 0.970	102.23	0.001046 0.001174	
4.00	A	0.0003	0.448	0.622	3.750 3.250 2.750 2.250 1.750	0.968 1.032 1.071 1.002 1.017	97.47	0.004457 0.002112 0.003336	*
3.75	A	0.0003	0.407	0.795	3.750 3.250 2.750 2.250 1.750 1.250 0.750 0.250	0.936 0.695 0.695 0.720	100.70 0.001770 0.003950 0.002222	0.001847 0.003342	*
3.50	b	0.0003	0.375	0.982	3.750 3.250	0.982 1.010	99.50 0.002597	0.003950 0.002597	*
3.25	b	0.0003	0.343	1.023	2.750 2.250 1.750 1.250 0.750	1.023 0.989 1.014 0.914 0.828	101.99 0.002091 0.003040 0.002188 0.002776	0.001899 0.004620 0.005146 0.001658	*
3.00	b	0.0003	0.311	0.937	3.750 3.250 2.750 2.250 1.750 1.250 0.750	0.937 1.020 1.033 1.039 0.996 0.942 0.908	103.70 0.002364 0.001715 0.004620 0.005146 0.001658 0.004610	0.005701 0.002364 0.001715 0.004620 0.005146 0.001658	*
2.75	b	0.0003	0.279	1.006	3.250 2.750 2.250	1.006 1.019 0.993	96.58	0.002155 0.002149 0.002197	
2.50	b	0.0003	0.247	1.019	2.750 2.250	1.019 0.952		0.002149 0.001729 0.001896 0.002183	
2.25	b	0.0003	0.215	0.981	2.250	0.981		0.002633 0.002124	
2.00	b	0.0003	0.183	0.908	2.00	0.908			

NOTE

THOSE VALUES OF C_{FS} WHICH ARE MARKED WITH AN ASTERISK WERE NOT USED IN PLOTTING THE CHARACTERISTIC ROUGHNESS CURVES.

TABLE A-4 [CONTINUED]

WELL SHAPE S/L = 1/32

DEPTH (FT) (IN.)	SECTION NO. 1	SLOPE OF FLUME WALL (FT/FT)	DISCHARGE FLUME (CFS)	MEAN VELOCITY (FPS)	PROBE EL. ABOVE DATUM (IN.)	VELOCITY AT PROBE (FPS)	CHEZY'S C	KS
3.75	b	0.00035	0.407	3.795	2.250	0.981	96.58	0.001807
					1.750	0.934		0.002139
	c	0.00035	0.407	3.795	1.250	0.924		0.002604
					0.750	0.852		0.001816
	b	0.00044	0.375	3.786	3.250	1.016		0.001955
					2.750	1.011		0.001678
	c	0.00044	0.375	3.786	2.250	0.993		0.001956
					1.750	1.000		0.001473
	b	0.00044	0.375	3.786	1.250	0.938		0.001786
					0.750	0.864		0.002022
	c	0.00044	0.375	3.786	3.250	0.963	84.74	0.007572 *
					2.750	1.011		0.004886 *
	b	0.00044	0.375	3.786	2.250	0.993		0.004455 *
					1.750	0.983		0.003739
	c	0.00044	0.375	3.786	1.250	0.944		0.003733
					0.750	0.889		0.003374
	b	0.00044	0.375	3.786	3.250	0.943		0.004933 *
					2.750	0.980		0.008680 *
	c	0.00044	0.375	3.786	2.250	0.973		0.006001 *
					1.750	0.956		0.005132
	b	0.00044	0.375	3.786	1.250	0.930		0.004747
					0.750	0.835		0.004148
	c	0.00044	0.375	3.786	3.250	0.936		0.005059
					2.750	1.024		0.009189 *
	b	0.00044	0.375	3.786	2.250	0.993		0.004456
					1.750	0.970		0.004617
	c	0.00044	0.375	3.786	1.250	0.935		0.004298
					0.750	0.872		0.003995
	b	0.00044	0.331	3.747	3.250	0.954		0.006006 *
					2.750	0.941		0.005543
	c	0.00044	0.331	3.747	2.250	0.910		0.005467
					1.750	0.894		0.004500

NOTE
THOSE VALUES OF KS WHICH ARE MARKED WITH AN ASTERISK WERE NOT USED IN PLOTTING THE CHARACTERISTIC ROUGHNESS CURVES.

TABLE A-4 [CONTINUED]

DUNE SHAPE $\kappa/L = 1/32$

DEPTH IN FT	SECTION NO. LINE	SLANT OF FLAT	DISCHARGE CFS	MEAN VELOCITY CFS	PROBE EL. ABOVE DATUM	VELOCITY AT PROBE	CHEZY'S C		KS
							(IN.)	(FPS)	
2.02	A	0.0004	0.331	0.747	0.750 0.250	0.816 0.652	82.77	0.004944 0.005838 *	
	E				2.750 2.250 1.750 1.250 0.750	0.909 0.926 0.869 0.845 0.788		0.007942 * 0.006091 * 0.007110 * 0.006318 * 0.0036015 *	
	C				2.750 2.250 1.750 1.250 0.750	0.930 0.952 0.931 0.898 0.818		0.006974 * 0.005124 * 0.004727 * 0.004384 * 0.004890	
	A	0.0004	0.296	0.725	2.750 2.250 1.750 1.250 0.750	0.852 0.881 0.866 0.833 0.774	82.80	0.010048 * 0.006842 * 0.006196 * 0.005814 * 0.005644 *	
	E				0.250	0.616		0.006521 *	
	C				2.750 2.250 1.750 1.250 0.750	0.835 0.858 0.829 0.785		0.012088 * 0.007923 * 0.007813 * 0.007948	
	A	0.0004	0.677	2.250 1.750 1.250 0.750	0.845 0.624 0.793 0.756		0.010234 * 0.005674 * 0.005965 * 0.005396 *		
2.01								0.005764	

NOTE
THESE VALUES OF KS WHICH ARE MARKED WITH AN ASTERISK WERE NOT USED IN PLOTTING THE CHARACTERISTIC ROUGHNESS CURVES.

TABLE A-4 [CONTINUED]

DUNE SHAPE $K/L = 1/32$

DEPTH OF FLUME (IN.)	SECTION ON DUNE (IN.)	SLOPE OF FLUME (FT/FT)	DISCHARGE (CFS)	MEAN VELOCITY (FPS)	PROBE EL. ABOVE DATUM (IN.)	VELOCITY AT PROBE (FPS)	CHEZY'S C		KS	
							(IN.)	(FT.)		
2.75	A	0.0004	0.254	0.677	0.250	0.580	79.95	0.007265 *	*	
					2.250	0.825	0.008234 *	0.008234 *		
					1.750	0.797		0.008109 *		
2.50	A	0.0005	0.238	0.700	2.250	0.825	0.007283	0.007283	*	
					1.750	0.830		0.006910		
					1.250	0.773		0.006910		
2.25	A	0.0006	0.223	0.728	2.250	0.794	0.008054	0.008054	*	
					1.750	0.847		0.008657		
					1.250	0.816		0.007940		
2.00	A	0.0007	0.218	0.750	2.250	0.794	0.0051460 *	0.0051460 *	*	
					1.750	0.858		0.008027		
					1.250	0.830		0.007283		
1.75	A	0.0008	0.213	0.778	2.250	0.826	0.008657	0.008657	*	
					1.750	0.882		0.007940		
					1.250	0.854		0.008593		
1.50	A	0.0009	0.208	0.800	2.250	0.799	0.005889	0.005889	*	
					1.750	0.892		0.017556 *		
					1.250	0.826		0.006906		
1.25	A	0.0010	0.203	0.822	2.250	0.632	0.006311	0.006311	*	
					1.750	0.911		0.007475		
					1.250	0.892		0.006414		
1.00	A	0.0011	0.198	0.844	2.250	0.750	0.006263	0.006263	*	
					1.750	0.858		0.011911		
					1.250	0.834		0.009335		
0.75	A	0.0012	0.193	0.866	2.250	0.734	0.006668	0.006668	*	
					1.750	0.906		0.007704		
					1.250	0.878		0.007704		

NOTE
THESE VALUES OF KS WHICH ARE MARKED WITH AN ASTERISK * WERE NOT USED IN PLOTTING THE CHARACTERISTIC ROUGHNESS CURVES.

TABLE A-4 [CONTINUED]

DUNE SHAPE $K/L = 1/32$

DEPTH IN FLUID (IN.)	SECTION IN FLUID (IN.)	SLOPE OF FLUME	DISCHARGE (CFS)	MEAN VELOCITY (FPS)	PROBE EL. ABOVE DATUM (IN.)	VELOCITY AT PROBE (FPS)	CHEZY'S C (FT.)	KS
2.025	C	0.223	0.726	1.250 0.750	0.902 0.832	76.10	0.006034 0.006061	

NOTE
THOSE VALUES OF KS WHICH ARE MARKED WITH AN ASTERISK WERE NOT USED IN PLOTTING THE CHARACTERISTIC ROUGHNESS CURVES.

TABLE A-5
EXPERIMENTAL DATA

DUNE SHAPE $K/L = 1/4$

DEPTH OF FLUID (IN.)	SECTION ON DUNE (IN.)	SLOPE OF FLUME (FT/FT)	DISCHARGE (CFS)	MEAN VELOCITY (FPS)	PROBE EL. ABOVE DATUM (IN.)	VELOCITY AT PROBE (FPS)	CHEZY'S C (FT.)	KS
4.075	A	0.0002	0.947	4.250	1.120	129.70	0.000053	*
				3.750	1.145		0.000037	
				3.250	1.134		0.000035	
				2.750	1.080		0.000050	
				2.250	1.105		0.000032	
				1.750	1.068		0.000036	
				1.250	0.970		0.000066	
				0.750	0.958		0.000044	
				0.250	0.733		0.000124	*
4.075	B	0.0002	0.947	4.250	1.105		0.000070	*
				3.750	1.123		0.000052	
				3.250	1.136		0.000040	
				2.750	1.116		0.000040	
				2.250	1.091		0.000043	
				1.750	1.060		0.000045	
				1.250	1.005		0.000054	
				0.750	0.933		0.000065	
				0.500	0.835		0.000112	*
4.075	C	0.0002	0.947	4.250	1.138		0.000037	*
				3.750	1.170		0.000024	
				3.250	1.131		0.000030	
				2.750	1.197		0.000014	
				2.250	1.104		0.000027	
				1.750	1.090		0.000024	
				1.250	1.050		0.000026	
				0.750	0.971		0.000033	
4.045	A	0.0002	0.945	3.750	1.004	120.13	0.000175	*
				3.250	1.023		0.000125	
				2.750	1.004		0.000128	
				2.250	0.944		0.000190	
				1.750	0.928		0.000175	
				1.250	0.901		0.000163	
				0.750	0.891		0.000108	
				0.250	0.672		0.000325	*
				3.750	1.000		0.000187	*

NOTE
THE VALUES OF K WHICH ARE MARKED WITH AN ASTERISK WERE NOT USED IN PLOTTING THE CHARACTERISTIC ROUGHNESS CURVES.

TABLE A-5 [CONTINUED]

DUNE SHAPE $K/L = 1/40$

DEPTH L _f FLC _u (IN.)	SECTION U. L _u (IN.)	SLOPE OF FLUME (FT/FT)	DISCHARGE (CFS)	MEAN VELOCITY (FPS)	PROBE EL. ABOVE DATUM (IN.)	VELOCITY AT PROBE (FPS)	CHEZY'S C		KS (FT.)
							PROBE EL. ABOVE DATUM (IN.)	VELOCITY AT PROBE (FPS)	
4.25	b	0.002	0.484	0.845	3.250	1.002	120.13	0.000160	
					2.750	1.014		0.000120	
					2.250	0.992		0.000122	
					1.750	0.923		0.000190	
					1.250	0.903		0.000166	
					0.750	0.820		0.000228	
					0.250	0.742		0.000166	
					3.750	1.023			
					3.250	1.016		0.000120	*
					2.750	1.012		0.000111	
					2.250	0.985		0.000098	
					1.750	0.983		0.000104	
					1.250	0.983		0.000083	
					1.250	0.922		0.000109	
					0.750	0.886		0.000094	
					0.500	0.790		0.000164	*
5.75	a	0.002	0.365	0.715	3.250	0.932	106.26	0.000227	
					2.750	0.918		0.000222	
					2.250	0.907		0.000205	
					1.750	0.882		0.000207	
					1.250	0.842		0.000225	
					0.750	0.760		0.000317	*
					0.250	0.551		0.002842	*
					3.250	0.889		0.000563	
					2.750	0.884		0.000500	
					2.250	0.858		0.000535	
					1.750	0.839		0.000509	
					1.250	0.798		0.000559	
					0.750	0.732		0.000672	*
					0.500	0.669		0.000866	*
					3.250	0.901		0.000434	
					2.750	0.907		0.000343	
					2.250	0.921		0.000243	
					1.750	0.883		0.000284	
					1.250	0.799		0.000487	
					0.750	0.760		0.000440	

NOTE
THOSE VALUES OF KS WHICH ARE MARKED WITH AN ASTERISK WERE NOT USED IN PLOTTING THE CHARACTERISTIC ROUGHNESS CURVES.

TABLE A-5 [CONTINUED]

DPIH of Flow (in.)	SECTION No. of Duct (in.)	SLUPE of Flow (ft/ft)	DISCHARGE FLUME (CFS)	MEAN VELOCITY (FPS)	PROBE EL. ABOVE DATUM (IN.)	VELOCITY AT PROBE (FPS)	CHEZY'S C		KS
							(IN.)	(FT.)	
2.025	A	0.0002	0.303	0.634	2.750	0.824	107.30	0.000584 *	
					2.250	0.641		0.000394	
					1.750	0.823		0.000373	
					1.250	0.799		0.000348	
					0.750	0.738		0.000410	
					0.250	0.545		0.002129 *	
					2.750	0.793		0.001156 *	
					2.250	0.794		0.000938	
					1.750	0.755		0.001115	
					1.250	0.732		0.001027	
					0.750	0.648		0.001565	
					0.500	0.621		0.001397	
					2.750	0.826		0.000551 *	
					2.250	0.823		0.000466	
					1.750	0.805		0.000443	
					1.250	0.767		0.000481	
					0.750	0.716		0.000507	
					2.250	0.731		0.000977	
					1.750	0.724		0.000830	
					1.250	0.692		0.000865	
					0.750	0.602		0.001499	
					0.500	0.565		0.002247	
					2.250	0.786		0.000267	
					1.750	0.766		0.000264	
					1.250	0.734		0.000275	
					0.750	0.665		0.000372	
2.025	A	0.0005	0.227	0.607	2.250	0.728	101.39	0.001049	
					1.750	0.725		0.000841	
					1.250	0.683		0.000992	
					0.750	0.642		0.000966	
					0.250	0.436		0.005734 *	
					2.250	0.731		0.000977	
					1.750	0.724		0.000830	
					1.250	0.692		0.000865	
					0.750	0.602		0.001499	
					0.500	0.565		0.002247	
					2.250	0.786		0.000267	
					1.750	0.766		0.000264	
					1.250	0.734		0.000275	
					0.750	0.665		0.000372	
					2.250	0.919		0.004078	
					1.750				

NOTE
THOSE VALUES OF KS WHICH ARE MARKED WITH AN ASTERISK WERE NOT USED IN PLOTTING THE CHARACTERISTIC ROUGHNESS CURVES.

TABLE A-5 [CONTINUED]

DUNE SHAPE $K/L = 1/40$

DEPTH OF FLUID (IN.)	SECTION NUMBER DUNE NUMBER (IN.)	SULPHT OF FLUID (FT/FT)	DISCHARGE (CFS)	MEAN VELOCITY (FPS)	PROBE EL. ABOVE DATUM (IN.)	VELOCITY AT PROBE (FPS)	CHEMYS C	KS
2.25	A	0.0005	0.227	0.741	1.250	0.906	84.91	0.003209
					0.750	0.824		0.003770
					0.250	0.616		0.006485 *
b					1.750	0.883		0.005440
					1.250	0.868		0.004424
					0.750	0.757		0.006269
					0.500	0.702		0.006468
c					1.750	0.959		0.002886
					1.250	0.935		0.002448
					0.750	0.871		0.002474
1.75	b	0.0005	0.193	0.609	1.500	0.972	81.29	0.005717 *
					1.250	1.001		0.004051
					1.000	0.985		0.003633
					0.750	0.956		0.003335
					0.500	0.903		0.003224
b					0.250	0.745		0.004906 *
					1.500	0.937		0.006943 *
					1.250	0.943		0.005824
					1.000	0.904		0.006091
c					0.750	0.866		0.005981
					0.500	0.772		0.007371 *
					1.500	1.014		0.004423 *
					1.250	1.033		0.003227
1.25	A	0.0010	0.110	0.647	1.000	0.756	67.32	0.022681 *
					0.750	0.783		0.008345
					0.500	0.771		0.006416
					0.250	0.673		0.006515
					0.0	0.446		0.0

NOTE
THOSE VALUES OF KS WHICH ARE MARKED WITH AN ASTERISK WERE NOT USED IN PLOTTING THE CHARACTERISTIC ROUGHNESS CURVES.

TABLE A-5 [CONTINUED]

DRYING SHAPE $K/1 = 1/40$

DEPTH OF FLUID (IN.)	SECTION OF CHANNEL (IN.)	SLOPE OF FLUID FLANE (FT/FT)	DISCHARGE OF FLUID (CFS)	MEAN VELOCITY AT PROBE (FPS)	PROBE EL. ABOVE DATUM (IN.)	VELOCITY AT CHEZY'S C PROBE (FPS)	KS	UNIT SHAPE R/L = 1/40	
								(FT.)	(FT.)
1.025	b	0.0010	0.110	0.647	1.000	0.680	67.32	0.017141	*
					0.750	0.693		0.055831	*
					0.500	0.655		0.027063	*
					0.250	0.616		0.009580	*
	c								
					1.000	0.765		0.017881	*
					0.750	0.650		0.005581	
					0.500	0.825		0.004583	

הנְּצָר
הנְּצָר

TABLE A-6
EXPERIMENTAL DATA

BUXT SHAPE $K/L = 1/8R$

DET IN ($\frac{L}{R}$)	SECTION IN BUXT (in.)	SLOPE OF FLUX (F_1/F_2)	DISCHARGE (Q)	MEAN VELOCITY (Q/F_1)	PROBE EL. ABOVE DATUM ($IN.$)	VELOCITY AT PROBE ($IN./SEC$)	CHEZY'S C	KS
4.75	4	0.0014	0.510	3.798	4.250	0.935	40.76	0.352527 *
					3.750	0.928		0.318426 *
					3.250	0.919		0.286384
					2.750	0.961		0.276879
					2.250	0.858		0.246348
					1.750	0.822		0.218625
					1.250	0.742		0.209266
					0.750	0.599		0.211957
					4.250	0.933		0.354958 *
					3.750	0.921		0.327279
					3.250	0.902		0.303400
					2.750	0.870		0.288533
					2.250	0.843		0.260985
					1.750	0.721		0.315975
					1.250	0.701		0.242749
					0.750	0.605		0.206778
					4.250	0.917		0.375532 *
					3.750	0.903		0.251722 *
					3.250	0.889		0.221178
					2.750	0.971		0.199912
					2.250	0.689		0.221307
					1.750	0.869		0.185133
					1.250	0.805		0.166123
					0.750	0.654		0.172948
					4.250	0.730		0.345122 *
					3.750	0.923		0.240706 *
					3.250	0.987		0.213336
					2.750	0.981		0.218674
					2.250	0.899		0.199935
					1.750	0.841		0.192817
					1.250	0.743		0.193797
					0.750	0.647		0.170157
					4.250	0.448		0.357413 *
					3.750	0.914		0.277647 *
					3.250	0.948		0.231378

NOTE
THESE VALUES IF K/L WHICH ARE MARKED WITH AN ASTERISK WERE NOT USED IN PLOTTING THE CHARACTERISTIC DRAUGHNESS CURVES.

TABLE A-6 [CONTINUED]

DUNE SHAPE K/L = 1/8R	SECTION NO.	SECTION LINE (ft.)	SLOPE OF FLUME (ft./ft.)	DISCHARGE FLUME (CFS)	MAN VELOCITY (FPS)	PROBE EL. ABOVE DATUM (IN.)	VELOCITY AT PROBE (FPS)	CHEZY'S C	KS
4.025	B	0.0014	0.448	0.730	2.750	0.937	38.49	0.212340	
					2.250	0.910		0.192154	
					1.750	0.793		0.230652	
					1.250	0.724		0.212554	
					0.750	0.631		0.180713	
	C				4.250	0.903		0.372220	*
					3.750	0.967		0.258517	
					3.250	0.943		0.245399	
					2.750	0.926		0.220828	
					2.250	0.666		0.226348	
4.025	D	0.0014	0.543	0.678	1.750	0.802		0.222720	
					1.250	0.747		0.195705	
					0.750	0.658		0.163388	
	E				3.750	0.933	36.45	0.274000	*
					3.250	0.942		0.229468	
					2.750	0.921		0.210026	
					2.250	0.835		0.237954	
					1.750	0.803		0.208955	
4.025	F	0.0014	0.543	0.678	1.250	0.751		0.182017	
					0.750	0.654		0.157846	*
	G				3.750	0.929		0.279735	*
					3.250	0.929		0.241570	
					2.750	0.913		0.216729	
					2.250	0.859		0.217796	
					1.750	0.826		0.191527	
	H				1.250	0.699		0.221972	
					0.750	0.611		0.185746	

NOTE

THESE VALUES OF KS WHICH ARE MARKED WITH AN ASTERISK WERE NOT USED IN PLOTTING THE CHARACTERISTIC ROUGHNESS CURVES.

TABLE A-6 [CONTINUE]

DUNE SHAPE $K/L = 1/3R$

LENGTH OF FLL. (IN.)	SECTION IN DUNE FLLE	SLOPE OF FLLE	DISCHARGE	MEAN VELOCITY	PROBE EL. ABOVE DATUM	VELOCITY AT PROBE	CHEZY'S C	KS	C	
									(IN.)	(FPS)
4.000	A	0.0014	0.358	0.657	3.750	0.817	36.10	0.397267	*	
					3.250	0.872		0.278263	*	
					2.750	0.863		0.243841		
					2.250	0.843		0.216170		
					1.750	0.767		0.225498		
					1.250	0.671		0.233200		
					0.750	0.608		0.179031		
					3.750	0.813		0.404282	*	
					3.250	0.861		0.291133	*	
					2.750	0.874		0.234426		
					2.250	0.812		0.243633		
					1.750	0.784		0.210781		
					1.250	0.709		0.201846		
					0.750	0.592		0.189787		
					3.750	0.843		0.359758	*	
					3.250	0.897		0.253464		
					2.750	0.820		0.288791		
					2.250	0.805		0.250113		
					1.750	0.769		0.223444		
					1.250	0.703		0.206010		
					0.750	0.601		0.183526		
					3.750	0.814		0.351766		
					3.250	0.789		0.328464		
					2.750	0.816		0.280632		
					2.250	0.798		0.248302		
					1.750	0.725		0.248166		
					1.250	0.693		0.200940		
					0.750	0.560		0.204197		
					3.250	0.793		0.345007	*	
					2.750	0.768				
					2.250	0.757				
					1.750	0.735		0.238363		
					1.250	0.647		0.241436		
					0.750	0.517		0.242799		
					3.250	0.798				

NOTE
TABLE VALUES WHICH ARE MARKED WITH AN ASTERISK WERE NOT USED IN PLOTTING THE CHARACTERISTIC ROUGHNESS CURVES.

TABLE A-6 [CONTINUED]

DEPTH L _f FLL _n (IN.)	SECTION NUMBER A _n	SLOPE OF FLL _n (FT/FT)	DISCHARGE (CFS)	MEAN VELOCITY (FPS)	PROBE EL. ABOVE DATUM (IN.)	VELOCITY AT PROBE (FPS)	CHEZY'S C		KS
							(FT.)	(FT.)	
3.72	C	0.0014	0.314	0.615	2.750	0.790	34.55	0.301224	
					2.250	0.793		0.244259	
					1.750	0.711		0.262649	
					1.250	0.663		0.226764	
					0.750	0.558		0.206034	
3.72	A	0.0014	0.269	0.563	3.250	0.719	32.47	0.438925	*
					2.750	0.694		0.411509	*
					2.250	0.683		0.351434	*
					1.750	0.648		0.315637	
					1.250	0.593		0.298023	
					C.750	0.497		0.249915	
3.72	B	0.0014	0.269	0.563	3.250	0.714	32.47	0.438925	*
					2.750	0.743		0.336738	*
					2.250	0.724		0.297428	
					1.750	0.659		0.301933	
					1.250	0.579		0.298344	
					0.750	0.507		0.239796	
3.72	C	0.0014	0.269	0.563	3.250	0.713	32.47	0.438925	*
					2.750	0.726		0.336738	*
					2.250	0.674		0.297428	
					1.750	0.632		0.301933	
					1.250	0.598		0.298344	
					0.750	0.516		0.239796	
3.72	D	0.0014	0.230	0.520	2.750	0.666	30.79	0.427959	*
					2.250	0.652		0.361304	*
					1.750	0.622		0.365143	*
					1.250	0.565		0.336597	
					0.750	0.502		0.276362	
								0.231501	
3.72	E	0.0014	0.230	0.520	2.750	0.649		0.457918	*
					2.250	0.654		0.367074	
					1.750	0.609		0.345380	
					1.250	0.536		0.334241	
					0.750	0.469		0.265370	

L_fL_n

LAST VALUES OF KS WHICH ARE MARKED WITH AN ASTERISK WERE NOT USED IN PLOTTING THE CHARACTERISTIC ROUGHNESS CURVES.

TABLE A-6 [CONTINUED]

DUNE SHAPE $K/L = 1/88$

DEPTH IN FT.	SECTION LINE LUM.	SLUPE OF FLUME	DISCHARGE	MEAN VELOCITY	PROBE EL. ABOVE DATUM	VELOCITY AT PROBE	CHEZY'S C	KS	A	
									(FT.)	(FT.)
3.025	C	0.0014	0.230	0.520	2.750	0.679	30.79	0.404391	*	
					2.250	0.675		0.334529		
					1.750	0.629		0.316746		
					1.250	0.575		0.282894		
					0.750	0.494		0.249182		
3.035	A	0.0014	0.193	0.472	2.750	0.619	28.82	0.480327	*	
					2.250	0.661		0.327710		
					1.750	0.593		0.356536		
					1.250	0.540		0.305941		
					0.750	0.470		0.249610		
3.045	B	0.0014	0.193	0.472	2.750	0.645		0.429772	*	
					2.250	0.628		0.378604		
					1.750	0.590		0.346325		
					1.250	0.522		0.331787		
					0.750	0.442		0.280771		
3.055	C	0.0014	0.193	0.472	2.750	0.624		0.469543	*	
					2.250	0.626		0.380451		
					1.750	0.606		0.323518		
					1.250	0.543		0.302487		
					0.750	0.456		0.263559		
3.075	A	0.0012	0.150	0.415	2.250	0.574	27.24	0.398410	*	
					1.750	0.555		0.338056		
					1.250	0.482		0.337892		
					0.750	0.438		0.248534		
3.085	B	0.0012	0.150	0.415	2.250	0.573		0.390104	*	
					1.750	0.544		0.356180		
					1.250	0.494		0.320140		
					0.750	0.402		0.293743		
3.095	C	0.0012	0.150	0.415	2.250	0.562		0.419770	*	
					1.750	0.549		0.347604		
					1.250	0.520		0.283905		
					0.750	0.413		0.273032		

NOTE

THESE VALUES OF KS WHICH ARE MARKED WITH AN ASTERISK WERE NOT USED IN PLOTTING THE CHARACTERISTIC ROUGHNESS CURVES.

TABLE A-6 [CONTINUED]

DUNE SHAPE $K/L = 1/8K$

DEPTH OF FLUME (IN.)	SECTION OF FLUME (IN.)	SLOPE OF FLUME (FT/FT)	DISCHARGE (CFS)	MEAN VELOCITY (FPS)	PROBE EL. ABOVE DATUM (IN.)	VELOCITY AT PROBE (FPS)	CHEZY'S KS	
							C	FT
2.50	A	0.0013	0.127	0.372	2.250	0.517	25.33	0.472882 *
					1.750	0.510		0.379274
					1.250	0.481		0.311366
B					0.750	0.398		0.278556
					2.250	0.510	0.488521 *	
					1.750	0.496	0.405508	
					1.250	0.461	0.343912	
C					0.750	0.393		0.285695
					2.250	0.524		0.456092 *
					1.750	0.520	0.362516	
					1.250	0.468	0.331701	
					0.750	0.413		0.259595
2.25	A	0.0013	0.163	0.337	1.750	0.557	23.94	0.270473
					1.250	0.529		0.222968
					0.750	0.453		0.194341
					1.750	0.556		0.270984
					1.250	0.510		0.244094
B					0.750	0.409		0.242779
					1.750	0.542		0.290568
					1.250	0.516		0.236392
					0.750	0.453		0.194341
C								

NOTE
THESE VALUES FOR KS WHICH ARE MARKED WITH AN ASTERISK ARE NOT USED IN PLOTTING THE CHARACTERISTIC ROUGHNESS CURVES.

TABLE A-7
EXPERIMENTAL DATA

LUNE SHAPE $K/L = 1/16R$

DEPTH OF FLOOR (in.)	SECTION NUMBER L-1	SLOPE OF LUNE (ft/ft)	DISCHARGE (CFS)	MEAN VELOCITY (FPS)	PROBE EL. ABOVE DATUM (IN.)	VELOCITY AT PROBE (FPS)	CHEZY'S KS	
							C	GS
4.075	A	0.0011	3.0965	0.873	4.0250	1.118	50.95	0.107206 *
					3.0750	1.178		0.073812 *
					3.0250	1.136		0.076101
					2.0750	1.142		0.062719
					2.0250	1.095		0.062193
					1.0750	1.022		0.065447
					1.0250	0.993		0.052676
					0.0750	0.903		0.044868
					4.0250	1.128		0.107811 *
					3.0750	1.127		0.091138 *
					3.0250	1.143		0.073892
					2.0750	1.119		0.068939
					2.0250	1.083		0.065457
					1.0750	1.039		0.061132
					1.0250	0.913		0.071603
					0.0750	0.848		0.057322
					4.0250	1.118		0.107206 *
					3.0750	1.168		0.076848
					3.0250	1.140		0.074815
					2.0750	1.164		0.057414
					2.0250	1.057		0.072735
					1.0750	1.063		0.055186
					1.0250	0.961		0.060095
					0.0750	0.895		0.047223
4.050	A	0.0011	0.498	0.809	4.0250	1.047	48.10	0.132257 *
					3.0750	1.110		0.089504 *
					3.0250	1.104		0.079556
					2.0750	1.080		0.074475
					2.0250	1.050		0.069249
					1.0750	0.988		0.069672
					1.0250	0.920		0.066231
					0.0750	0.830		0.057959
					4.0250	1.033		0.140437 *
					3.0750	1.108		0.090499 *
					3.0250	1.114		0.076355

NOTE
THESE VALUES OF KS WHICH ARE MARKED WITH AN ASTERISK WERE NOT USED IN PLOTTING THE CHARACTERISTIC ROUGHNESS CURVES.

TABLE A-7 [CONTINUED]

DUNE SHAPE $K/L = 1/16R$

NOTE.—THEST VALUES OF δ WHICH ARE MARKED WITH AN ASTERISK WERE NOT USED IN PLOTTING THE CHARACTERISTIC BRIGHTNESS CURVES.

TABLE A-7 [CONTINUED]

DUNE SHAPE $K/L = 1/16R$

DEPTH IN FT.	STATION IN FT.	SLOPE OF FLUME (IN/FT.)	DISCHARGE (CFS)	MEAN VELOCITY (FPS)	PROBE EL. ABOVE DATUM (IN.)	VELOCITY AT PROBE (FPS)	CHEZY'S C		KS
							(IN.)	(FT.)	
A									
4.00	0.3611	0.404	0.741	0.916	3.750	45.89	0.171799	*	
				0.968	3.250		0.118647		
				0.946	2.750		0.110629		
				0.883	2.250		0.119139		
				0.863	1.750		0.101274		
				0.802	1.250		0.094591		
				0.733	0.750		0.076696	*	
				0.888	3.750		0.194363	*	
				0.931	3.250		0.139638		
				0.893	2.750		0.139746		
				0.891	2.250		0.115282		
				0.855	1.750		0.105007		
				0.760	1.250		0.113545		
				0.702	0.750		0.087486	*	
				0.910	3.750		0.176963	*	
				0.957	3.250		0.124856		
				0.923	2.750		0.122309		
				0.903	2.250		0.109550		
				0.871	1.750		0.097835		
				0.829	1.250		0.083747		
				0.734	0.750		0.076193	*	
				0.653	3.250		0.180209	*	
				0.868	2.750		0.142792		
				0.823	2.250		0.142272		
				0.814	1.750		0.115608		
				0.710	1.250		0.130991		
				0.665	0.750		0.087982	*	
				0.839	3.250		0.191472	*	
				0.855	2.750		0.150951		
				0.825	2.250		0.141079		
				0.794	1.750		0.126400		
				0.728	1.250		0.121024		
				0.623	0.750		0.116161		
				0.845	3.250		0.186382	*	

Note

These values of C_s which are marked with an asterisk were not used in plotting the characteristic roughness curves.

TABLE A-7 [CONTINUED]

DEPTH OF FLUID (IN.)	SLOPE OF DUNES (IN.)	DISCHARGE (CU. FT./FT.)	MEAN VELOCITY (FPS)	PROBE EL. ABOVE DATUM (IN.)	VELOCITY AT PROBE (FPS)	CHEZY'S C		KS (FT.)
						PROBE EL. ABOVE DATUM (IN.)	VELOCITY AT PROBE (FPS)	
3.75	C	0.0011	0.674	2.750	0.860	42.74	0.147932	
				2.250	0.835		0.134808	
				1.750	0.797		0.124290	
				1.250	0.743		0.113331	
				0.750	0.669		0.094589 *	
3.50	A	0.0011	0.503	3.250	0.841	41.33	0.172797	
				2.750	0.822		0.159399	
				2.250	0.806		0.140470	
				1.750	0.787		0.119107	
				1.250	0.739		0.105940	
				0.750	0.644		0.098391	
3.25	B	0.0011	0.436	3.220	0.838		0.174597	
				2.750	0.804		0.173175	
				2.250	0.840		0.119835	
				1.750	0.779		0.123243	
				1.250	0.709		0.121634	
				0.750	0.613		0.113358	
3.00	C	0.0011	0.363	3.220	0.814		0.195327	
				2.750	0.826		0.156130	
				2.250	0.813		0.135936	
				1.750	0.781		0.122233	
				1.250	0.747		0.102166	
				0.750	0.662		0.090564 *	
2.75	D	0.0011	0.299	3.220	0.749		0.202084 *	
				2.750	0.747		0.166815	
				2.250	0.700		0.161980	
				1.750	0.651		0.145991	
				1.250	0.596		0.113712	
2.50	E	0.0011	0.235	2.750	0.742		0.209016 *	
				2.250	0.745		0.168901	
				1.750	0.710		0.154948	
				1.250	0.620		0.168567	
				0.750	0.558		0.135801	

NOTE
THOSE VALUES OF KS WHICH ARE MARKED WITH AN ASTERISK WERE NOT USED IN PLOTTING THE CHARACTERISTIC ROUGHNESS CURVES.

TABLE A-7 [CONTINUED]

DUNE SHAPE $K/L = 1/16R$

DEPTH OF FLUID (IN.)	SECTION OF DUNE (IN.)	SLOPE OF DUNE (FT/FT)	DISCHARGE (CFS)	MEAN VELOCITY (FPS)	PROBE EL. ABOVE DATUM (IN.)	VELOCITY AT PROBE (FPS)	CHEV'S C		KS (FT.)
							39.10	0.212382	
3.025	C	0.0011	0.299	0.585	2.750	0.739	39.10	0.212382	0.196062
					2.250	0.713			
					1.750	0.680			
					1.250	0.673			
					0.750	0.573			
3.040	A	0.0011	0.216	0.524	2.750	0.696	36.46	0.234170	0.226723
					2.250	0.662			
					1.750	0.656			
					1.250	0.638			
					0.750	0.570			
3.040	B	0.0011	0.216	0.524	2.750	0.644	0.301992 *	0.301992 *	0.181247
					2.250	0.685			
					1.750	0.635			
					1.250	0.606			
					0.750	0.495			
3.040	C	0.0011	0.216	0.524	2.750	0.677	0.257547 *	0.257547 *	0.141089
					2.250	0.691			
					1.750	0.657			
					1.250	0.583			
					0.750	0.548			
2.12	A	0.0011	0.176	0.471	2.250	0.607	33.54	0.267739	0.196925
					1.750	0.596			
					1.250	0.581			
					0.750	0.507			
2.12	B	0.0011	0.176	0.471	2.250	0.621	0.249160	0.249160	0.169493
					1.750	0.575			
					1.250	0.553			
					0.750	0.461			
2.12	C	0.0011	0.176	0.471	2.250	0.619	0.252006 *	0.252006 *	0.147087
					1.750	0.607			
					1.250	0.550			
					0.750	0.497			

NOTE
THESE VALUES OF KS WHICH ARE MARKED WITH AN ASTERISK WERE NOT USED IN PLOTTING THE CHARACTERISTIC ROUGHNESS CURVES.

TABLE A-7 [CONTINUED]

DOME SHAPE $K/L = 1/10 R$

DEPTH L FT M M	STITCH D FT E M	SLOPE UP FLUID (IN/FT)	DISCHARGE (CFS)	MEAN VELOCITY FT/SEC	PROBE EL. ABOVE DATUM (IN.)	VELOCITY AT PROBE (FPS)	CHEZY'S C		KS
							(IN.)	(FT.)	
2.50	A	0.0011	0.145	0.425	2.250	0.546	31.42	0.326874	*
					1.750	0.539		0.263907	
					1.250	0.527		0.201134	
					0.750	0.461		0.169541	
	B				2.250	0.549		0.321776	*
					1.750	0.542		0.259280	
					1.250	0.503		0.231248	
					0.750	0.450		0.179483	
	C				2.250	0.565		0.296368	
					1.750	0.562		0.234095	
					1.250	0.502		0.228537	
					0.750	0.455		0.175645	
	D				1.750	0.495	29.14	0.295150	
					1.250	0.469		0.244356	
					0.750	0.417		0.194957	
	E				1.750	0.481		0.319719	
					1.250	0.453		0.265784	
					0.750	0.394		0.220476	
	F				1.750	0.496		0.294546	
					1.250	0.480		0.230251	
					0.750	0.427		0.184458	

NOTE
THESE VALUES OF KS WHICH ARE MARKED WITH AN ASTERISK WERE NOT USED IN PLOTTING THE CHARACTERISTIC ROUGHNESS CURVES.

TABLE A-8
EXPERIMENTAL DATA

DUNE SHAPE $K/L = 1/24.8$

DEPTH OF FLY (IN.)	SECTION OR DYN. FLY	SLOPE OF FLY (FT/FT)	DISCHARGE VELOCITY (CFS)	MEAN VELOCITY (FPS)	PROBE EL. ABOVE DATUM (IN.)	VELOCITY AT PROBE (FPS)	CHEZY'S C	KS
4.00	A	0.0007	6.634	0.979	4.250	1.191	71.66	0.022906 *
					3.750	1.235		0.016101 *
					3.250	1.254		0.012662
					2.750	1.259		0.010974
					2.250	1.193		0.012010
					1.750	1.126		0.013202
					1.250	1.062		0.013122
					0.750	0.977		0.012168
b								
					4.250	1.173		0.024424 *
					3.750	1.227		0.016304 *
					3.250	1.217		0.015259
					2.750	1.201		0.014064
					2.250	1.191		0.012127
					1.750	1.039		0.021628
					1.250	0.979		0.020283
					0.750	0.843		0.024352
c								
					4.250	1.177		0.024566 *
					3.750	1.201		0.019141 *
					3.250	1.226		0.014592
					2.750	1.233		0.011899
					2.250	1.162		0.014085
					1.750	1.112		0.014186
					1.250	1.065		0.012894
					0.750	0.938		0.014893
d								
					4.250	1.117		0.032069 *
					3.750	1.170		0.020070 *
					3.250	1.184		0.016230
					2.750	1.182		0.013815
					2.250	1.174		0.011829
					1.750	1.114		0.012629
					1.250	1.072		0.011215
					0.750	0.902		0.016432
e								
					4.250	1.072		0.038208 *
					3.750	1.151		0.022246 *
					3.250	1.155		0.013902

NOTE

THESE VALUES OF KS WHICH ARE MARKED WITH AN ASTERISK WERE NOT USED IN PLOTTING THE CHARACTERISTIC ROUGHNESS CURVES.

TABLE A-8 [CONTINUED]

$$D_{\text{LNL}} = 3\Delta p_E = k/L = 1/24\pi$$

LEAD	STATION	STRAIGHT	DISCHARGE	MEAN	PROBE EL.	VELOCITY	CHEZY'S	KS
FLD.	FLD.	FLD.	FLD.	FLD.	FLD.	FLD.	FLD.	FLD.
(FT.)	(FT.)	(FT.)	(FT.)	(FT.)	(IN.)	(FPS)	(FPS)	(FT.)
4.5	6	0.3377	0.579	0.944	0.944	2.750	1.137	70.35
						2.250	1.162	0.017265
						1.750	1.049	0.017752
						1.250	0.968	0.019330
						0.750	0.609	0.026741 *
						4.250	1.085	0.035579 *
						3.750	1.156	0.021595 *
						3.250	1.193	0.015263
						2.750	1.190	0.013278
						2.250	1.164	0.012479
						1.750	1.101	0.013508
						1.250	1.036	0.013589
						0.750	0.910	0.015794
						3.750	1.114	67.83
						3.250	1.141	0.023982 *
						2.750	1.149	0.017972
						2.250	1.113	0.014605
						1.750	1.052	0.014476
						1.250	0.980	0.015516
						0.750	0.872	0.016403
								0.017569
						3.750	1.113	0.024176 *
						3.250	1.121	0.020002
						2.750	1.115	0.017480
						2.250	1.056	0.019637
						1.750	1.016	0.018956
						1.250	0.951	0.019201
						0.750	0.795	0.026363 *
						3.750	1.126	0.022527 *
						3.250	1.119	0.020246
						2.750	1.109	0.018091
						2.250	1.117	0.014159
						1.750	1.061	0.014907
						1.250	1.020	0.013270
						0.750	0.850	0.016973

FIGURE 1. THE VARIOUS STAGES OF THE MANUFACTURE OF ASBESTOS CLOTHES NOT USEFUL IN PRINTING THE CHARACTERISTIC BRIGHTNESS CURVES

TABLE A-8 [CONTINUED]

LINE SHAPE $K/L = 1/24.8$

DEPTH D FT. (IN.)	SECTION NUMBER N	SLOPE OF FLUME (FT/FT) (IN.)	DISCHARGE (CFS)	MEAN VELOCITY (FPS)	PROBE EL. ABOVE DATUM (IN.)	VELOCITY AT PROBE (FPS)	CHEZY'S C	KS
4.00	K	0.007	0.750	0.654	3.750	1.001	64.79	0.039225 *
					3.250	1.074		0.022784
					2.750	1.037		0.023549
					2.250	1.085		0.014827
					1.750	1.058		0.013406
					1.250	0.956		0.016678
					0.750	0.652		0.017682
					3.750	0.964		0.043129 *
					3.250	1.068		0.023597
					2.750	1.049		0.022136
					2.250	1.048		0.018224
					1.750	1.019		0.017421
					1.250	0.875		0.025561 *
					0.750	0.775		0.026988 *
					3.750	1.012		0.036948 *
					3.250	1.062		0.024339
					2.750	1.080		0.018653
					2.250	1.055		0.017451
					1.750	1.011		0.017314
					1.250	0.958		0.016575
					0.750	0.811		0.022232 *
					3.250	0.984		0.032813 *
					2.750	1.002		0.025143
					2.250	0.981		0.023104
					1.750	0.943		0.022287
					1.250	0.886		0.021895
					0.750	0.787		0.022888
					3.250	0.963		0.036931 *
					2.750	1.004		0.024379
					2.250	1.011		0.019555
					1.750	0.939		0.022714
					1.250	0.826		0.030563
					0.750	0.719		0.033468 *
					3.250	1.010		0.028426 *

NOTE: VALUES OF KS WHICH ARE MARKED WITH AN ASTERISK ARE USED IN PLOTTING THE CHARACTERISTIC ROUGHNESS CURVES.

TABLE A-8 [CONTINUED]

DUNE SHAPE $K/L = 1/24K$

DEPTH OF FLUID (IN.)	SECTION NUMBER (L) L/D	SLOPE OF DUNE (FT/FT)	DISCHARGE (CFS)	MEAN VELOCITY (FPS)	PROBE EL. ABOVE DATUM (IN.)	VELOCITY AT PROBE (FPS)	CHEZY'S C (FT.)	KS
3.01	L	0.0007	0.409	0.801	2.750 2.250 1.750 1.250 0.750	1.028 1.007 0.973 0.890 0.777	63.66 0.021735 0.020057 0.018824 0.021393 0.024179	*
3.02	L	0.0007	0.362	0.766	3.250 2.750 2.250 1.750 1.250 0.750	0.509 0.933 0.936 0.881 0.865 0.742	62.41 0.044046 0.032303	*
3.03	L	0.0007	0.362	0.766	3.250 2.750 2.250 1.750 1.250 0.750	0.916 0.899 0.887 0.893 0.851 0.695	0.042088 0.039342	*
3.04	L	0.0007	0.320	0.722	3.250 2.750 2.250 1.750 1.250 0.750	0.934 0.997 0.989 0.942 0.881 0.778	0.038099 0.022409 0.019229 0.019519 0.019884 0.021497	*
3.05	L	0.0007	0.320	0.722	2.750 2.250 1.750 1.250 0.750	0.873 0.922 0.885 0.851 0.741	0.039702 0.024323 0.023528 0.020624 0.023646	
3.06	L	0.0007	0.320	0.722	2.750 2.250 1.750 1.250 0.750	0.873 0.840 0.822 0.774 0.643	0.039702 0.039598 0.034194 0.032401 0.040970	

NOTE: VALUES OF KS WHICH ARE MARKED WITH AN ASTERISK WERE NOT USED IN PLOTTING THE CHARACTERISTIC ROUGHNESS CURVES.

TABLE A-8 [CONTINUED]

DUNE SHAPE $K/L = 1/24R$

Depth L _D FL _D (in.)	Station L _D L _{Unit} (in.)	SLOPE OF F _L (ft/ft)	DISCHARGE VOLUME (cu ft)	MEAN VELOCITY (fps)	PROBE EL. ABOVE DATUM (in.)	VELOCITY AT PROBE (fps)	CHEZY'S C	KS	(ft.)			
2.025	C	0.320	0.722	2.750 2.250 1.750 1.250 0.750	0.840 0.895 0.897 0.784 0.706	60.48 60.48 60.48 60.48 60.48	0.035999 0.028614 0.022009 0.030580 0.029083	0.032312 0.025363 0.024693 0.027272				
3.000	A	0.691	0.242	2.750 2.250 1.750 1.250 0.750	0.840 0.848 0.846 0.796 0.695	59.68 59.68 59.68 59.68 59.68	0.041536 0.032312					
4.075	C	0.0007	0.251	2.750 2.250 1.750 1.250 0.750	0.805 0.826 0.803 0.741 0.605	0.051296 0.036995 0.033095 0.034515 0.047403	*					
				2.750 2.250 1.750 1.250 0.750	0.820 0.834 0.822 0.773 0.649	0.046799 0.035255 0.029509 0.028336 0.036162	*					
				2.750 2.250 1.750 1.250 0.750	0.778 0.774 0.739 0.628	0.034449 0.029861 0.036161	*					
				2.250 1.750 1.250 0.750	0.710 0.721 0.649 0.529	0.064523 0.046737 0.052520 0.067166	*					
				2.250 1.750 1.250 0.750	0.776 0.750 0.713 0.605	0.042701 0.039119 0.035089 0.041692	*					

Note
TRUST VALUES WHICH ARE VARIOUS AND AN ASTERISK WERE NOT USED IN PLOTTING THE CHARACTERISTIC ROUGHNESS CURVES.

TABLE A-8 [CONTINUED]

WAVE SHAPE $K/L = 1/24.8$

DEPTH OF FLU. (IN.)	STATION UN CF L/D	SLOPE OF FLUME (FT/FT)	DISCHARGE CF L/D	MEAN VELOCITY (CF-S)	PROBE EL. ABOVE DATUM (FPS)	VELOCITY AT PROBE (IN.)	CHEZY'S C PROBE (FPS)	KS
2.56	A	0.0009	0.234	0.688	2.250	0.765	56.25	0.068344 *
					1.750	0.743		0.058616
					1.250	0.718		0.050032
					0.750	0.628		0.050235
3.50	B	0.0009	0.234	0.688	2.250	0.716	0.091042	
					1.750	0.715		0.071273
					1.250	0.642		0.077427
					0.750	0.529		0.088949
4.50	C	0.0009	0.234	0.688	2.250	0.756	0.072002 *	
					1.750	0.736		0.063109
					1.250	0.704		0.053985
					0.750	0.596		0.060423
5.50	D	0.0009	0.234	0.697	1.750	0.886	53.78	0.035430
					1.250	0.847		0.031194
					0.750	0.739		0.033641
6.50	E	0.0009	0.234	0.707	1.750	0.809		0.053829
					1.250	0.753		0.051973
					0.750	0.654		0.053689
7.50	F	0.0009	0.234	0.716	1.750	0.837		0.046157
					1.250	0.783		0.044840
					0.750	0.716		0.038279

NOTE

THESE VALUES WHICH ARE MARKED WITH AN ASTERISK WERE NOT USED IN PLOTTING THE CHARACTERISTIC ROUGHNESS CURVES.

TABLE A-9
EXPERIMENTAL DATA

DUNE SHAPE $K/L = 1/32R$

BEDN LI FLLW (IN.)	SLOPE OF FLUKE (IN.)	DISCHARGE VELOCITY (CFS)	MEAN VELOCITY (FPS)	PROBE EL. ABOVE DATUM (IN.)	VELOCITY AT PROBE (FPS)	CHEZY'S C	KS
A							
4.75	0.0005	0.620	0.550	4.250	1.136	82.95	0.074071 *
				3.750	1.123		0.053398 *
				3.250	1.178		0.008920
				2.750	1.177		0.007234
				2.250	1.110		0.009706
				1.750	1.075		0.009014
				1.250	1.008		0.010361
				0.750	0.952		0.007879
B							
				4.250	1.092		0.013547 *
				3.750	1.117		0.069729 *
				3.250	1.151		0.012571
				2.750	1.150		0.008999
				2.250	1.121		0.008607
				1.750	1.046		0.013477
				1.250	1.020		0.009072
				0.750	0.846		0.099132 *
C							
				4.250	1.128		0.110009 *
				3.750	1.154		0.018966 *
				3.250	1.160		0.010972
				2.750	1.162		0.008021
				2.250	1.134		0.007739
				1.750	1.098		0.007446
				1.250	1.025		0.008589
				0.750	0.898		0.015879 *
D							
				4.250	1.056	81.25	0.014989 *
				3.750	1.082		0.127318 *
				3.250	1.122		0.014103
				2.750	1.110		0.011102
				2.250	1.078		0.011006
				1.750	1.027		0.012987
				1.250	0.988		0.010423
				0.750	0.883		0.014938
E							
				4.250	1.018		0.018990 *
				3.750	1.080		0.141526 *
				3.250	1.113		0.016958

NOTE
These values of K_s which are marked with an asterisk were not used in plotting the characteristic roughness curves.

TABLE A-9 [CONTINUED]

DURÉE SHARE $k/t = 1/328$

RELATIVE VALUES OF THE WHICH ARE MARKED WITH AN ASTERISK REFER TO FIGURE NOT USED IN PICTURING THE CHARACTERISTICS SOURCE: C. W.

TABLE A-9 [CONTINUED]

DUNE SHAPE $K/L = 1/32R$

DEP ^{IN}	SECTION # FLU.	SLP ^{FT} OF DUNE	DISCHARGE VOLUME (CU. FT.)	PROBE EL. ABOVE DATUM (FPS)	VELOCITY AT PROBE (FPS)	CHEZY'S C	KS	PROBE EL. ABOVE DATUM (IN.)	
								(IN.)	(FT.)
2.00	μ	0.0005	0.434	3.750	0.941	73.18	0.021187 *		
				3.250	1.008		0.150984 *		
				2.750	1.008		0.042184 *		
				2.250	0.968		0.027690 *		
				1.750	0.955		0.023948 *		
				1.250	0.901		0.025257 *		
				0.750	0.815		0.031317 *		
				3.750	0.947		0.020375 *		
				3.250	0.981		0.014211 *		
				2.750	0.987		0.110470 *		
				2.250	0.967		0.063091 *		
				1.750	0.914		0.136198 *		
				1.250	0.881		0.050802 *		
				0.750	0.730		0.016661		
				3.750	0.950		0.019933 *		
				3.250	1.002		0.214038 *		
				2.750	1.024		0.023901 *		
				2.250	0.998		0.021018 *		
				1.750	0.953		0.021453 *		
				1.250	0.920		0.015453		
				0.750	0.615		0.031726 *		
				3.250	0.933	71.01	0.016080 *		
				2.750	0.933		0.013777		
				2.250	0.938		0.079242 *		
				1.750	0.893		0.115094 *		
				1.250	0.863		0.041182		
				0.750	0.777		0.061381 *		
				3.250	0.901		0.020746 *		
				2.750	0.934		0.014090		
				2.250	0.908		0.013697		
				1.750	0.648		0.015847		
				1.250	0.786		0.017092		
				0.750	0.705		0.017502		
				3.250	0.949		0.015145 *		

1016

THESE VALUES OF KS WHICH ARE MARKED WITH AN ASTERISK WERE NOT USED IN PLOTTING THE CHARACTERISTIC ROUGHNESS CURVES.

TABLE A-9 [CONTINUED]

BIGHT, SHAPE, $K/L = 1/32R$

DEPTH OF FLOOR (IN.)	STATION ON FLOOR (IN.)	DISCHARGE OF FLOOR (CFS)	VELOCITY AT FLOOR (FPS)	VELOCITY ABOVE YATUM (FPS)	PROBE EL. ABOVE YATUM (IN.)	VELOCITY AT PROBE (FPS)	CHEVY'S C	
							71.01	0.128172 * 0.096607 * 0.035484 * 0.106392 * 0.223563 *
2.0	6	0.360	0.750	2.150	0.950	0.950	71.01	0.128172 * 0.096607 * 0.035484 * 0.106392 * 0.223563 *
				2.250	0.934	0.934		
				1.750	0.913	0.913		
				1.250	0.843	0.843		
				0.750	0.754	0.754		
3.0	5	0.333	0.700	3.250	0.650	0.650	68.27	0.023732 * 0.016571 * 0.074092 * 0.013624 * 0.070624 * 0.083440 *
				2.750	0.687	0.687		
				2.250	0.912	0.912		
				1.750	0.849	0.849		
				1.250	0.827	0.827		
				0.750	0.743	0.743		
3.0	6	0.300	0.700	3.250	0.832	0.832	0.028533 * 0.020132 * 0.015730 * 0.014157 * 0.014072 * 0.015454 *	0.028533 * 0.020132 * 0.015730 * 0.014157 * 0.014072 * 0.015454 *
				2.750	0.853	0.853		
				2.250	0.605	0.605		
				1.750	0.844	0.844		
				1.250	0.795	0.795		
				0.750	0.706	0.706		
3.0	7	0.300	0.700	3.250	0.652	0.652	0.024788 * 0.015543 * 0.057340 * 0.016339 * 0.158062 * 0.116523 *	0.024788 * 0.015543 * 0.057340 * 0.016339 * 0.158062 * 0.116523 *
				2.750	0.697	0.697		
				2.250	0.918	0.918		
				1.750	0.883	0.883		
				1.250	0.812	0.812		
				0.750	0.742	0.742		
3.0	8	0.300	0.684	2.750	0.793	0.793	0.027119 * 0.023628 * 0.023600 * 0.019078 * 0.023427 *	0.027119 * 0.023628 * 0.023600 * 0.019078 * 0.023427 *
				2.250	0.805	0.805		
				1.750	0.802	0.802		
				1.250	0.765	0.765		
				0.750	0.683	0.683		

NOTE
Velocity values in the table are marked with an asterisk were not used in plotting the characteristic roughness curves.

TABLE A-9 [CONTINUED]

DRAIN OF TUBE (IN.)	STRUCTURE UN DRAIN TUBE (IN.)	SUPPORT OR TUBE (IN.)	DISCHARGE VÉLOCITÉ (CFS)	MEAN VÉLOCITÉ (CFS)	PROFILÉ AOÛTÉ D'AMPA (IN.)	VELOCITY AT PROBE (FPS)	CHEZY'S C (FT.)	KS	DRAINE SHAPÉ K/L = 1.328	
									PROFILÉ (IN.)	VELOCITY AT PROBE (FPS)
3.00	C	0.0005	0.333	0.634	2.750	0.714	67.86	0.023332		
					2.250	0.612		0.019343		
					1.750	0.601		0.016238		
					1.250	0.701		0.015373		
					0.750	0.662		0.018387		
3.00	C	0.0002	0.202	0.640	2.750	0.716	65.45	0.039545 *		
					2.250	0.768		0.022247		
					1.750	0.754		0.019235		
					1.250	0.690		0.021677		
					0.750	0.611		0.022998		
3.00	C	0.0002	0.202	0.640	2.750	0.705		0.042899 *		
					2.250	0.704		0.035387		
					1.750	0.672		0.034759		
					1.250	0.647		0.029699		
					0.750	0.545		0.036980 *		
3.00	C	0.0002	0.202	0.640	2.720	0.698		0.045293 *		
					2.250	0.702		0.035773 *		
					1.750	0.691		0.030184		
					1.250	0.633		0.032836		
					0.750	0.591		0.026701		
3.00	C	0.0002	0.202	0.640	2.250	0.664		0.039944 *		
					1.750	0.665		0.030894		
					1.250	0.624		0.029966		
					0.750	0.565		0.027936		
3.00	C	0.0002	0.202	0.640	2.250	0.671		0.037976		
					1.750	0.642		0.036767		
					1.250	0.623		0.030304		
					0.750	0.512		0.041385 *		
3.00	C	0.0002	0.202	0.640	2.250	0.707		0.029168		
					1.750	0.692		0.025382		
					1.250	0.632		0.028250		
					0.750	0.548		0.031609		

NOTE
INSET VALUES OF KS AND MANNING AND MANNING ALL AS STRIKES NOT USED IN PLOTTING THE CHARACTERISTIC ROUGHNESS CURVES.

TABLE A-9 [CONTINUED]

UNITE SHAPE $K/L = 1/32R$

DEPTH IN. H	SOLUTION No. L	Slope OF FLOOR (FT/FT)	DISCHARGE CFS (CFS)	MEAN VELOCITY (FPS)	PROBE EL. ABOVE DATUM (IN.)	VELOCITY AT PROBE (FPS)	CHARAC- TERIS- TIC KS
					FL	EL.	
2.00	2	0.190	3.556	2.250	0.714	61.26	0.022555
				1.750	0.688		0.021450
				1.250	0.656		0.019572
				0.750	0.580		0.021097
				2.250	0.678		0.029837
				1.750	0.665		0.024961
				1.250	0.644		0.021548
				0.750	0.560		0.024765
				2.250	0.696		0.025941 *
				1.750	0.709		0.016273
				1.250	0.687		0.015411
				0.750	0.597		0.018557
				2.250	0.717		0.022312
				1.750	0.716		0.016070
				1.250	0.608		0.021388
				0.750			
				1.750	0.695		0.026209
				1.250	0.687		0.019845
				0.750	0.602		0.022236
				1.750	0.643		0.038338 *
				1.250	0.727		0.014745
				0.750	0.652		0.015371

NOTE
INLET VALUES WHICH ARE MARKED WITH AN ASTERISK WERE NOT USED IN PLOTTING THE CHARACTERISTIC ROUGHNESS CURVES.

TABLE A-10
EXPERIMENTAL DATA

DUNE SHAPE $K/L = 1/40$

DUNE OR FLAT HEIGHT (IN.)	SECTION OR LAYER NUMBER	SLIPPER UP TOPOE	DISCHARGE	MEAN VELOCITY	PROBE EL. ABOVE DATUM	VELOCITY AT PROBE	CHEZY'S C	KS	TIME	
									(IN.)	(FPS)
4.72										
4.00	4	0.0003	0.265	0.573	4.250	1.055	97.57	0.004046	*	
					3.750	1.040		0.004019	*	
					3.250	1.042		0.003423		
					2.750	1.053		0.002575		
					2.250	0.972		0.004130		
					1.750	0.991		0.002670		
					1.250	0.962		0.002377		
					0.750	0.883		0.002694		
					4.250	1.035		0.004744	*	
					3.750	1.055		0.003571	*	
					3.250	1.072		0.002613		
					2.750	1.072		0.002165		
					2.250	1.007		0.003087		
					1.750	1.015		0.002156		
					1.250	0.936		0.002987		
					0.750	0.815		0.004753	*	
					4.250	1.029		0.004961	*	
					3.750	1.095		0.002511	*	
					3.250	1.093		0.002175		
					2.750	1.078		0.002050		
					2.250	1.069		0.001764		
					1.750	0.983		0.002883		
					1.250	0.962		0.002377		
					0.750	0.781		0.006030	*	
4.50										
4.00	4	0.0003	0.510	0.831	4.250	0.933	94.66	0.008329	*	
					3.750	1.015		0.004244	*	
					3.250	1.024		0.003381		
					2.750	1.032		0.002614		
					2.250	0.986		0.003147		
					1.750	0.945		0.003417		
					1.250	0.883		0.004060	*	
					0.750	0.810		0.004385	*	
					4.250	0.886		0.013399	*	
					3.750	0.971		0.005874	*	
					3.250	1.011		0.003787		

NOTE
Last values of C which are marked with an asterisk were not used in plotting the characteristic roughness curves.

TABLE A-10 [continued]

DUNE SHAPE $K/L = 1/40$

RESULTS.—The results of the experiments with an asbestin are given in the following table.

TABLE A-10 [CONTINUED]

DUNIT SHAPE $K/L = 1/40K$

SECTION #	STATION IN FL. (IN.)	SWEAT UP FLUME (FT/FT)	DISCHARGE (CFS)	MEAN VELOCITY (FPS)	PROBE EL. ABOVE DATUM (IN.)	VELOCITY AT PHONE (FPS)	CHEZY'S C		KS
							IN.	FT.	
4.00	A	0.0003	0.400	0.733	3.750	0.845	86.97	0.011370	*
					3.250	0.892		0.006939	*
					2.750	0.917		0.004993	
					2.250	0.927		0.003755	
					1.750	0.858		0.005215	
					1.250	0.858		0.003685	
					0.750	0.743		0.005768	*
					3.750	0.796		0.036699	*
					3.250	0.840		0.007026	*
					2.750	0.914		0.005115	
					2.250	0.880		0.005540	
					1.750	0.835		0.006190	
					1.250	0.774		0.007091	*
					0.750	0.694		0.007779	*
					3.750	0.758		0.016571	*
					3.250	0.918		0.005806	*
					2.750	0.920		0.004873	
					2.250	0.912		0.004272	
					1.750	0.881		0.004303	
					1.250	0.851		0.003941	
					0.750	0.767		0.004793	
3.75	A	0.0003	0.351	0.688	3.250	0.868	83.48	0.007168	
					2.750	0.844		0.007355	
					2.250	0.836		0.006614	
					1.750	0.799		0.006988	
					1.250	0.740		0.007957	
					0.750	0.715		0.006289	
					3.250	0.840		0.008597	
					2.750	0.833		0.007908	
					2.250	0.838		0.006544	
					1.750	0.772		0.008377	
					1.250	0.727		0.008704	
					0.750	0.669		0.008580	
					3.250	0.849		0.008084	*

NOTE
THOSE VALUES OF KS WHICH ARE MARKED WITH AN ASTERISK WERE NOT USED IN PLOTTING THE CHARACTERISTIC ROUGHNESS CURVES.

TABLE A-10 [CONTINUED]

DUNN SHAPE $\kappa/L = 1/400$

DEPTH (FT.)	SECTION NUMBER (FLU.)	DISCHARGE OF FLUME (CFS)	MEAN VELOCITY (FPS)	PROBE EL. ABOVE DATUM (IN.)	VELOCITY AT PROBE (FPS)	CHEZY'S C (FT.)	KS
3.75	C	0.0003	0.688	2.750	0.862	83.48	0.006514
				2.250	0.835		0.006650
				1.750	0.805		0.006721
				1.250	0.793		0.005457
				0.750	0.690		0.007486 *
3.50	F	0.0003	0.303	3.250	0.774	79.14	0.013476 *
				2.750	0.758		0.012918 *
				2.250	0.776		0.008738
				1.750	0.719		0.011136
				1.250	0.712		0.008583
				0.750	0.659		0.008245
3.25	G	0.0003	0.306	3.250	0.713	0.150410 *	
				2.750	0.754		0.013842 *
				2.250	0.772		0.009003
				1.750	0.747		0.008785
				1.250	0.696		0.009598
				0.750	0.621		0.011263 *
3.00	H	0.0003	0.303	3.250	0.649	0.027281 *	
				2.750	0.785		0.009730
				2.250	0.789		0.007979
				1.750	0.759		0.008082
				1.250	0.714		0.008428
				0.750	0.650		0.008803
2.75	I	0.0003	0.202	2.750	0.715	75.66	0.019365 *
				2.250	0.710		0.013673
				1.750	0.707		0.010276
				1.250	0.660		0.011354
				0.750	0.615		0.010132
2.50	J	0.0003	0.291	2.750	0.680		0.090985 *
				2.250	0.681		0.027542 *
				1.750	0.681		0.014010 *
				1.250	0.620		0.024582 *
				0.750	0.576		0.017350 *

NOTE
THOSE VALUES OF KS WHICH ARE MARKED WITH AN ASTERISK WERE NOT USED IN PLOTTING THE CHARACTERISTIC ROUGHNESS CURVES.

TABLE A-10 [CONTINUED]

DRAFT SHAPE $K/L = 1/40K$

Depth in ft (in.)	Sediment Size in D ₅₀ ft (in.)	Slope of Flume Bottom (ft/ft)	Discharge (CFS) (ft ³ /ft)	Velocity (fps) (in.)	Profilé El. Above Datum (in.)	Velocity at Probe (fps)	Chezy's C	KS
2.025	0.0003	0.0002	0.591	2.750	0.710	75.66	0.022137	*
				2.250	0.713		0.013214	
				1.750	0.691		0.012181	
				1.250	0.642		0.014559	
				0.750	0.599		0.013500	
2.000	0.0005	0.220	0.539	2.750	0.642	71.15	0.276407	*
				2.250	0.664		0.022737	
				1.750	0.648		0.017209	
				1.250	0.608		0.018944	
				0.750	0.550		0.020733	
2.000	0.0005	0.220	0.539	2.750	0.612		0.023744	*
				2.250	0.621		0.264827	*
				1.750	0.617		0.053471	*
				1.250	0.593		0.025390	*
				0.750	0.522		0.066449	*
2.000	0.0005	0.220	0.539	2.750	0.631		0.019577	*
				2.250	0.661		0.024996	*
				1.750	0.653		0.015689	
				1.250	0.624		0.013861	
				0.750	0.552		0.019343	
2.075	0.0003	0.157	0.529	2.250	0.663	71.75	0.013848	
				1.750	0.654		0.011196	
				1.250	0.612		0.012093	
				0.750	0.528		0.021092	
2.075	0.0003	0.157	0.529	2.250	0.594		0.018692	
				1.750	0.592		0.055946	
				1.250	0.566		0.037930	
				0.750	0.536		0.017351	
2.075	0.0003	0.157	0.529	2.250	0.651		0.017374	
				1.750	0.628		0.016032	
				1.250	0.610		0.012423	*
				0.750	0.536		0.017495	

NOTE

THESE VALUES OF KS WHICH ARE MARKED WITH AN ASTERISK WERE NOT USED IN PLOTTING THE CHARACTERISTIC ROUGHNESS CURVES.

TABLE A-10 [CONTINUED]

DUNE SHAPE $R/L = 1/40K$

DRAIN L _D FL _D (IN.)	STATION L _{IN} L _{LINE} (IN.)	STRAIN OF FLUX (IN.)	DISCHARGE FLUX (CFS)	VELOCITY AT EL. (FPS)	VELOCITY ABOVE DUNUM (IN.)	PAUSE EL. ABOVE DUNUM (IN.)	VELOCITY AT PAUSE (FPS)	CHEZY'S C	KS
2.20	A	0.0004	0.172	0.506	2.250	0.516	62.04	0.065247	*
					1.750	0.543		0.040134	
					1.250	0.554		0.026082	
					0.750	0.508		0.023138	
	B				2.250	0.562		0.043843	*
					1.750	0.560		0.032368	
					1.250	0.539		0.029521	
					0.750	0.487		0.027861	
	C				2.250	0.516		0.064823	*
					1.750	0.592		0.026275	
					1.250	0.592		0.018768	
					0.750	0.536		0.018180	
	D	0.0004	0.154	0.503	1.750	0.622	64.46	0.154242	*
					1.250	0.598		0.062447	*
					0.750	0.556		0.031922	
	E				1.750	0.601		0.019333	
					1.250	0.581		0.202241	*
					0.750	0.511		0.018736	
	F				1.750	0.623		0.137587	*
					1.250	0.593		0.083909	
					0.750	0.558		0.029274	

NOTE

These values of C which were MARKED WITH AN ASTERISK WERE NOT USED IN PLOTTING THE CHARACTERISTIC ROUGHNESS CURVES.

ANALYSIS OF SAND SAMPLE

1) Sieve Analysis

The sand used to form the additional roughness coating on the bed forms was white Ottawa sand, 20-30 nominal size. That is, the grain sizes were between the #20 and #30 sieve sizes. The following results were obtained in a sieve analysis of a sample of the material:

Material larger than #20	2.4 gm.	0.126%
Material smaller than #30	4.2 gm.	0.221%
Material between #20, #30	1899.8 gm	99.653%
Mesh opening in #20 sieve	0.0331 inches	
Mesh opening in #30 sieve	0.0232 inches	
Average	0.0281 inches	

2) Settlement Analysis

A series of settlement analyses were performed on samples of the roughness coating material, using a Visual-Accumulation-Tube Apparatus. By observation of the recorder chart produced by this apparatus the grain size distribution of a sample may be found.

Some difficulty was encountered during the tests due to the uniform size of the sample grains. It was observed that the sample, when released, settled virtually as a unit,

making it impossible to accurately plot the time-depth curve of the sediment accumulation. The results obtained were as follows:

Test	D_{50}	Remarks
1	0.570 mm.	Test very inaccurate -results disregarded
2	0.620 mm.	
3	0.640 mm.	
Average	0.630 mm.	

3) Grain Measurement

A sample of the sand coating material was placed under a microscope, and the grains measured against the eyepiece grid. Maximum and minimum diameters were recorded for twenty-five grains, and the average diameter calculated.

Average diameter = 0.803 mm.

4) Average Grain Size

To summarize the results of both the tests:

Test	D_{50}
Settlement	0.630 mm.
Microscope	0.803 mm.
Average	0.716 mm.

Thus the average diameter according to these tests was 0.716 mm., or 0.0282 inches.

Referring again to the results of the sieve analysis, we see that by far the bulk of the material fell between the #20 and #30 sieve sizes, which have a mean opening of 0.0281 inches. This compares favorably with the average of 0.0282 inches determined from the other two tests.

APPENDIX B

DETAILED EXPERIMENTAL RESULTS

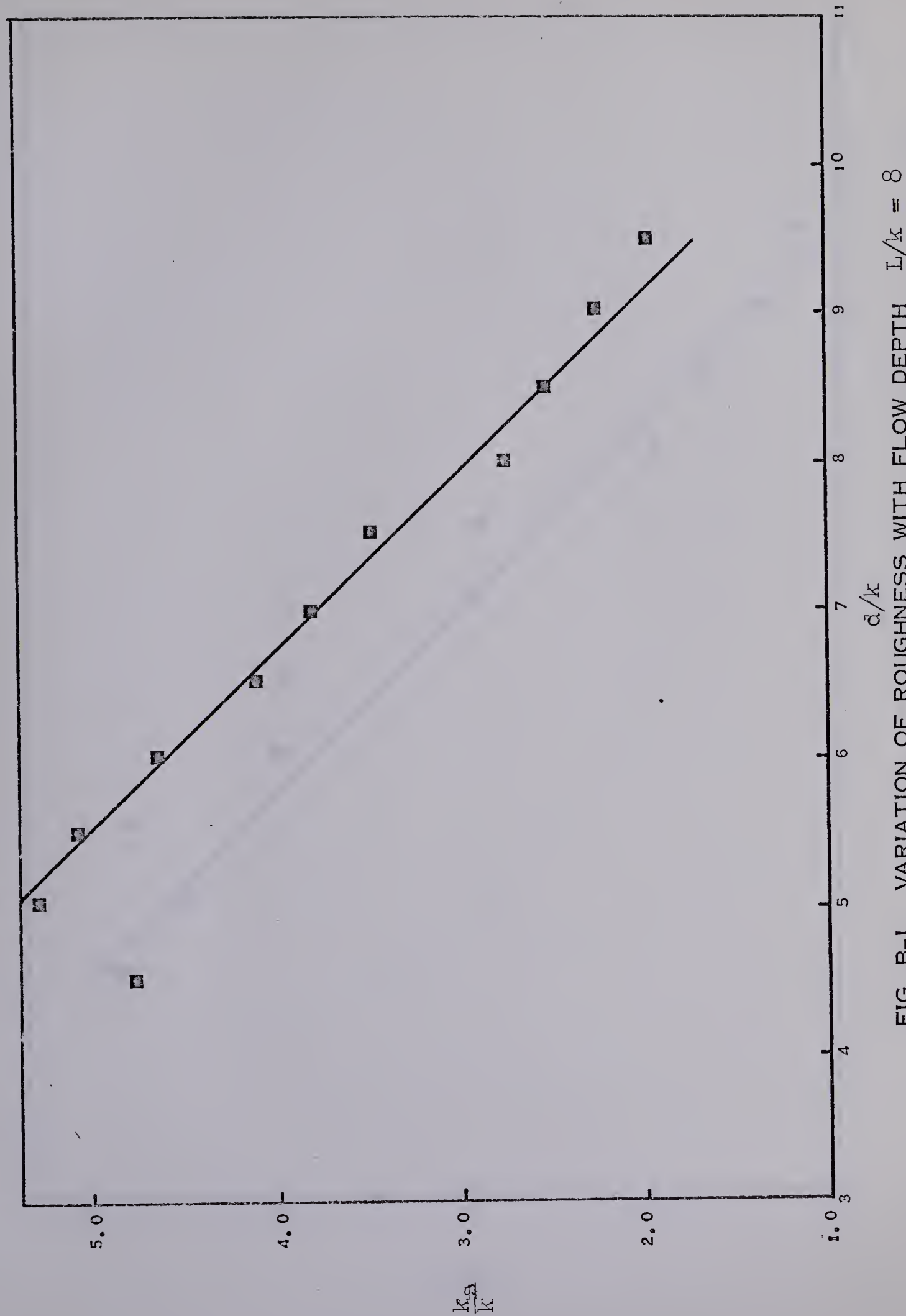


FIG. B-1 VARIATION OF ROUGHNESS WITH FLOW DEPTH $L/k = 8$

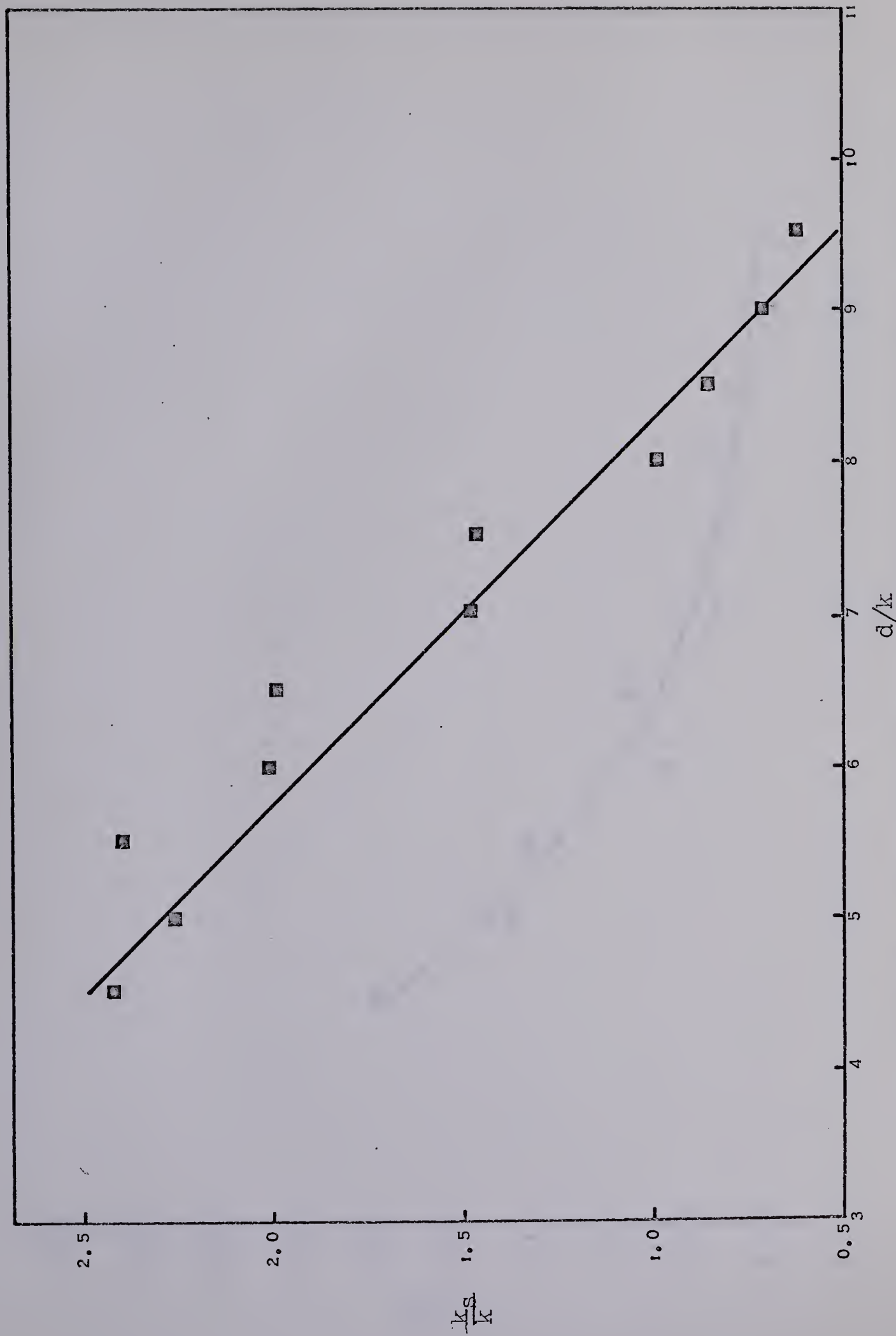


FIG. B-2 VARIATION OF ROUGHNESS WITH FLOW DEPTH $L/k = 16$

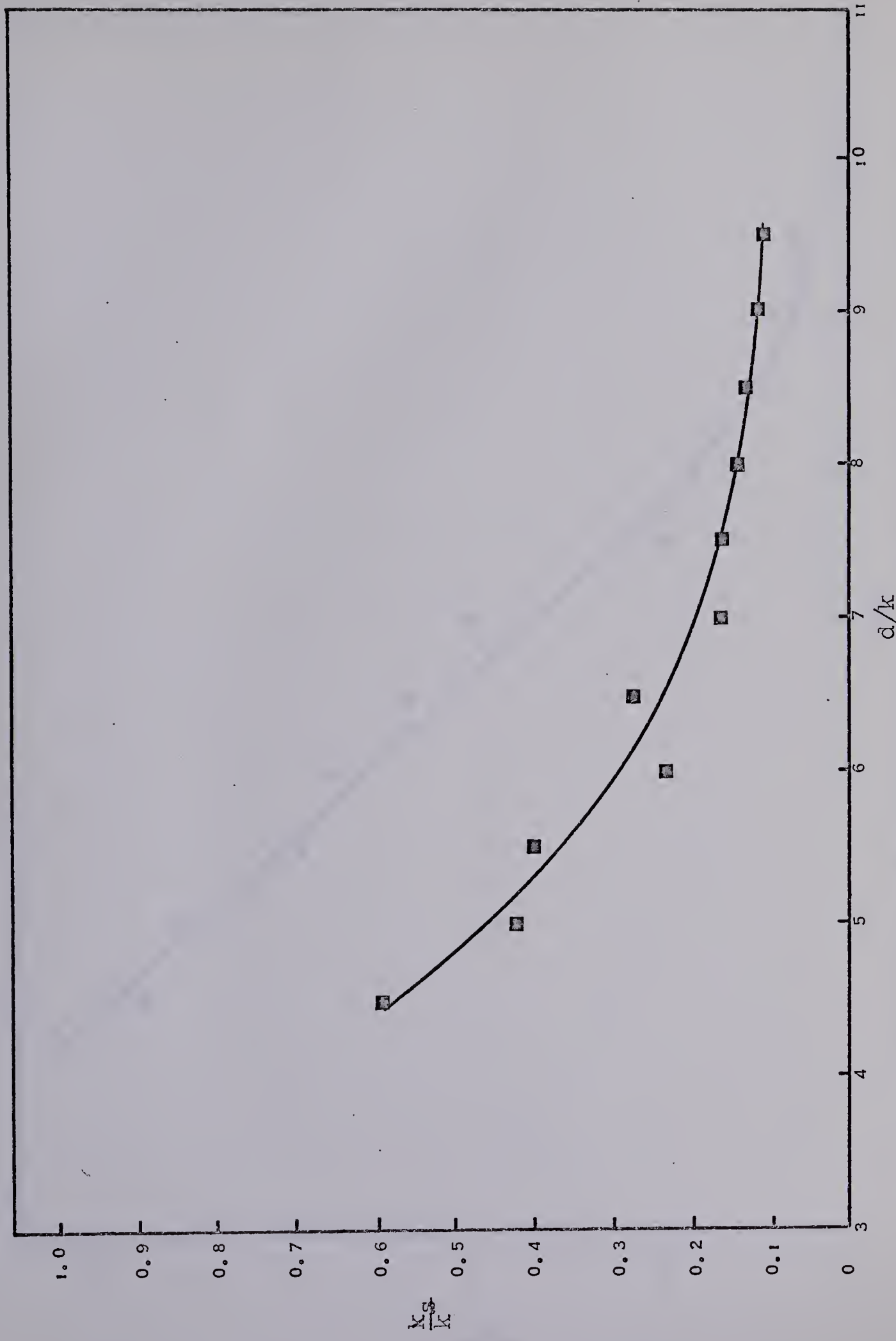


FIG. B-3 VARIATION OF ROUGHNESS WITH FLOW DEPTH $I_4/k = 24$

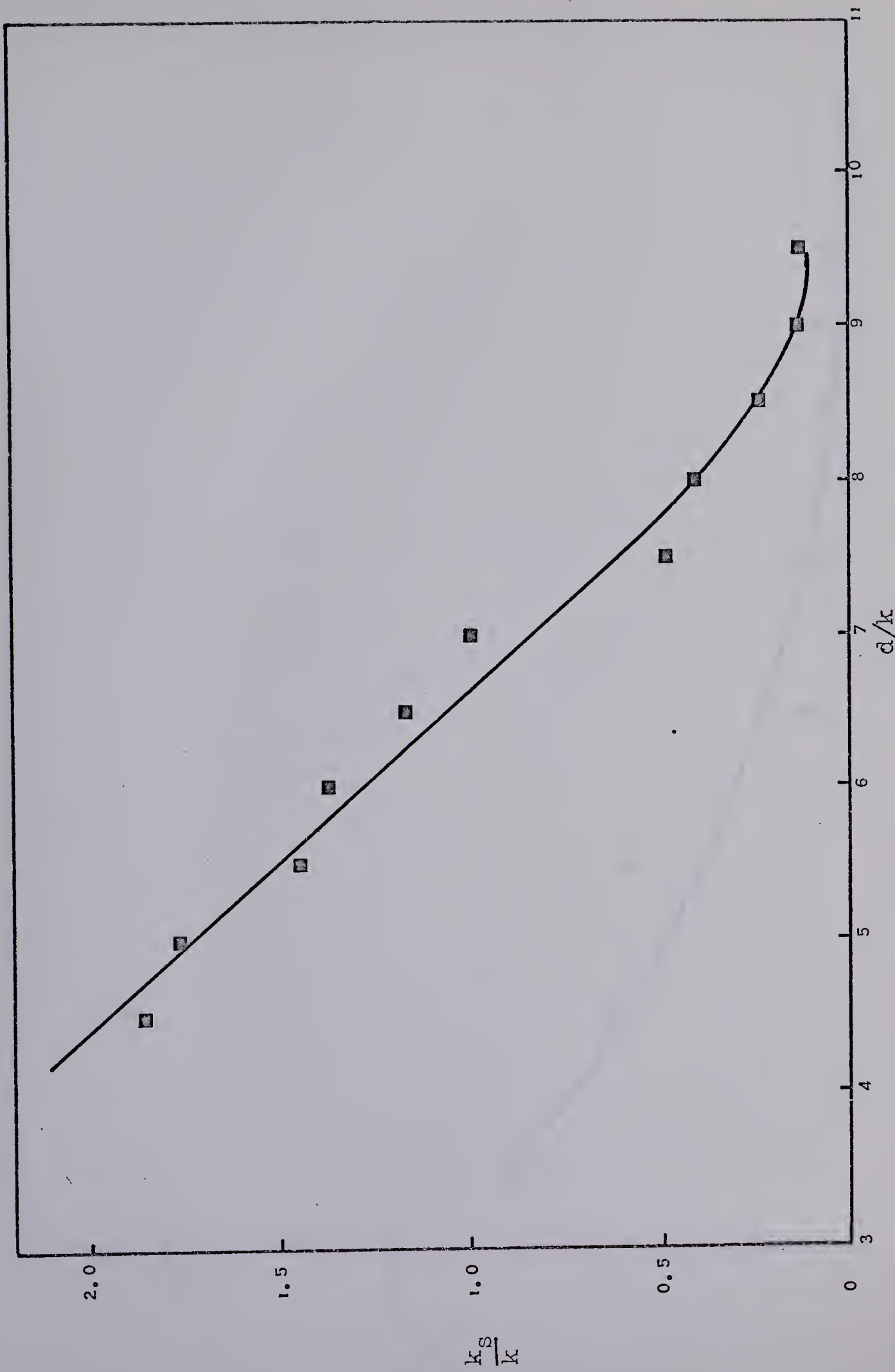


FIG. B-4 VARIATION OF ROUGHNESS WITH FLOW DEPTH $L/k = 32$

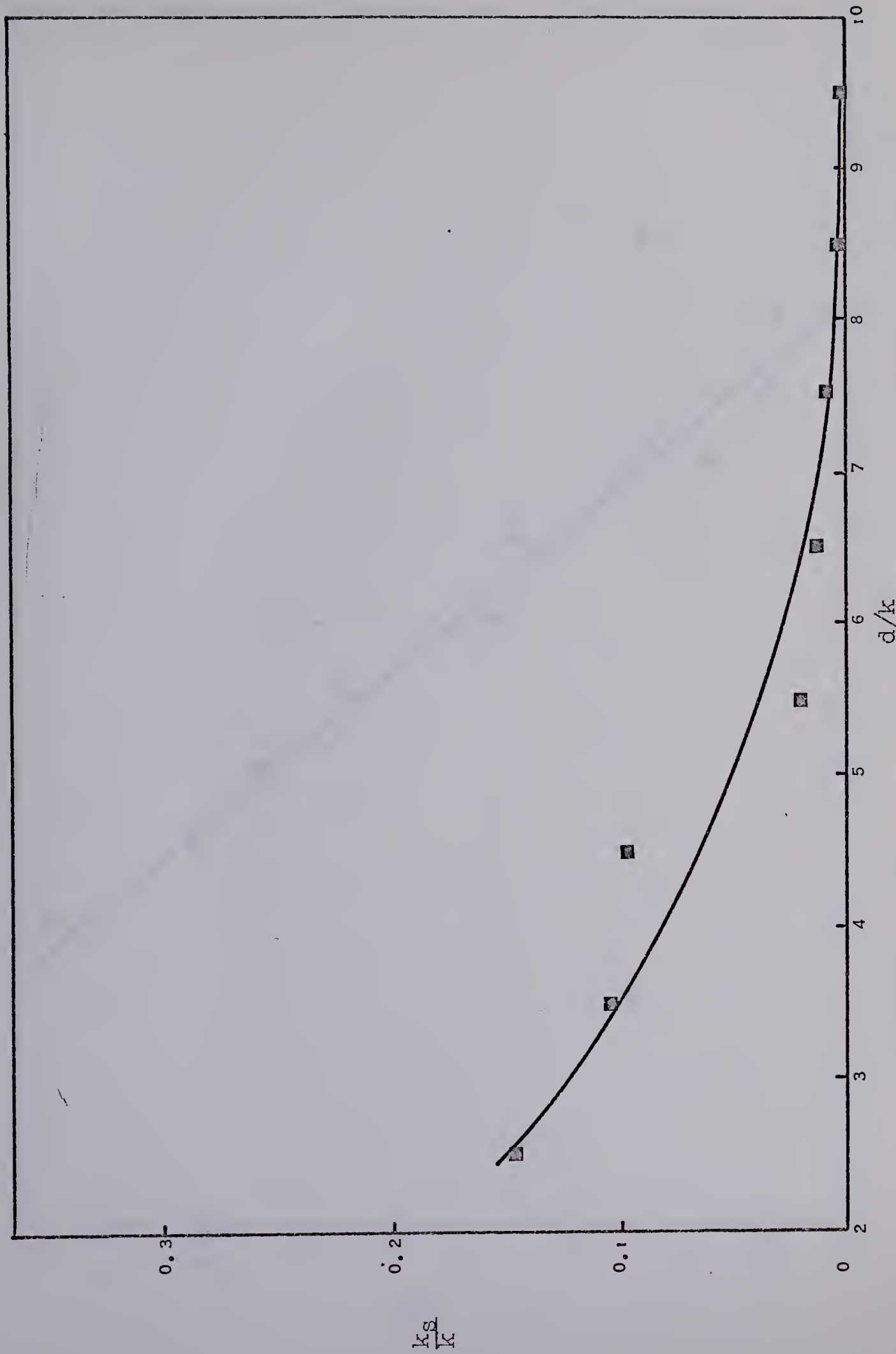


FIG. B-5 VARIATION OF ROUGHNESS WITH FLOW DEPTH $L/k = 40$

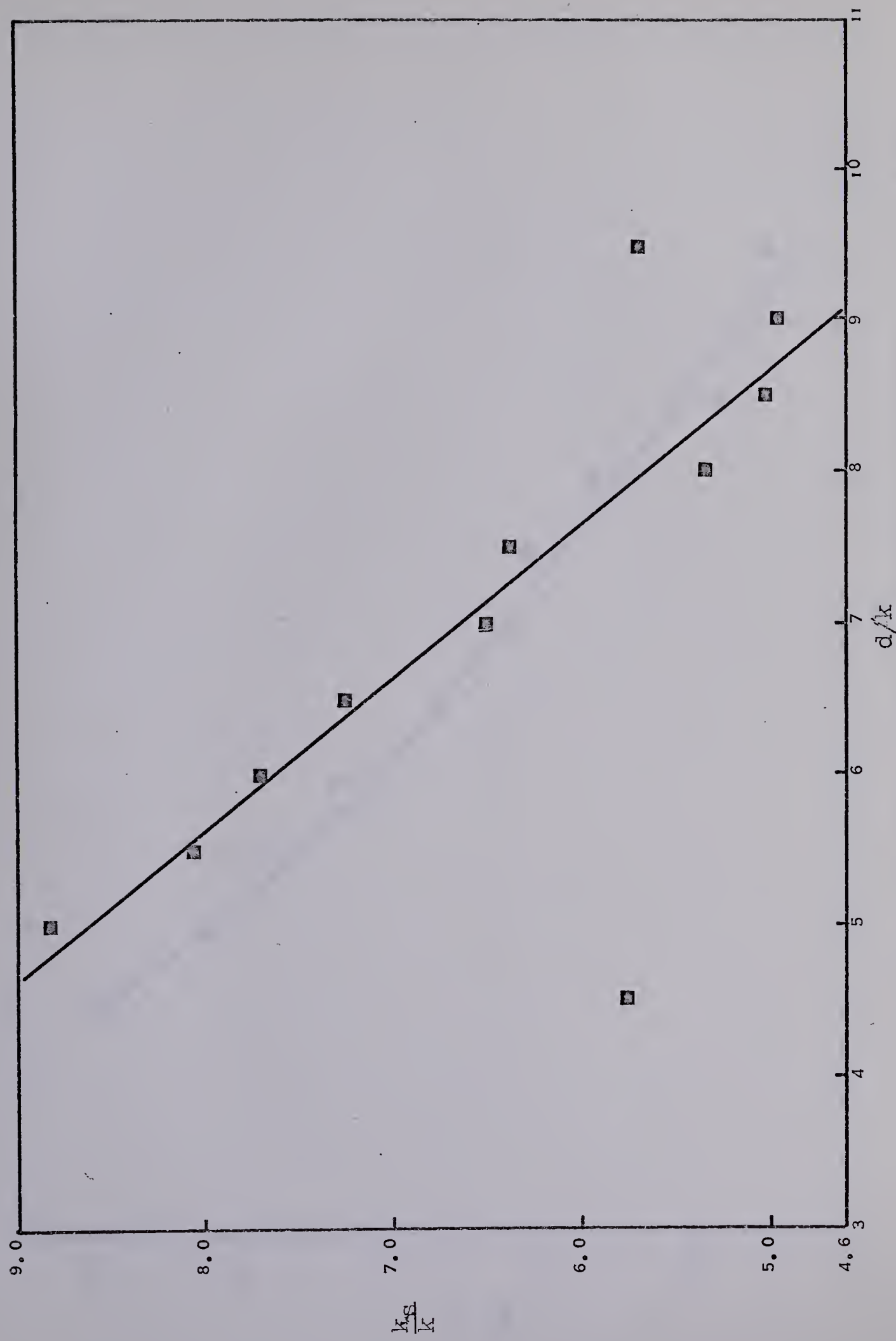


FIG. B-6 VARIATION OF ROUGHNESS WITH FLOW DEPTH $L/k = 8R$

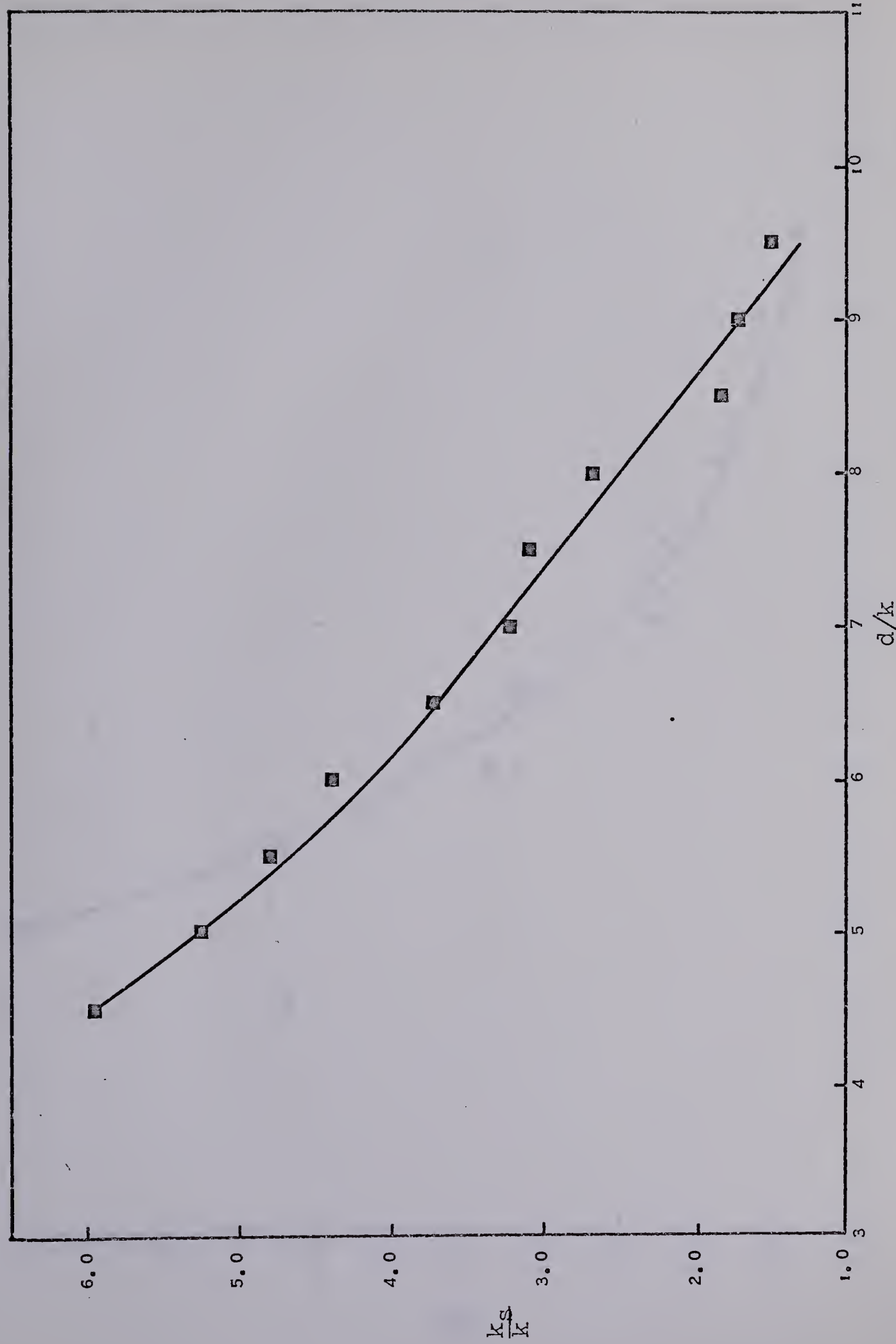


FIG. B-7 VARIATION OF ROUGHNESS WITH FLOW DEPTH $L/k = 16R$

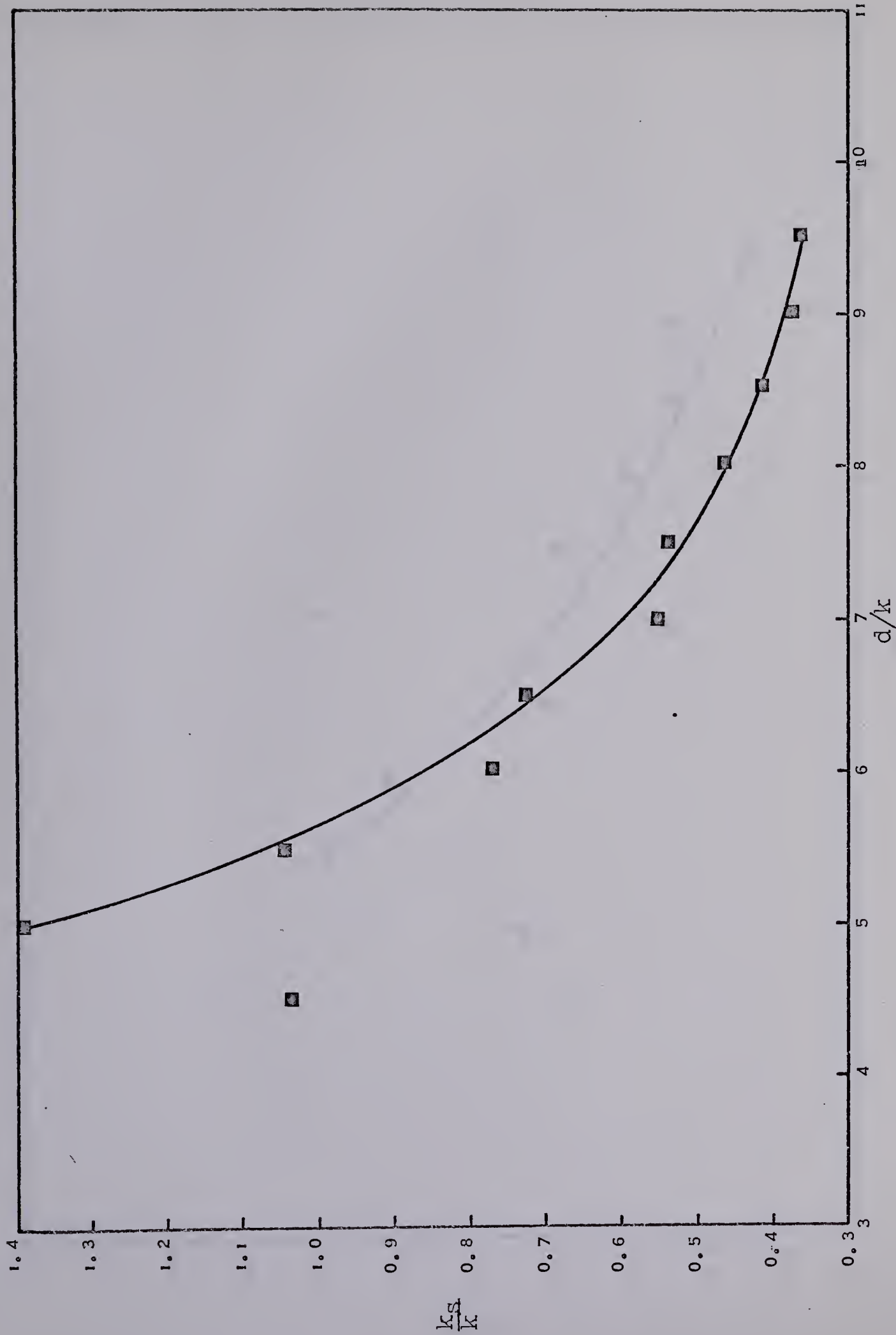


FIG. B-8 VARIATION OF ROUGHNESS WITH FLOW DEPTH $L/k = 24R$

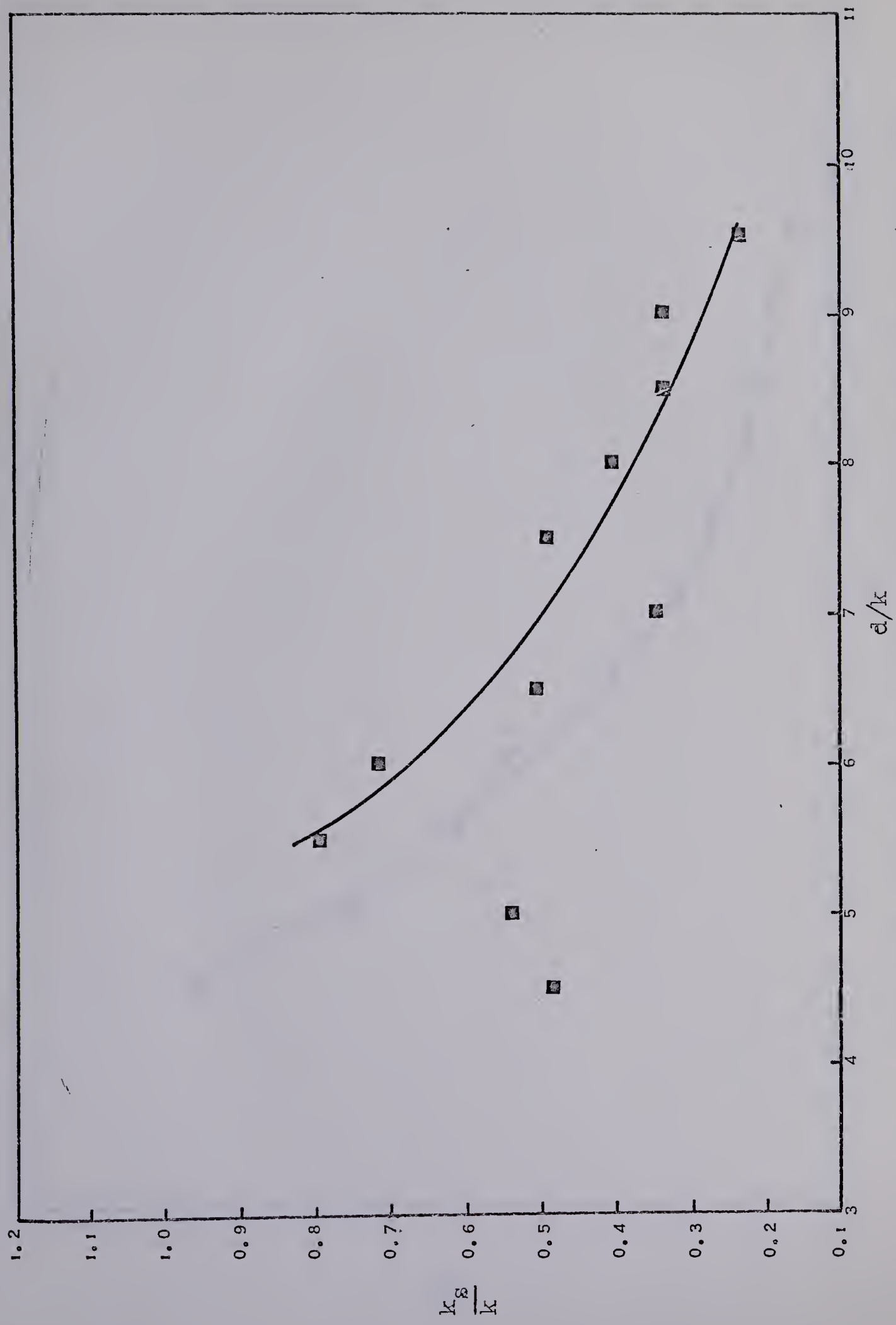


FIG. B-9 VARIATION OF ROUGHNESS WITH FLOW DEPTH $L/k = 32R$

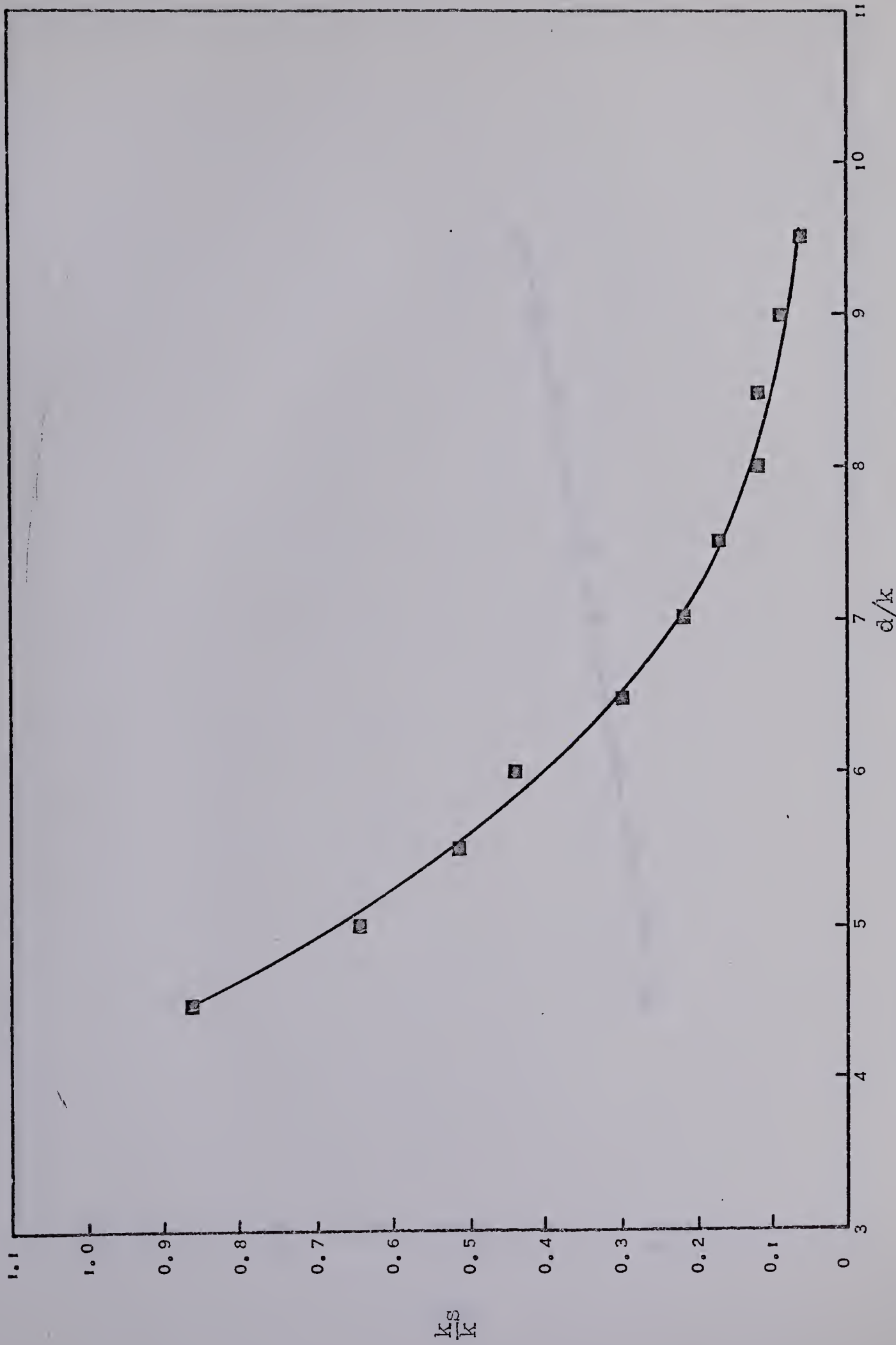


FIG. B-10 VARIATION OF ROUGHNESS WITH FLOW DEPTH $L/k = 4$ OR

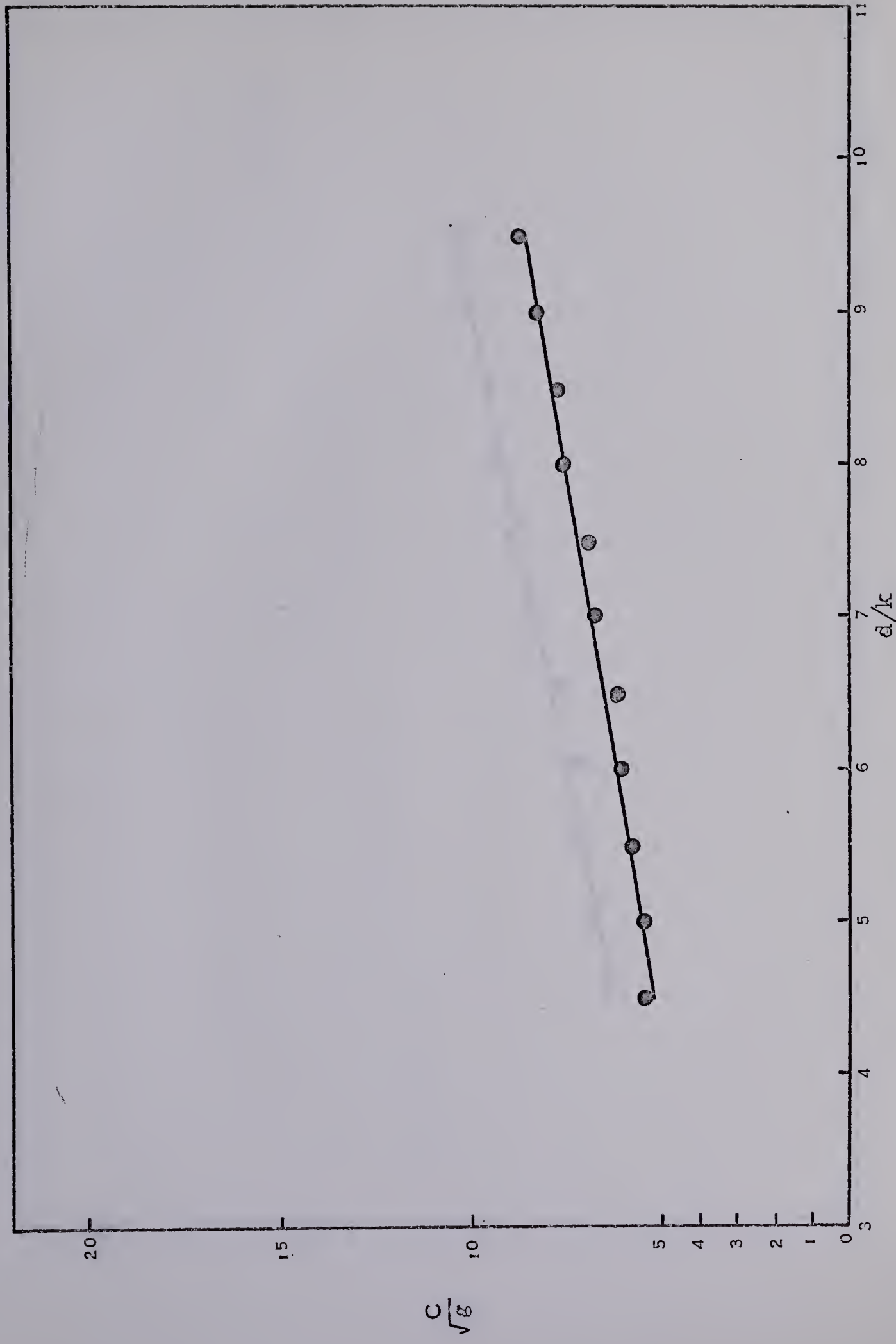


FIG. B-II VARIATION OF ROUGHNESS WITH FLOW DEPTH $L/k = 8$

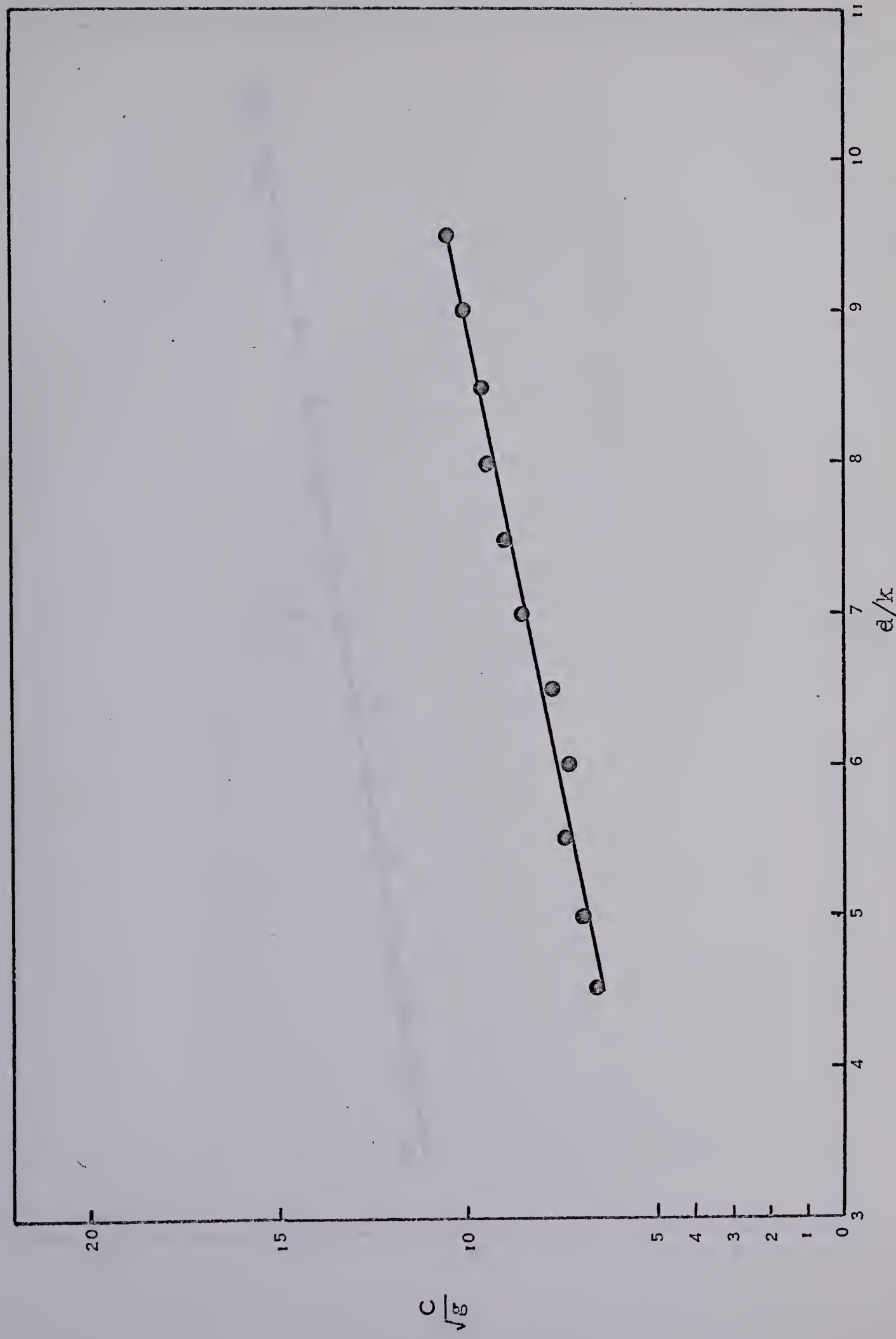


FIG. B-12 VARIATION OF ROUGHNESS WITH FLOW DEPTH $L/k = 16$

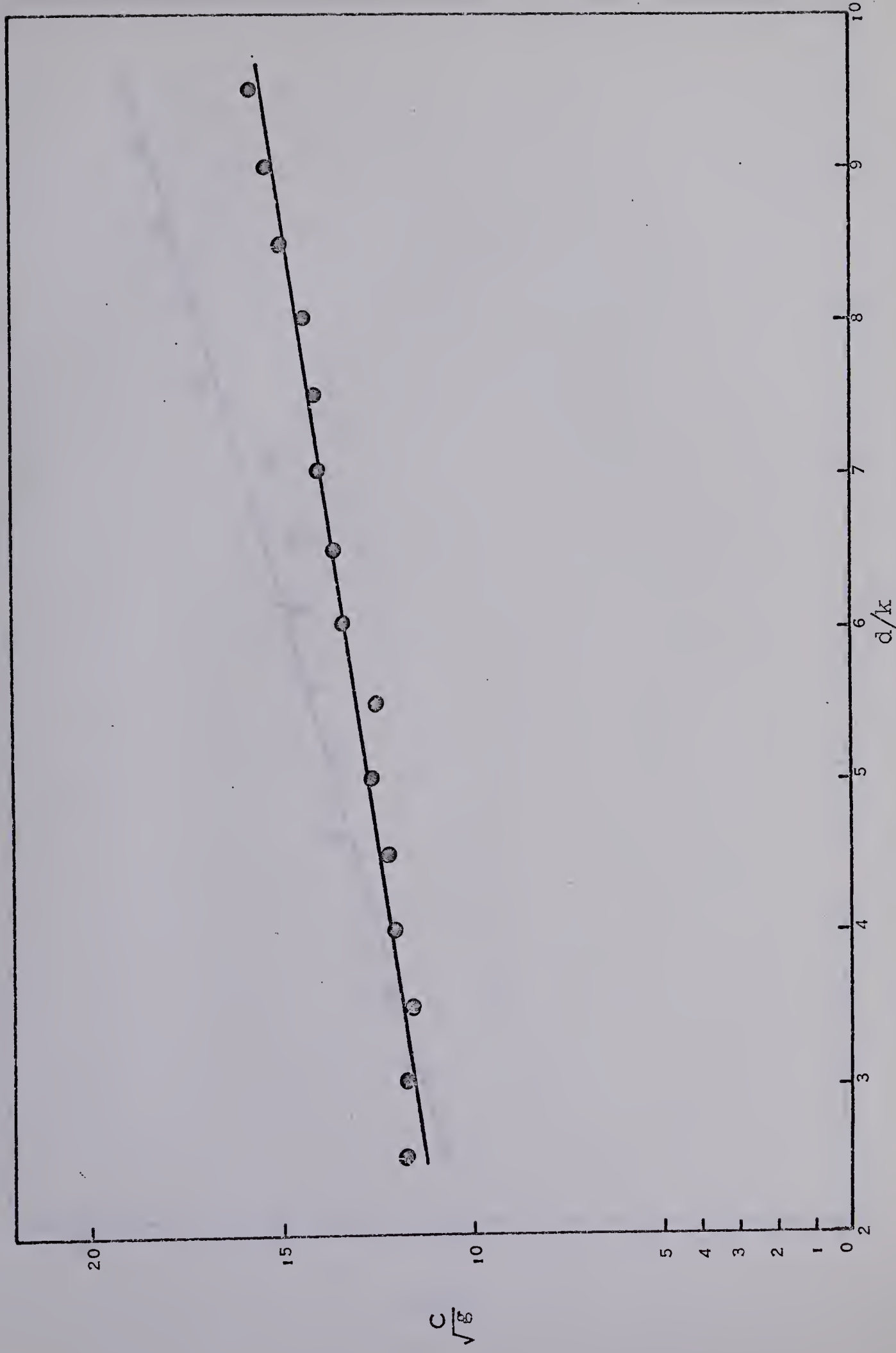


FIG. B-13 VARIATION OF ROUGHNESS WITH FLOW DEPTH $L/k = 24$

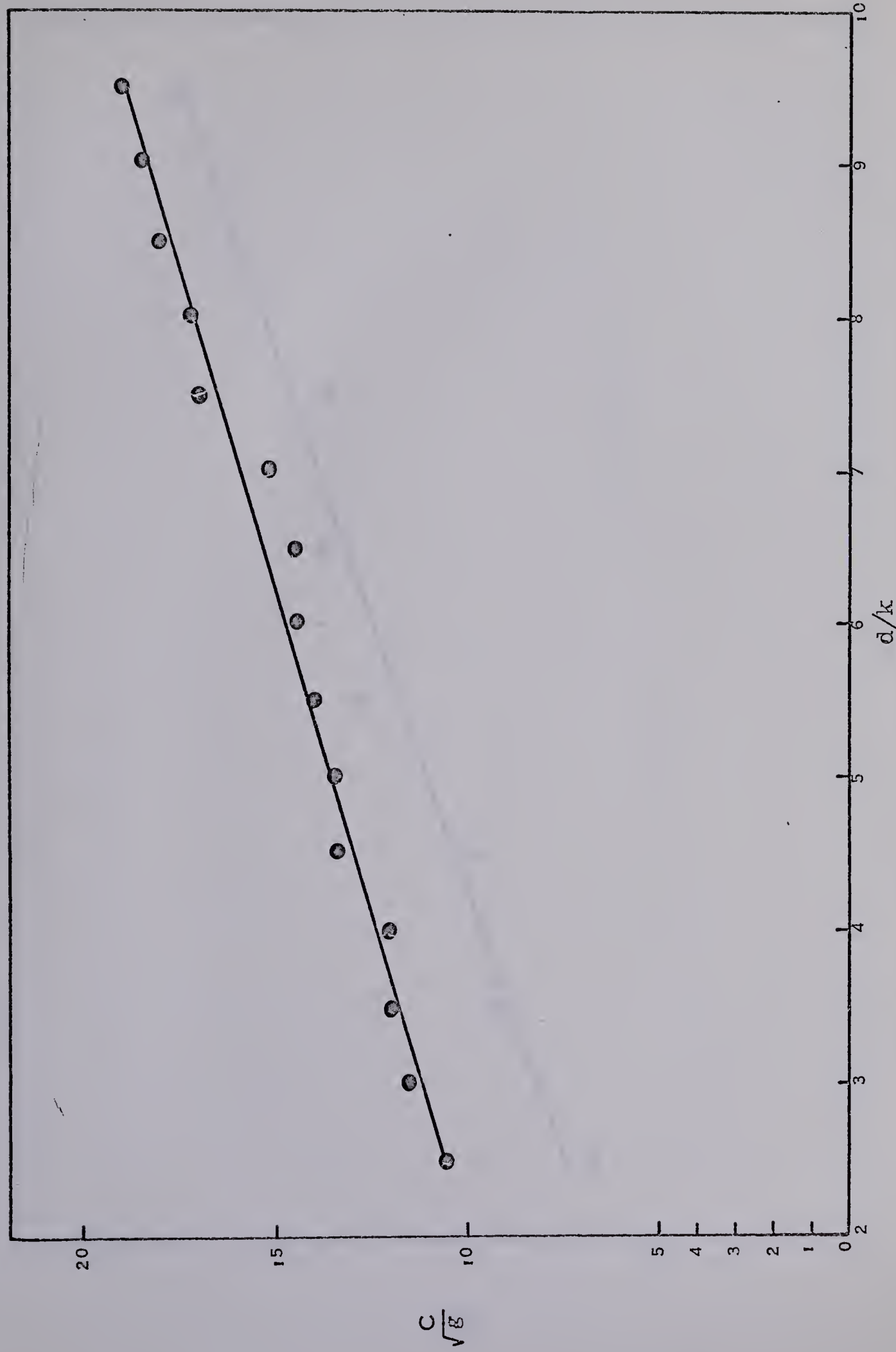


FIG. B-14 VARIATION OF ROUGHNESS WITH FLOW DEPTH $L/k = 32$

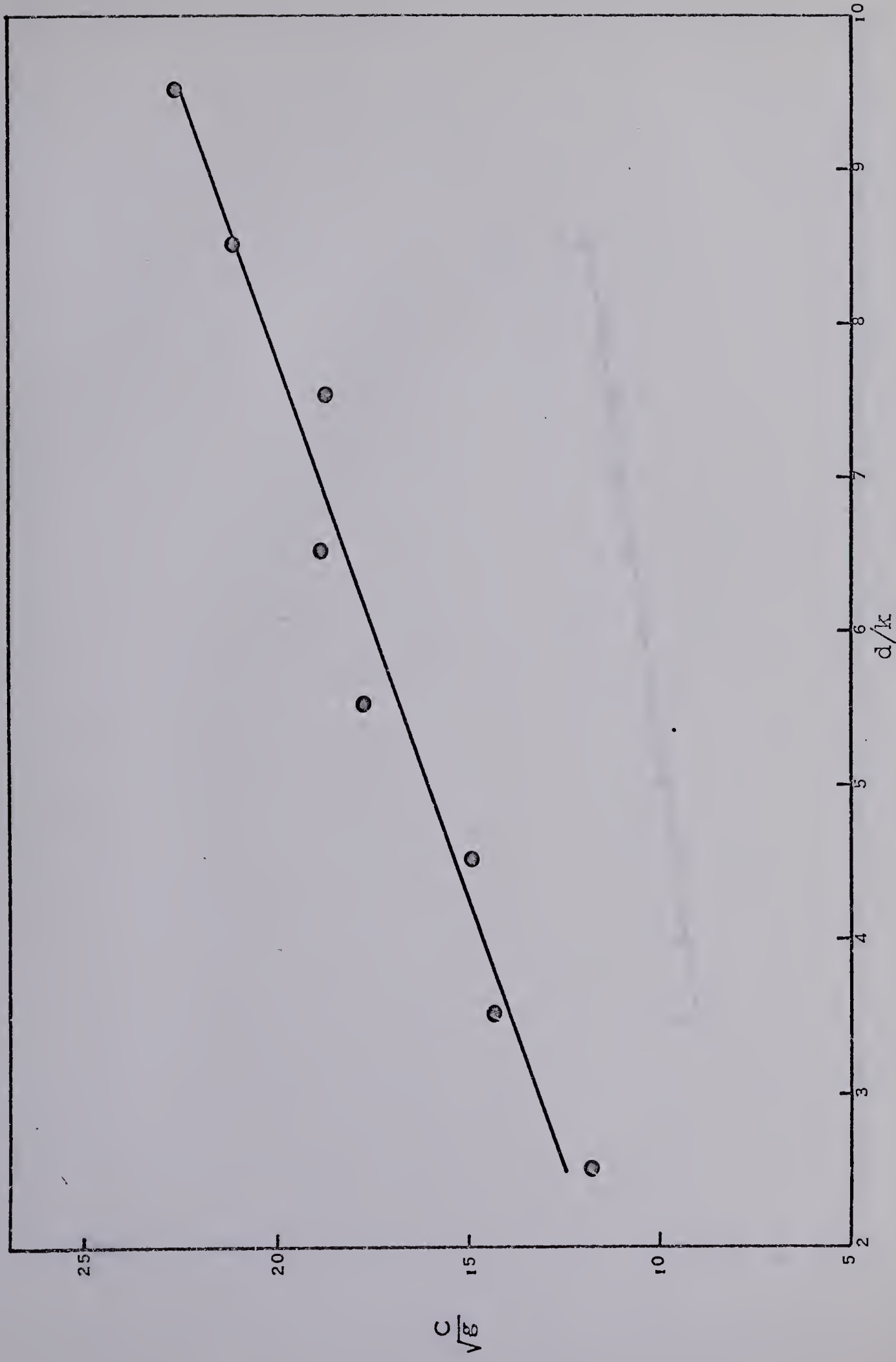
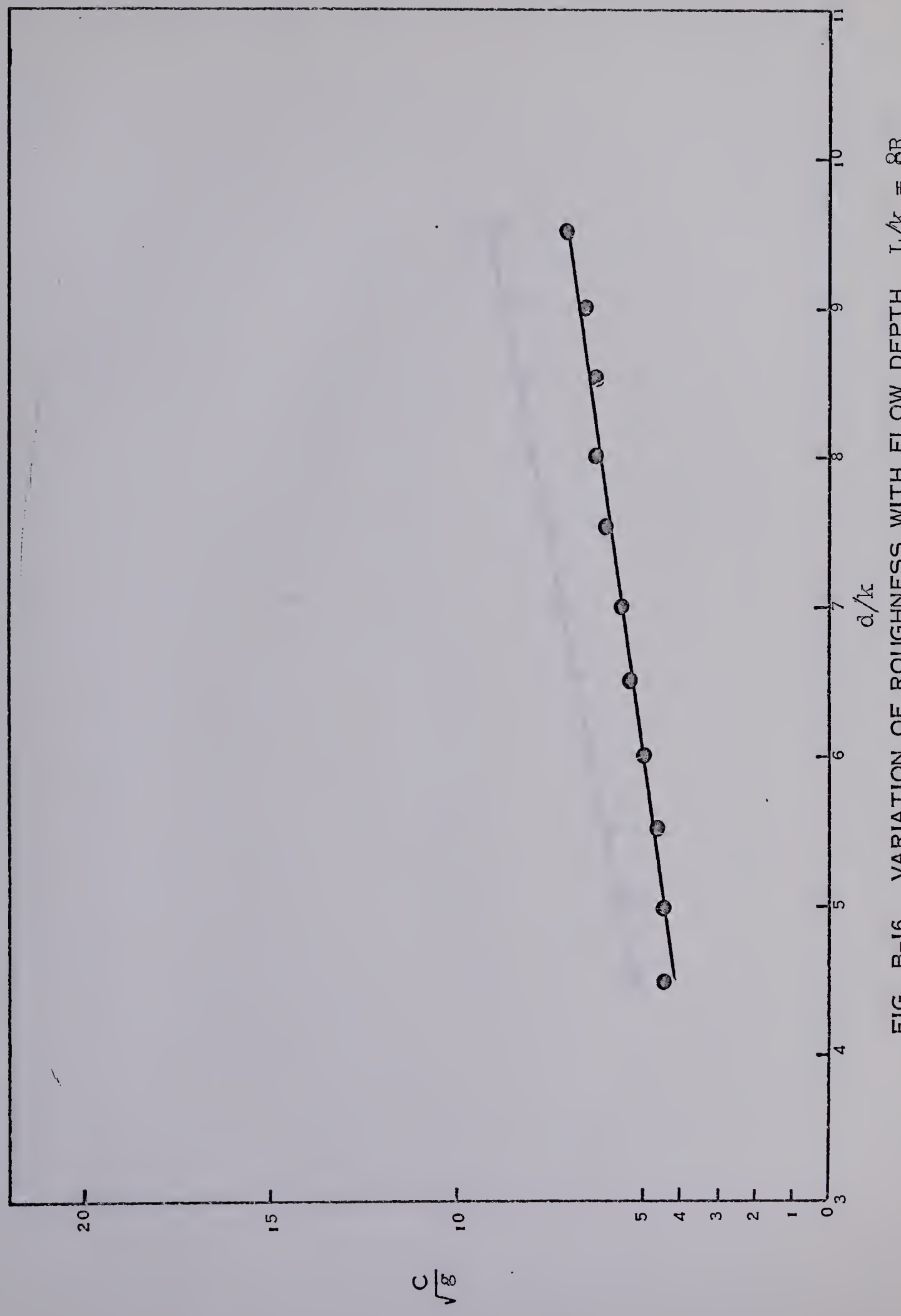


FIG. B-15 VARIATION OF ROUGHNESS WITH FLOW DEPTH $L/k = 40$

FIG. B-16 VARIATION OF ROUGHNESS WITH FLOW DEPTH $L/k = 8R$

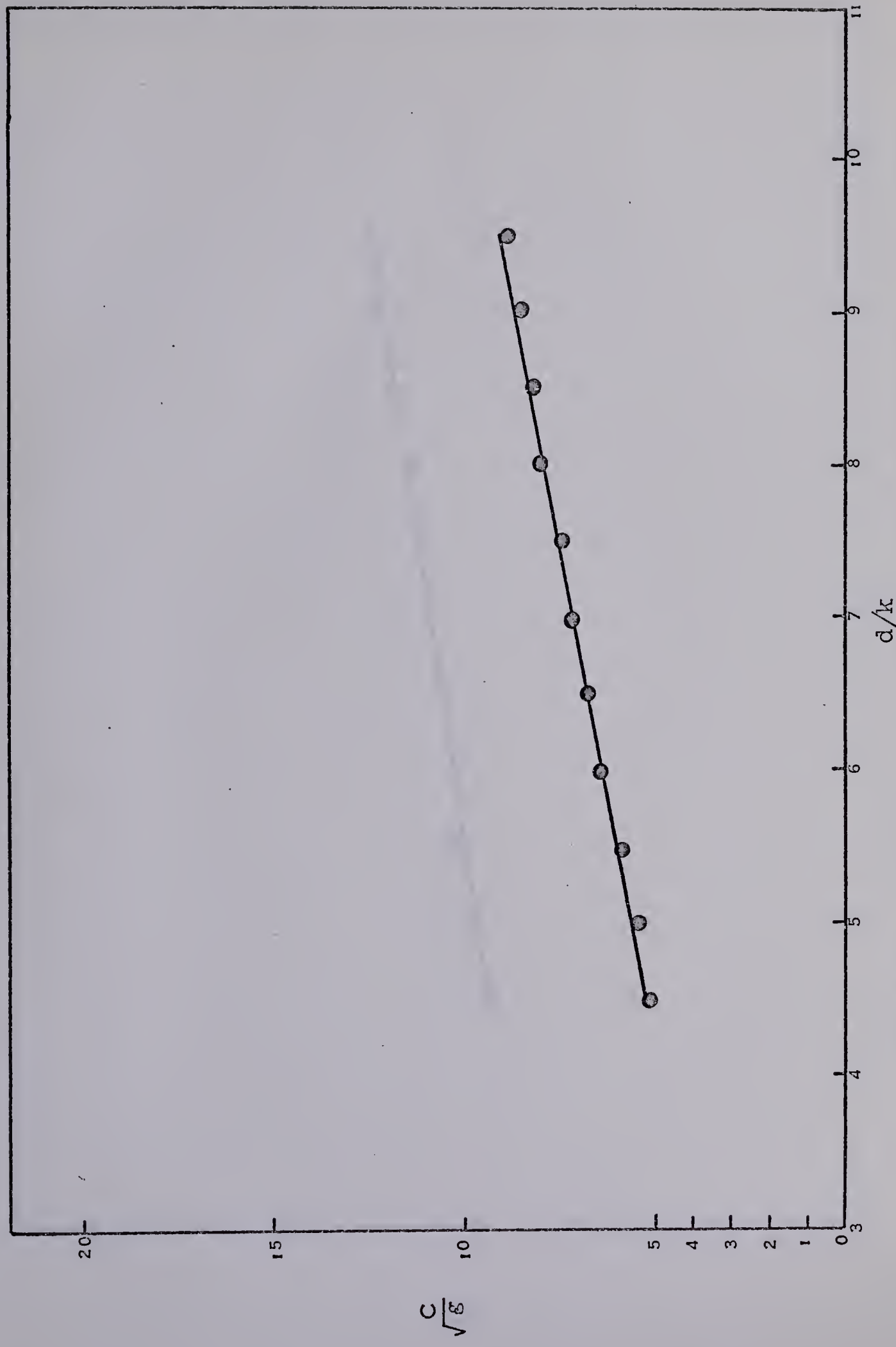
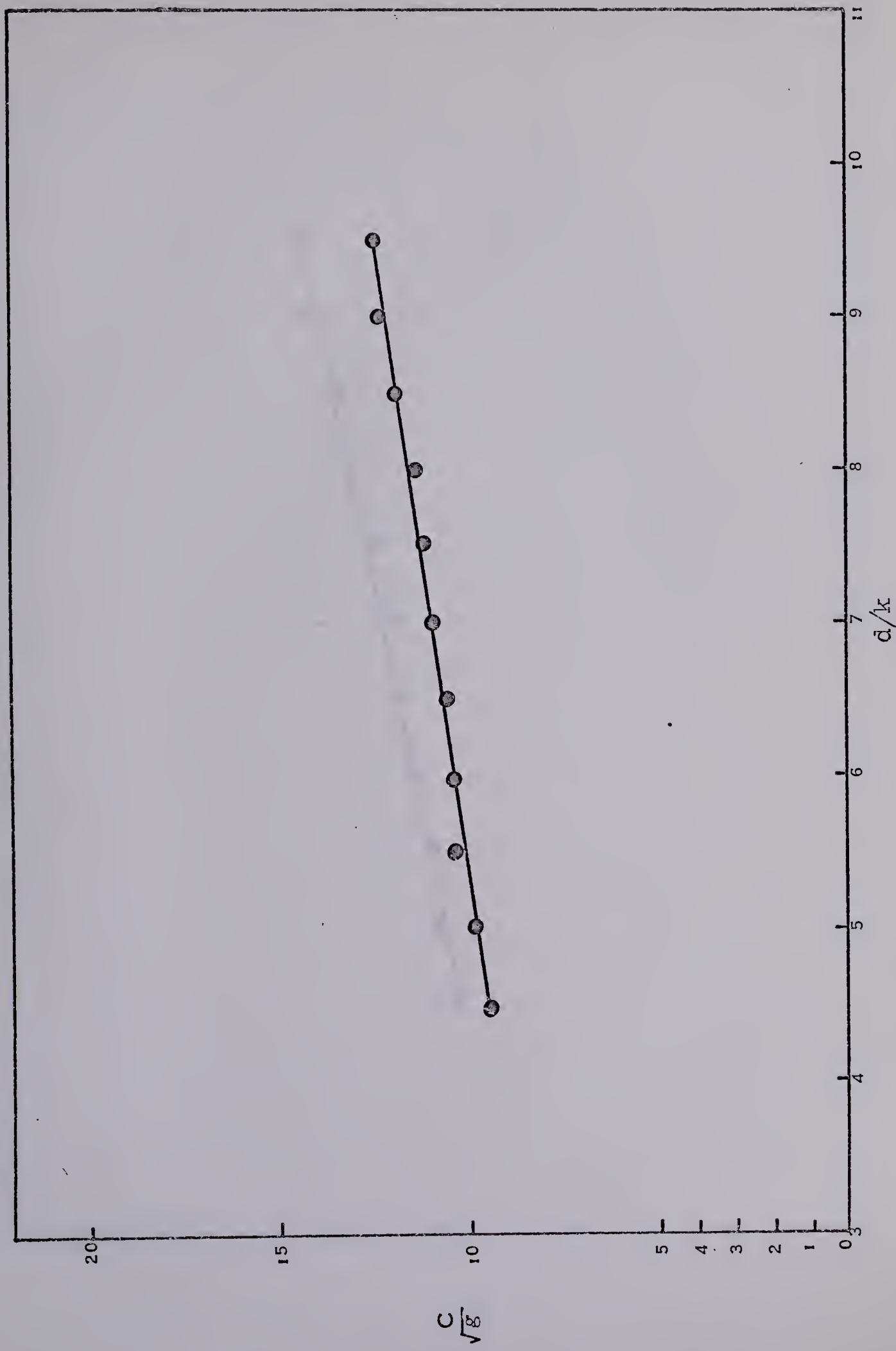
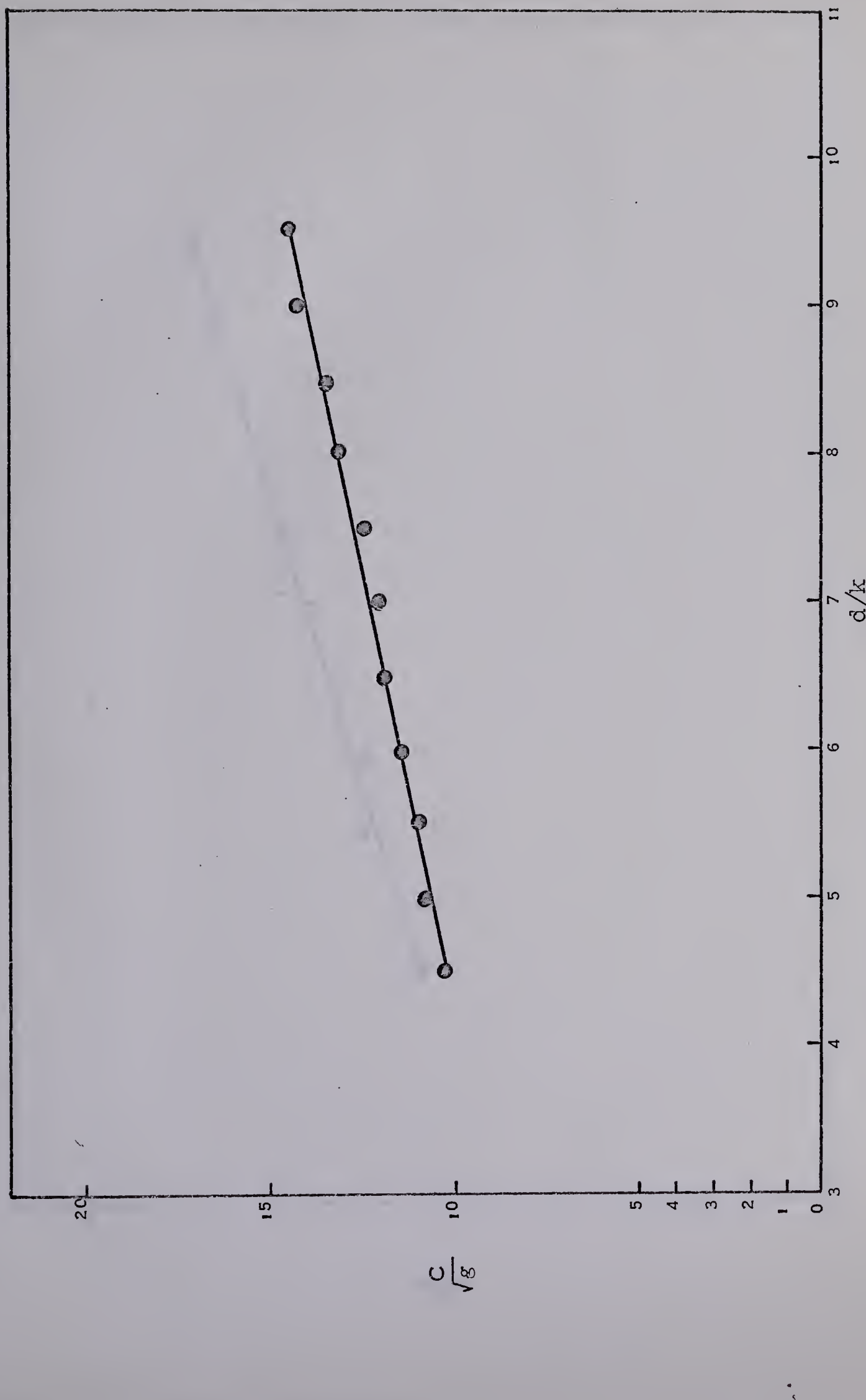
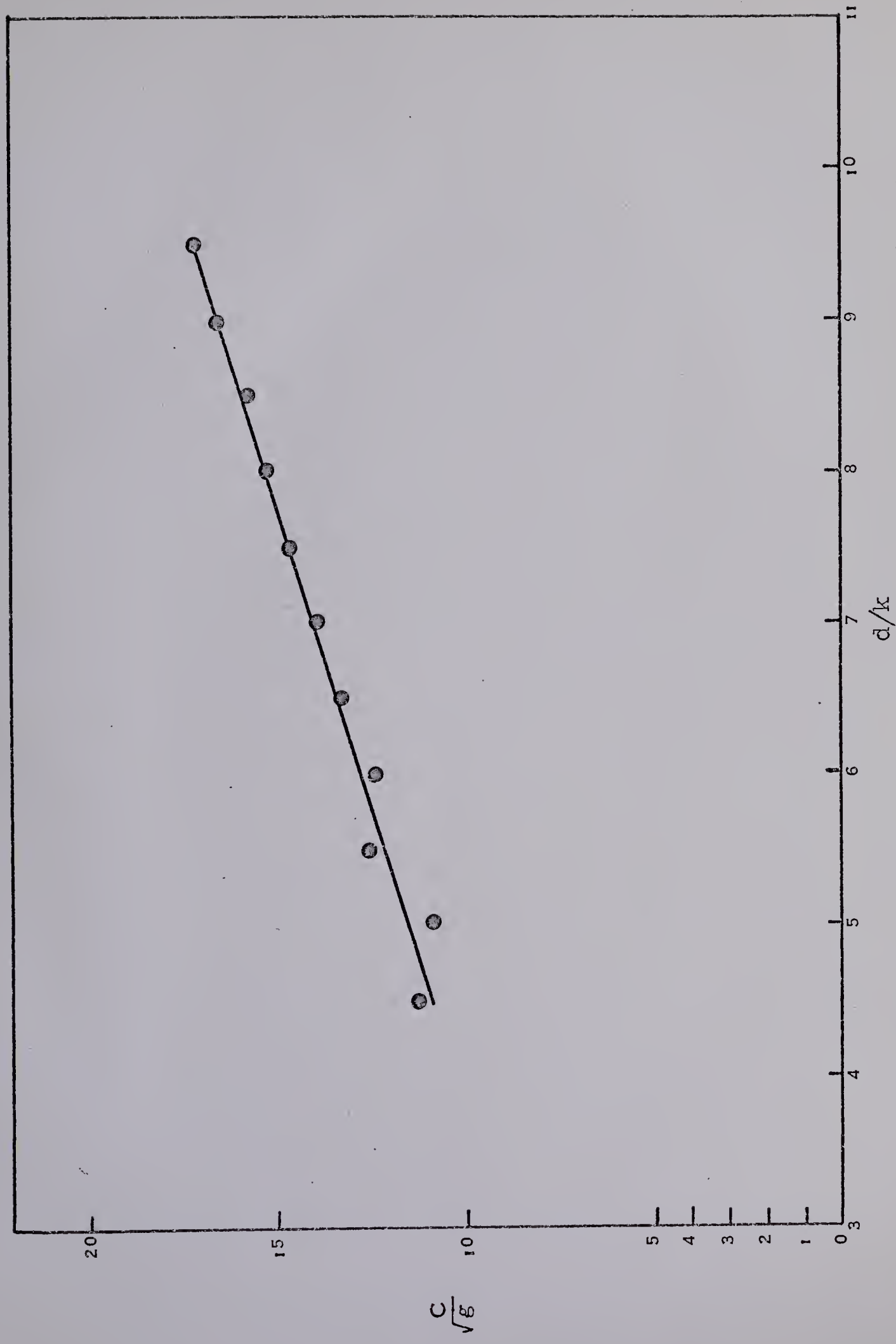


FIG. B-17 VARIATION OF ROUGHNESS WITH FLOW DEPTH $L/k = 16R$

FIG. B-18 VARIATION OF ROUGHNESS WITH FLOW DEPTH $L/k = 24R$

FIG. B-19 VARIATION OF ROUGHNESS WITH FLOW DEPTH $L/k = 32R$



B29881